Volatile Messenger of Death

- Grapevine Fatty Acid Hydroperoxide Lyase Acts in Cell-Death Related Immunity

Zur Erlangung des akademischen Grades eines

DOKTORS DER NATURWISSENSCHAFTEN

(Dr. rer. nat.)

der KIT-Fakultät für Chemie und Biowissenschaften

des Karlsruher Instituts für Technologie (KIT)

genehmigte

DISSERTATION

von

Sahar Akaberi

aus

Chaloos, Iran

KIT-Dekan: Prof. Dr. Willem Klopper

Referent: Prof. Dr. Peter Nick

Korreferent: Prof. Dr. Eva Zyprian

Tag der mündlichen Prüfung: 16. Dezember. 2016

Die vorliegende Dissertation wurde am Botanischen Institut des Karlsruher Instituts für Technologie (KIT), Botanisches Institut, Lehrstuhl 1 für Molekulare Zellbiologe, von Dezember 2012 bis Oktober 2016 angefertigt.

Hiermit erkläre ich, dass ich die vorliegende Dissertation, abgesehen von der Benutzung der angegebenen Hilfsmittel, selbständig verfasst habe.

Alle Stellen, die gemäß Wortlaut oder Inhalt aus anderen Arbeiten entnommen sind, wurden durch Angabe der Quelle als Entlehnungen kenntlich gemacht.

Diese Dissertation liegt in gleicher oder ähnlicher Form keiner anderen Prüfungsbehörde vor.

Zudem erkläre ich, dass ich mich beim Anfertigen dieser Arbeit an die Regeln zur Sicherung guter wissenschaftlicher Praxis des KIT gehalten habe, einschließlich der Abgabe und Archivierung der Primärdaten, und dass die elektronische Version mit der schriftlichen übereinstimmt.

Karlsruhe, im Oktober 2016

Sahar Akaberi

Acknowledgements

First and foremost, I would like to appreciate Prof. Dr. Peter Nick for his wonderful personality, his patience and motivation, as well as for his continuous support during my study. I am deeply thankful to him for giving me a chance to work in his lab, which opened a great chapter in my life.

I would like to thank Dr. Michael Riemann for his help and suggestions during my work and for critical appreciation of my thesis.

I thank Prof. Dr. Philippe Hugueney and Ms. Patricia Claudel for the wonderful time I spent in their lab at the Colmar University in Colmar, France. I would like to thank Prof. Dr. Bettina Hause for hormone analysis, Leibniz Institute of Plant Biochemistry. I thank Prof. Dr. Jaideep Mathur, University of Guelph, Canada for providing me the stroma marker tpFNR-mEosFP.

I appreciate the excellent work of our lab technicians Sybille Wörner, Sabine Purper and Ernst Heene as well as our Azubi Ronja Kammerrich and Lena Draheim. I thank Joachim Daumann and all the staff of the KIT botanical garden for the technical support.

My sincere thanks also go to all my colleagues at Botanical Institute 1 for such a friendly and helpful working environment. I thank especially Dr. Qiong Liu for her support and companionship during the period of my PhD study. My special thanks also go to Dr. Jan Maisch and Dr. Vaidurya Sahi for reviewing this thesis. I am also thankful to Beatrix, Viktoria, Rita, Natalie, Sebastian, Ningning, Mohamed, Lixin, Peijie, Rohit and Preshobha from whom I learned many things.

Finally, I would like to thank my parents, my sister Azin and my brothers, Bardia and Amir for their unconditional love and support. I thank especially James Moossa for his infinite supports during the last four years.

This work was supported by funds from the Federal Ministry for Food, Agriculture and Consumer Protection (BMELV) in frame of the programme Federal

Programme for the Support of Ecological and other Forms of Sustainable Agriculture (BÖLN) to project 2810OE067.

Sahar Akaberi

Table of contents

Abbreviations

AOS: allene oxide synthase

BY-2: Tobacco *Nicotiana tabacum* L. cv. bright yellow 2

CYP: cytochrome P_{450}

DPI: diphenyleneiodonium

ETI: effector-triggered immunity

GC-MS: gas chromatography mass spectrometry

GFP: green fluorescent protein

GLVs: green leaf volatiles

HPL: hydroperoxide lyase

HPOD: hydroperoxy octadecadienoic acid

HPOT: hydroperoxy octadecatrienoic acid

H_2O_2 : hydrogen peroxide

HR: hypersensitive response

JA: Jasmonic acid

JA-Ile: (+)-7-iso-jasmonoyl-L-isoleucine

LOX: lipoxygenase

PAMPs: pathogen-associated molecular patterns

PCD: programmed cell death

PRRs: pattern recognition receptors

PTI: PAMP-triggered immunity

ROS: reactive oxygen species

SBSE: stir bar sorptive extraction

SPME: solid phase microextraction

VOCs: volatile organic compounds

WT: wild type

Zusammenfassung

Die Weinrebe (*Vitis vinifera*) ist eine weltweit verbreitete, wertvolle landwirtschaftliche Nutzpflanze, die allerdings sehr leicht von Pflanzenpathogenen infiziert werden kann. Oxylipine agieren als wichtige Signalmoleküle bei der pflanzlichen Antwort auf biotischen und abiotischen Stress. Es handelt sich dabei um chemische Verbindungen, die von Fettsäuren abstammen. Zusätzlich sind einige Oxylipin- Verbindungen als “green leaf volatiles” bekannt und diese sind maßgeblich beteiligt an der Geruchszusammensetzung von frisch gemähtem Gras. In Weinreben werden die flüchtigen Volatile aus den Fettsäure-Hydroperoxiden mittels der Aktivität des Enzyms Hydroperoxid Lyase (HPL) gebildet und diese tragen zum Geschmack und Aroma der Trauben und Weine maßgeblich bei.

In dieser Dissertation wurde eine HPL aus Weinreben, angefangen bei ihrer zellulären Funktionen bis hin zu den Auswirkungen ihrer heterologen Expression in BY-2 Tabakzellkultur, untersucht und charakterisiert. HPL befindet sich in den Plastiden aufgrund einer N-terminalen Lokalisierungssequenz. Durch eine quantitative Phänotypisierung konnte gezeigt werden, dass sich die überexprimierte Zelllinie unter Kontrollbedingungen gleich wie die Kontrollzelllinie verhält. Allerdings neigt die überexprimierte Zelllinie dazu, als Antwort auf Salzstress einem signalabhängigen Zelltod zu erliegen. Auf den bakteriellen Elicitor Harpin reagieren die Zellen mit der Aktivierung eines Verteidigungsmechanismus, der zu Zelltod führt. Diese signalabhängige Mortalität wurde entweder durch die Zugabe von exogener Jasmonsäure (einem wichtigem Signalmolekül der Grundimmunität bei Pflanzen) oder durch die Behandlung mit Diphenyleneiodonium (DPI) abgeschwächt. DPI ist ein Inhibitor der NADPH-Oxidasen, die apoplastische Superoxide erzeugen.

Durch die Zugabe verschiedener Substrate zu dem rekombinanten exprimierten Enzym konnte die HPL als 13-HPL bestätigt werden- passend zu der Prognose, die aus den Sequenzvergleichen gezogen wurde. Die Produkte, die durch die 13-HPL entstehen, sind cis-3- Hexenal und trans-2- Hexenal. Das Vorhandensein von cis-3 Hexenal verursacht eine schnelle Reaktion der Aktinfilamente, wie sie sich

auch beim Rezeptor-vermitteltem Zelltod abspielt, während das Isomer trans-2-Hexenal diese Reaktion nicht auslöst. Die Ergebnisse werden im Kontext eines Lipoxygenase-abhängigem Signalweg betrachtet, welcher die Abwehrantwort fördert. Dieser Signalweg zweigt von der Jasmonat-abhängigen basalen Immunität ab und führt letztendlich zu der mit dem Zelltod endenden Abwehrantwort.

Falscher Mehltaubefall wird durch das obligat-biotroph lebende Pathogen *Plasmopara viticola* hervorgerufen. Es handelt sich um eine ernstzunehmende Gefahr für die Weingüter Europas und besonders Deutschlands. Im zweiten Teil dieser Dissertation wurde die potentielle Rolle von volatilen Komponenten auf die Pflanzen-Pathogen Interaktion getestet. Hierfür wurde *Plasmopara viticola* als Modellorganismus verwendet. Die Zoosporen von *Plasmopara viticola* gelangen durch die Stomata der Weinrebe in das Blattgewebe. Es ist bereits aus früheren Studien bekannt, dass die Zoosporen durch Wirtsfaktoren, die von der Weinpflanze durch die geöffneten Stomata ausdünsten, angelockt werden und diese Faktoren den Zoosporen als Wegweiser zur Spaltöffnung dienen. Der genauen Rolle zweier dieser volatilen Komponenten, die als Kandidaten für diese Wirtsfaktoren in Betracht kommen, wurden in dieser Arbeit identifiziert und funktionell analysisert. Es zeigte sich, dass das Zielfindungsverhalten von *Plasmopara* Zoosporen in der Anwesenheit exogener Quellen von Farnesen und β- Caryophyllen verändert war. Die Beobachtungen dieser Arbeit lassen den Schluss zu, dass Volatile als Wegweiser und Anlockungsmittel für die Zoosporen zu den Stomata dienen.

Abstract

Grapevine is a widespread and valuable agricultural crop, but easily infected by plant pathogens. Oxylipins are fatty acid-derived compounds acting as important signal molecules in plant responses to biotic and abiotic stresses. In addition, some oxylipins known as "green leaf volatiles" participate in the distinctive smell of freshly cut grass. In grapevine (*Vitis vinifera*), green leaf volatiles are produced from fatty acid hydroperoxides by, Hydroperoxide Lyase (HPL) and contribute to the flavour and aroma of grapes and wines.

In this work, a grapevine HPL has been characterised with respect to its cellular functions upon heterologous expression in tobacco BY-2 cells. HPL is located in plastids due to an N-terminal localisation sequence. Quantitative phenotyping demonstrates that the overexpressor line is not distinct under control conditions, but is prone to signal-dependent cell death in response to salinity stress or the bacterial elicitor harpin, which activates cell-death related defence. This signal-dependent mortality is mitigated either by addition of exogenous jasmonic acid (an important transducer of basal immunity), or diphenyleneiodonium (DPI), an inhibitor of NADPH oxidases that generate apoplastic superoxide.

By feeding different substrates to recombinantly expressed enzyme, the HPL has been confirmed as 13-HPL consistent with the prediction derived from sequence comparisons. The cognate products generated by this 13-HPL were cis-3-hexenal and trans-2-hexenal. Cis-3-hexenal, but not its isomer trans-2-hexenal, elicited a rapid response of actin filaments indicative of a receptor-mediated programmed cell-death response. These results are discussed in the context of a lipoxygenase dependent signalling pathway, which triggers cell-death related defence and bifurcates from jasmonate-dependent basal immunity.

Downy mildew caused by the obligate biotrophic pathogen *Plasmopara viticola*, is an important threat to vineyards in Europe and especially in Germany. In the second part of this study, the potential roles of volatile compounds on plant-pathogen interaction have been investigated by using Grapevine-*Plasmopara* as an experimental model. Zoospores of *Plasmopara viticola* use the stomata to enter

grapevine and it is known from previous works that host factors released from the open stomata are used by zoospores as guiding signals. The potential roles of two volatile compounds as candidates for host factors have been followed. The results of this study showed that targeting behaviour of *Plasmopara* zoospores was affected in the presence of an exogenous source of farnesene or β-caryophyllene. These observations suggest that zoospores use volatiles as attractants to find the stomata.

1. INTRODUCTION

1.1 Grapevine Pathogens

Grapevine (*Vitis vinifera*) is an important fruit crop throughout the world, but it is susceptible to numerous pathogenic microorganisms, such as bacteria, fungi, oomycetes and viruses (Figure 1.1), causing the need for intense plant protection to control grape diseases. As a result, viticulture consumes around 70% of fungicides used in Europe (Eurostat, 2007). Dependance on chemical fungicides is not only costly, but also has a negative impact on the environment, which motivates the search for alternative strategies by improving the innate mechanisms of plant defence.

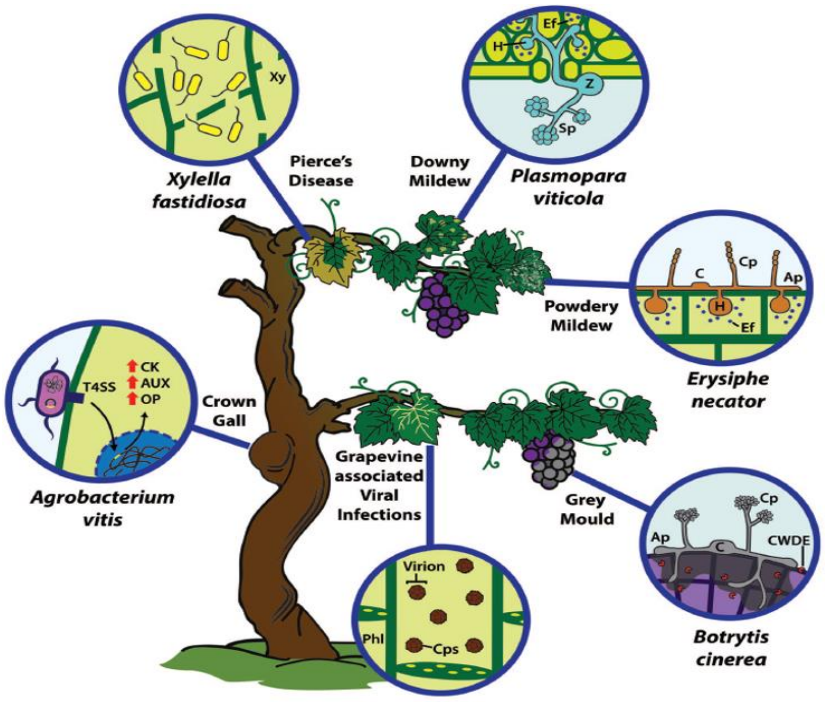

(Adapted from Armijo *et al.,* 2016)

Figure 1.1 Grapevine Pathogenic Microorganisms. *Agrobacterium vitis* causes the grapevine crown gall through the injection of T-DNA sequences via a type-IV secretion system (T4SS), which induce the synthesis of cytokinins (CK), auxins (AUX) and opines (OP). *Xylella fastidiosa* is transmitted by insect vectors; it grows and accumulates within the xylem (Xy) vessels causing Pierce's Disease. *Plasmopara viticola* zoospores (Z), generating the sporangium (Sp) and causes the grapevine downy mildew (DM) disease. Conidia (C) of *E. necator*, the causal agent of the powdery mildew (PM), infects epidermal layers. *P.viticola* and *E. necator* develop haustoria (H) and secret effectors (Ef) into the host. *Botritys cinerea* conidia (C) germinate and penetrate through the secretion of cell wall degrading enzymes (CWDE), causing the gray mold disease. Viruses are phloem-limited (Phl) microorganisms. Ap, appresorium; C, conidium; Cp, conidiophore. Cps, capside.

1.2 Plant Defence Mechanisms

As sessile organisms, plants have evolved a survival strategy that is mainly based on developmental plasticity. Plant defence is a central element of this strategy, and therefore consists of several elements with a high degree of flexibility: In addition to preformed barriers that can be physical, such as cuticles, or cell walls, plants can employ chemical barriers such as secondary compounds that often preexist already prior to any pathogen attack (Garcia-Brugger *et al.,* 2006), plants rely on inducible defence.

1.2.1 Inducible Defences

The reason for defence inducibility has to be searched considering the fact that defence is costly and diverts resources that otherwise could be used for growth (Stamp, 2003). From an evolutionary perspective the sluggish defence of many crop plants is the price paid for higher yields and shorter cultivation cycles. Although there exist cases of qualitative resistance based on single genes, most interactions between plants and pathogens are of a quantitative nature, and the velocity, by which defence is elicited, often decides about the outcome of the interaction (Poland *et al.,* 2009). Mechanisms that accelerate induced defence in response to a pathogen attack confer, therefore, a considerable selective advantage. In fact, plants have developed at least two mechanisms to achieve such a potentiated form of defence.

Activation of defence in tissues far from the site of pathogen attack by systemic acquired resistance (SAR) allows to remain ahead of the spreading pathogen (Durrant & Dong, 2004; Fu & Dong, 2013). A second phenomenon relevant in this context is the so called priming, whereby the experience of a different (mild) form of biotic or abiotic stress will lead to a faster and much stronger defence response to subsequent challenge with a pathogen (Conrath, 2011). The fact that defence can be modulated either based on signals that act across space (in SAR) or based on signals that act across time (in priming), already demonstrates that plant immunity is complex and must be composed of several layers.

1.2.2 PAMP-Triggered Immunity and Effector-Triggered Immunity

A lot of the apparent discrepancies characteristic for the field, could be resolved by a model, where a basal, broad-band immunity coexists with a pathogen-specific level of immunity originating from a coevolutionary history between host and pathogen (Jones & Dangl, 2006). It seems that these two layers are triggered by two types of receptors, located at either the cell surface (for basal immunity), or in the cytoplasm (for the specific layer of immunity). The receptors located on cell surface, are called pattern recognition receptors (PRRs) and recognize conserved pathogen–associated molecular patterns (PAMPs), such as flagellin, the main substituent building the filament of bacterial flagellum, or peptidoglycan fragments, composing the bacterial cell wall, or chitin, the building block of fungal cell walls (Vance *et al.,* 2009). Binding of these conserved ligands activates a so called PAMP-triggered immunity (PTI) that can contain further spread of the pathogen (Dangl *et al.,* 2013).

In consequence of a coevolutionary history with their host, advanced pathogens have developed effector molecules. Most of the microbial pathogens can deliver their effectors to the host cells by using type-III secretion systems (T3SS). When these effectors reach the cytosol of the host cell, they are able to quell PTI responses and initiate various pathogenesis related functions (Vance *et al.,* 2009). The host, in turn, has evolved novel receptors, mostly belonging to the class of the nucleotide binding-leucine rich repeat (NB-LRR) receptors, able to recognize these pathogen effectors (Figure 1.2). Since most effectors translocate into the cytoplasm, these receptors (also referred to as R-proteins) are usually located inside of the cell. After recognition of the pathogens by either PRR, or NB-LRR receptors different signaling pathways and cellular responses are activated. Among them, calcium influx, oxidative burst, activation of mitogen-activated protein kinases (MAPK) or programmed cell death are common events happening in plant cells during both PTI and ETI responses (Dodds & Rathjen, 2010). The effector-triggered immunity (ETI), activated by these receptors often, but not always, culminates in a form of rapid plant cell death termed as hypersensitive response (HR) as efficient strategy against biotrophic pathogens.

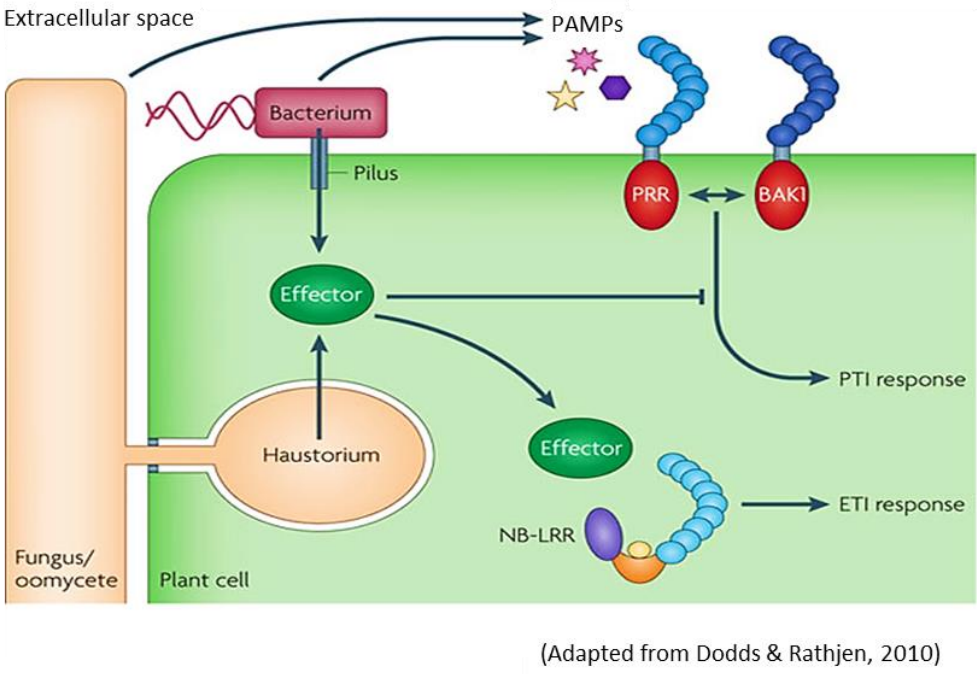

Figure 1.2 The principles of plant immunity. Pathogen-associated molecular patterns (PAMPs) are recognized by cell surface pattern recognition receptors (PRRs) and elicit PAMP-triggered immunity (PTI). PRRs generally consist of an extracellular leucine-rich repeat (LRR) domain (mid-blue), and an intracellular kinase domain (red). Many PRRs interact with the related protein Brassinosteroid Insensitive 1-Associated Kinase 1 (BAK1) to initiate the PTI signalling pathway. Bacterial pathogens deliver effector proteins into the host cell by a type-III secretion pilus. These intracellular effectors often act to suppress PTI. However, many are recognized by intracellular nucleotide-binding (NB)-LRR receptors, which induces effector-triggered immunity (ETI).

1.2.3 Hypersensitive Response (HR)

Plants as well as animals have evolved different modes of cellular suicide referred to as programmed cell death (PCD). When tracheary elements develop in the xylem of vascular plants, for instance, they undergo a form of PCD. From a morphological point of view, this form of PCD initiates from vacuolare swelling and cell wall thickening. These changes are followed by fragmentation of nuclear DNA, cell autolysis, and ends with formation of perforated cell walls. The Hypersensitive Response (HR), represents a different form of plant PCD and has the function to inhibit growth of (mainly biotrophic) pathogens. In contrast to xylem differentiation, chromatin condensation precedes vacuolar disruption in HR, culminating in

destruction of cell organelles, breakup of the cell membrane and release of cell contents into the apoplastic space (Figure 1.3) (Lam, 2004).

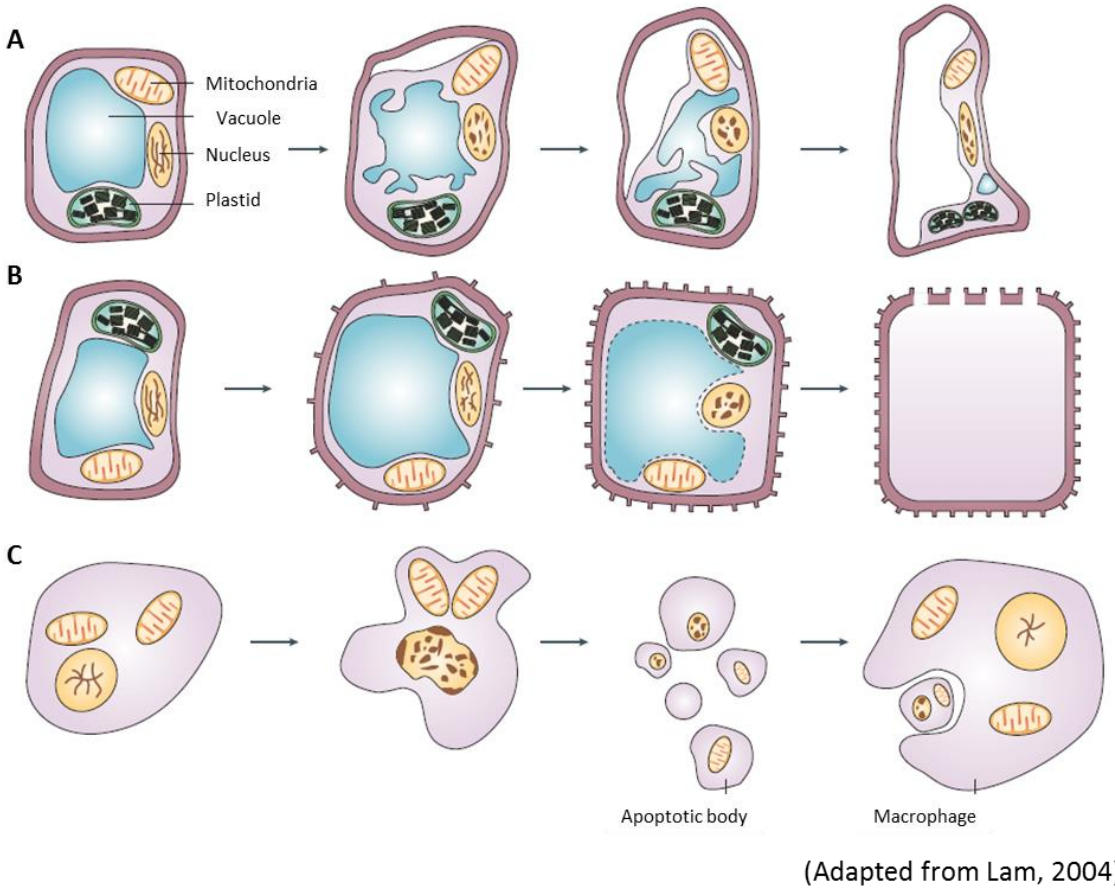

Figure 1.3 Morphological comparison between programmed cell death in plants and animal apoptosis. **A.** The hypersensitive response (HR), **B.** Differentiation of tracheary elements, **C.** Apoptosis in animal cells.

The HR was firstly observed in 1902, where in wheat plants infected by *Puccinia glumarum,* regions of necrotic spots were found at the site of infection (Ward, 1902). Resistance in many plants against microbial pathogens is associated with rapid and localised cell death (Mur *et al.,* 2008). For instance, resistance against downy mildew disease of grapevine is accompanied by the appearance of necrotic spots on leaves in genotypes of different resistance. Nevertheless, these observations are based on the phenotype of HR (Peressotti *et al.,* 2010). As molecular and cellular events accompanying HR, rapid changes of ionic fluxes, accumulation of salicylic acid (SA), nitric oxide, jasmonic acid (JA), ethylene (ET),

and reactive oxygen species (ROS) have been also observed in the context of pathogen infection (Lam, 2004).

The qualitatively different output of PTI and ETI would suggest that the underlying signalling must be different. However, there are several arguments for a strong molecular overlap: for instance, the recognition of effectors does not always lead to HR , a situation for which the term of a "blurred dichotomy" had been coined (Thomma *et al.,* 2011). Second, Resistance (R) proteins can recognize pathogen effectors from various kingdoms, but activate similar defence responses suggesting that many events must have been conserved over evolution (Jones & Dangl, 2006). In fact, a comparative study in grapevine cells (Chang & Nick, 2012) has revealed that the early signals for PTI and ETI are mostly identical, but are generated in a different temporal pattern.

1.3 Oxidative Burst

One of these generic cellular signals is reactive oxygen species (ROS), such as superoxide (O_2^-), hydroxyl radicals ($HO\cdot$) and hydrogen peroxide (H_2O_2). These molecules are produced as byproducts of oxidative metabolism, such as the respiratory chain in mitochondria or photosynthetic electron transport chain in chloroplast (Elstner, 1982). Superoxide and hydroxyl radicals have a short half-life, compared to the uncharged and more stable hydrogen peroxide which is also able to diffuse through membranes. H_2O_2 and $HO\cdot$ can react with membrane lipids and produce lipid peroxides, leading to membrane damage and causing cell death (Garcia-Brugger *et al.,* 2006). So far, two main mechanisms have been described with respect to ROS generation during early defence responses in the context of plant-pathogen interactions: NADPH oxidases and cell wall peroxidases. It has been shown that in some plants like cultured cells of rose (*Rosa damascena*) treated with *Phytophothora* derived elicitor (Bolwell, 1998), oxidative burst caused by NADPH oxidases, whereas in French bean (*Phaseolus vulgaris*) cell cultures treated with elicitors derived from the cell wall of *Colletotrichum lindemuthianum,* peroxidases are responsible for ROS production (Blee *et al.,* 2001). Furthermore, there are cases where both mechanisms are responsible for oxidative burst dependent cell death, where peroxidases are active during basal immunity, while

NADPH oxidases are responsible for the second level of immunity (Bindschedler *et al.,* 2006).

While ROSs can act as executors of cell death as a result of oxidative burst and hypersensitive response, they also can act as signaling molecules, that modulate cellular responses to biotic and abiotic stresses including gene expression (Baxter *et al.,* 2014).

1.3.1 NADPH Oxidase

In plants, NADPH oxidases (Respiratory burst oxidase Homologs, RboHs) also play a key role in signal-related ROS production (Marino *et al.,* 2012). Located in cell membranes, NADPH oxidases can transfer electrons to O_2 and generate superoxide which is later converted to H_2O_2, which is also used for signal transduction itself. H_2O_2, as a key signal molecule, can induce a variety of responses in plant cells. The role of H_2O_2 in activation of the oxylipin pathway, leading to the biosynthesis of JA-related compounds, HR- cell death, and defence gene expression following biotic and abiotic challenges has been shown in many studies (Almagro *et al.,* 2009). In grapevine cells, for instance, RboH can regulate defence-related cell death through modulating actin organisation (Chang *et al.,* 2015), or it can activate innate immunity by activation of the transcription factors *MYB14* that upregulates stilbene synthase, a key enzyme of phytoalexin synthesis in this species (Duan *et al.,* 2016).

When such simple molecules can convey so many different cellular functions, this leads to the question, through what mechanisms specificity is established. In addition to differences in concentration (Dat *et al.,* 2000), it is the temporal and spatial pattern of these molecules that confers specificity (Miller *et al.,* 2010; Ismail *et al.,* 2014). When a molecule is used as a signal, there must be a way to control its accumulation in time.

1.3.2. Lipid peroxidation

Similar to the overlap between PTI and ETI, the dichotomy between damage and signalling is blurred: When membrane lipids encounter ROS, they will be converted to oxygenated fatty acids by nonenzymatic lipid peroxidation. The degraded membrane lipids loose their functionality and impair membrane integrity, which is often accompanied with plant cell death (Farmer & Mueller, 2013). Thus, whereas non-enzymatic lipoxygenation is considered as stress damage event, it coexists with enzymatic lipoxygenation. The enzymatic lipid peroxidation proceeds by the action of Lipoxygenases (LOX). This enzymatic process culminates in the formation of jasmonates, as central stress regulators (Wasternack, 2014) and Green Leaf Volatiles, as important signaling molecules within and between plants (Matsui, 2006).

1.4 Volatile Organic Compounds (VOCs)

Plants cannot move. However, releasing a broad range of Volatile Organic Compounds (VOCs) simplify their interactions with their environment (Holopainen & Gershenzon, 2010). VOCs are low molecular weight compounds with high vapor pressure, that can easily pass the cellular membrane and emit into the air (Dudareva *et al.,* 2013). VOCs, as relatively considerable group of plant natural products, comprise of terpenoids, phenylpropanoids, benzenoids, oxylipins and amino acid derivatives, and are synthesized via four major pathways (Figure 1.4) (Holopainen & Gershenzon, 2010).

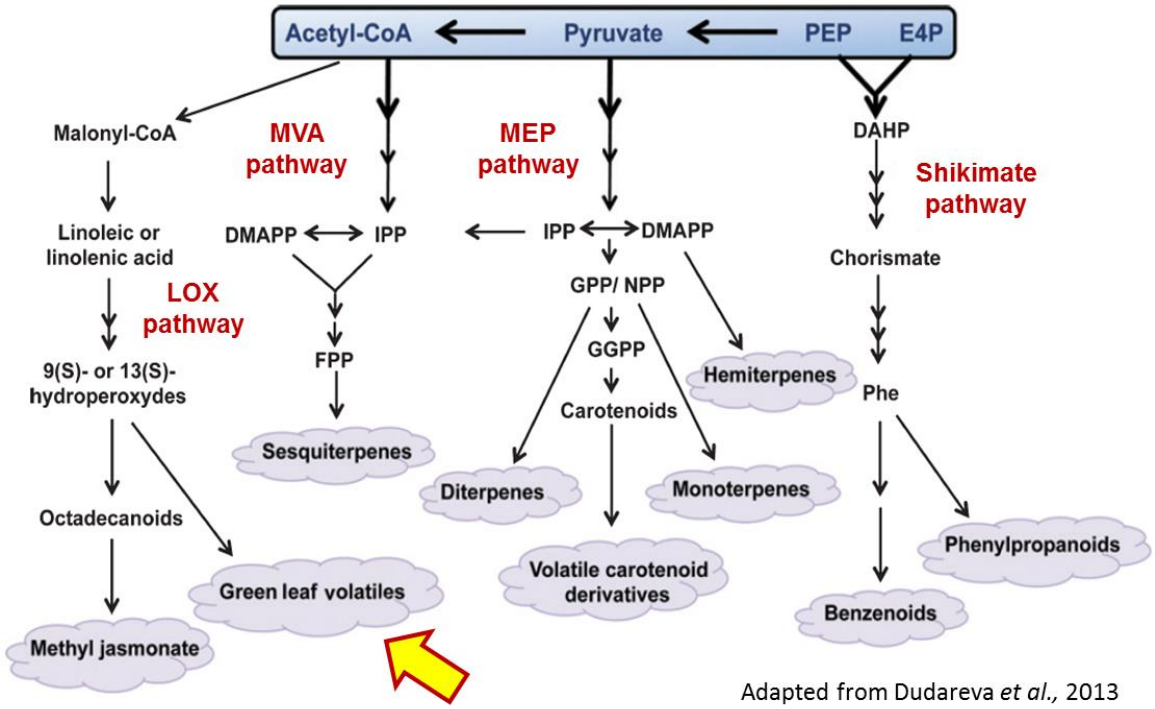

Figure 1.4 Overview of biosynthetic pathways leading to the emission of plant volatile organic compounds (VOCs). Precursors for plant VOCs originate from the primary metabolism (represented in the blue box). The four major VOC biosynthetic pathways, namely the shikimate/phenylalanine, the mevalonic acid (MVA), the methylerythritol phosphate (MEP) and lipoxygenase pathways lead to the emission of VOCs. Abbreviations: DAHP, 3-deoxy-D-arabinoheptulosonate-7 phosphate; DMAPP, dimethylallyl pyrophosphate; E4P, erythrose 4-phosphate; FPP, farnesyl pyrophosphate; GGPP, geranylgeranyl pyrophosphate; GPP, geranyl pyrophosphate; IPP, isopentenyl pyrophosphate; NPP, neryl pyrophosphate; PEP, phosphoenolpyruvate; Phe, phenylalanine.

VOCs are released mainly from flowers (Knudsen *et al.,* 2006), but leaves and stems also emit VOCs. Generally, emission of VOCs from vegetative tissues could be induced upon herbivore feeding, pathogen infection or even mechanical wounding. Biosynthesis of VOCs in plants is regulated during development. For instance, young leaves, immature fruits or flowers shortly before pollination emit higher levels of these compounds (Dudareva *et al.,* 2000). VOCs are involved in different aspects in plants. Plants make extremely use of VOCs for attracting pollinators (Raguso, 2008) and seed dispersers (Dudareva *et al.,* 2013), and they indirectly defend themselves against herbivores by inducing the emission of volatiles, that attracts carnivorous, natural enemies of herbivores (Arimura *et al.,* 2004). VOCs are involved in plant protection against various pathogens (Huang *et*

al., 2012). They mediate plant-plant communication. If released from neighbouring herbivore-attacked plants VOCs could act as warning signals to prime other plants (Baldwin *et al.,* 2006). Furthermore, VOCs protect plants under diverse abiotic stress conditions such as high temperature or drought by mediating oxidative stress (Vickers *et al.,* 2009).

A group of VOCs includes Green Leaf Volatiles (GLVs) and methyl jasmonate. These volatile compounds also called oxylipins, are synthesized from linoleic and linolenic acids through the lipoxygenase pathway (Figure 1.4) (Holopainen & Gershenzon, 2010).

1.4.1 Green Leaf Volatiles (GLVs)

GLVs include C_6 and C_9 aldehydes, alcohols and their esters (Dudareva *et al.,* 2013). GLVs are termed due to their typical scent produced when leaves are injured. Although intact and undamaged plants produce GLVs, their levels are very low. Plants immediately emit GLVs in response to various biotic and abiotic stress conditions (Matsui, 2006; Scala *et al.,* 2013).

In direct defence against herbivores, plants make use of GLVs to increase herbivore resistance. For instance, (Z)-3-hexenal formation at the site of herbivore attack can deter subsequent herbivores (Arimura *et al.,* 2009). In addition, GLVs have antibacterial and antifungal activities that protect plants from pathogen infection (Matsui, 2006), e.g. GLV treatment in *Arabidopsis thaliana* enhanced resistance against necrotrophic fungal pathogen *Botrytis cinerea* (Kishimoto *et al.,* 2005). Indirect defence is also induced by GLVs. It has been shown that GLVs could prime corn plants (*Zea mays*) against herbivorous insects by enhancing JA level and VOC emission (Engelberth *et al.,* 2004). GLVs are also involved in tritrophic (plant-herbivore-natural enemy) systems, where caterpillar-damaged corn and cotton plants attract parasitic wasps (Turlings *et al.,* 1995). In addition, GLVs emit in response to abiotic stimuli. GLVs are detected in tobacco *(Nicotiana tabacum)* plants exposed to ozone (Beauchamp *et al.,* 2005).

1.4.2 Biosynthesis of Oxylipins: Jasmonates versus Green Leaf Volatiles

As discussed earlier, both groups of oxylipins are produced through the lipoxygenase pathway. Lipoxygenase generates hydroperoxy fatty acids including 13-hydroperoxides (13-HPOD/T) and 9-hydroperoxides (9-HPOD/T). These hydroperoxides are subsequently converted into Green Leaf Volatiles and Jasmonates by enzymes belonging to a specific clade of the cytochrome P_{450} superfamily (Figure 1.5). This clade, CYP74 differs from canonical members, because they do neither need molecular oxygen nor NADPH-oxidoreductase for their activity, and also show low affinity for carbon monoxide. The CYP74 clade is further divided into branches with different enzymatic activities (Howe *et al.,* 2000).

Allene oxide synthase (AOS, CYP74A), as the first committed step of jasmonate biosynthesis, and canonical hydroperoxide lyase (HPL, CYP74B) compete for the same substrate, 13-hydroperoxy octadecatrienoic acid (13-HPOT), which means that they should interact antagonistically. In fact, downregulation of the HPL branch has been shown to activate jasmonate synthesis (Liu *et al.,* 2012). In contrast, the CYP74C type HPL accepts both, 13- and 9-hydroperoxides. Both HPL types are responsible for the emission of green leaf volatiles. Whereas AOS and HPL seem to be present in all land plants, the third group, the divinyl ether synthases (DES, CYP74D) have been discovered only in some taxa and might represent a specific variant of CYP74C-HPL (Hughes *et al.,* 2009). The CYP74 subclades have arisen from gene duplications followed by divergent mutations in the active center. By exchange of individual amino acids it is possible to convert an AOS into a HPL (Lee *et al.,* 2008), or a DES into an AOS (Toporkova *et al.,* 2013).

Although the HPL branch competes with jasmonate synthesis, it is also involved in plant defence. However, jasmonates as products of the CYP74A dependent pathway are mostly involved in basal immunity warding off necrotrophic pathogens (Bostock, 2005), the volatile products of HPL have acquired considerable attention in the response to herbivory (Gershenzon, 2007), but there is evidence that they can act also as signals to activate systemic defence (Frost *et al.,* 2008; Farag *et al.,* 2005).

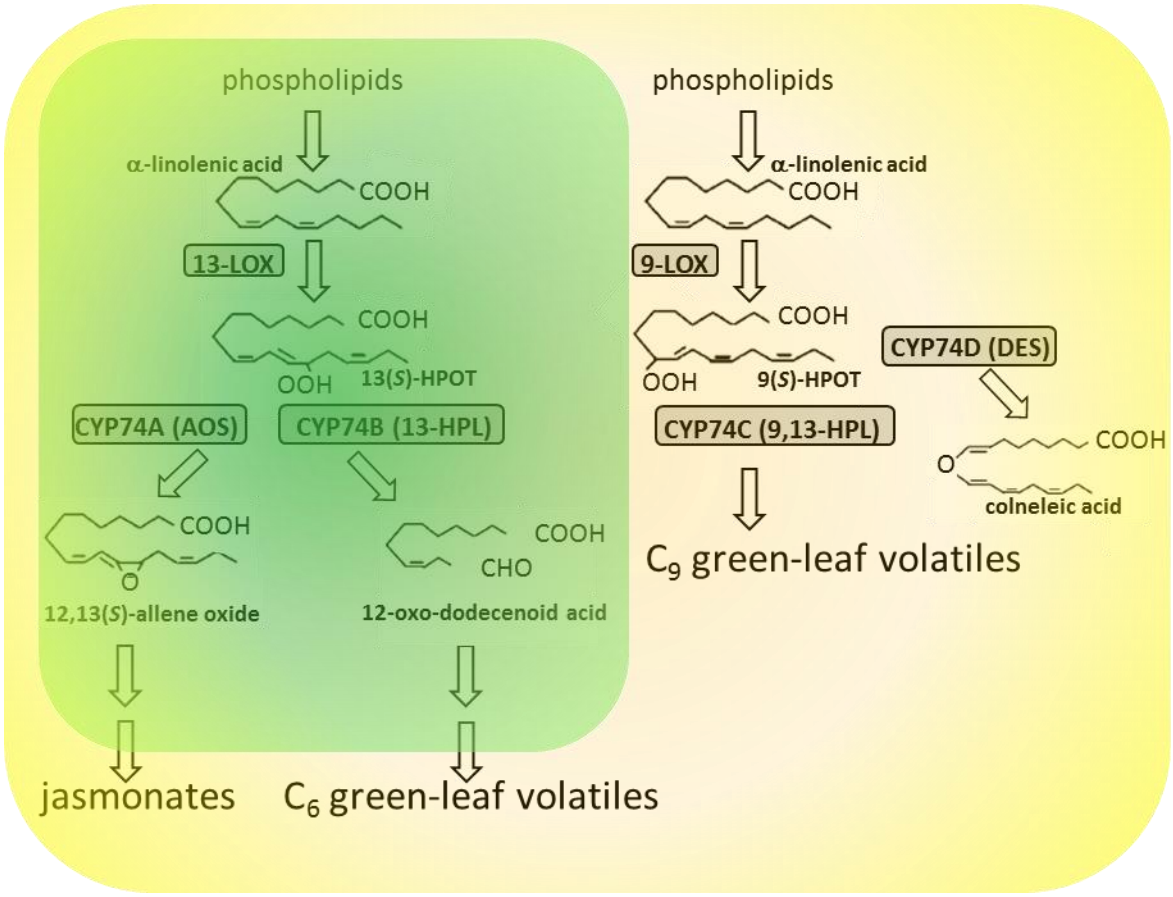

Figure 1.5 Simplified scheme for the metabolic pathways driven by the different CYP74 subclades according to (Hughes *et al.,* 2009). LOX, lipoxygenase; HPOT, hydroperoxy octadecatrienoic acid; AOS, allene oxide synthase; HPL, hydroperoxide lyase; DES, divinyl ether synthase. Plastidic localisation is indicated by green shading (Akaberi *et al.,* 2016 in preparation).

1.5 Hydroperoxide Lyase (HPL)

The Hydroperoxide Lyase gene was first isolated from green bell pepper *(Capsicum annuum)* fruits and characterised as a specific enzyme which belongs to the cytochrome P_{450} superfamily (Matsui *et al.,* 1996). Based on substrate preference, HPL could be classified into three groups: 13-HPL, 9-HPL and 9/13-HPL. The 13-HPL (CYP74B) can catalyse the cleavage of 13-HPOD/T derived from linoleic acid or linolenic acid, leading to the production of C_6 green-leaf volatiles, such as hexanal and cis-3-hexenal and 12-oxo-dodecenoid acid (Fauconnier & Marlier, 1997; Matsui, 2006).

The aldehydes are later reduced and converted to C_6-alcohols and esters such as trans-2-hexenal, cis-3-hexenol, trans-2-hexenol, cis-3-hexenyl acetate by the

action of alcohol dehydrogenase and isomerase (Bate & Rothstein, 1998). C_6-volatiles are considered to be involved directly in plant defence as antimicrobials. For instance, it has been shown that trans-2-hexenal produced in *Phaseolus vulgaris* leaves during HR has an antibacterial effect (Croft *et al.,* 1993). Hexanal as well as trans-2-hexenal could also inhibit hyphal growth in fungal pathogens (Hamilton-Kemp *et al.,* 1992). As indirect defence responses, C_6-volatiles act as signaling molecules. Treatment of *Arabidopsis* tissues with C_6-volatiles induced various defence genes (Bate & Rothstein, 1998). In addition to their role in plant defence either directly as antimicrobials or indirectly as signaling molecules, these compounds (Figure 1.6) are major constituents of flavor and aroma in various fruits and vegetables, thus they are also important in the food industry (Casey & Hughes, 2007).

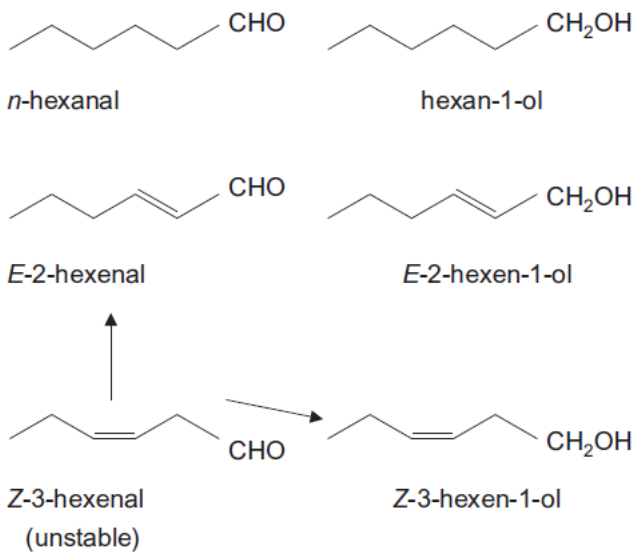

Figure 1.6 Some C_6 aldehydes and alcohols, formed by the action of hydroperoxide lyase (HPL) that contribute to flavor aromas in fruits and vegetables (Casey & Hughes, 2007).

The 12-oxo-dodecenoid acid also produced by the cleavage action of 13-HPL, is a precursor of the wound hormone traumatin. It has been shown that traumatin enhance cell division at the site of wounding and callus formation, thus traumatin is involved in direct defence (Siedow, 1991).

The 9-HPLs convert 9-HPOD/T into C_9 green-leaf volatiles such as cis-3-nonenal and 9-oxoacids (Mita *et al.,* 2005). C_9-volatiles are also involved in defence responses against pathogens. It has been shown that trans-2-nonenal and nonanal have inhibited the hyphal growth in *Alternaria alternata* and *Botrytis cinerea* (Hamilton-Kemp *et al.,* 1992).

In contrast, the 9/13-HPLs (CYP74C) accept both (13-HPOD/T) and (9-HPOD/T) hydroperoxy fatty acids, generating both C_6 and C_9 green-leaf volatiles.

The HPL gene is extensively distributed in plants. Recently, the HPL gene has been isolated from many plants. For instance, HPL from *Arabidopsis* (Bate *et al.,* 1998) and tomato *(Lycopersicon esculentum)* (Howe *et al.,* 2000) are characterised and clustered as CYP74B (13-HPL), whereas almond HPL (*Prunus dulcis)* is classified as 9-HPL (Mita *et al.,* 2005). HPL gene isolated from *Vitis vinifera* cv. 'Cabernet Sauvignon' and melon fruit (*Cucumis melo*) (Tijet *et al.,* 2001) are classified as 9/13-HPLs (Zhu *et al.,* 2012).

In addition to its substrate specificity, HPL from different plants shows also uncommon subcellular localisation patterns. For instance, HPL targeted to plastids in rice (*Oryza sativa)* (Chehab *et al.,* 2006) and tomato *(Lycopersicon esculentum)* (Froehlich *et al.,* 2001), to lipid bodies in almond seeds (*Prunus dulcis)* (Mita *et al.,* 2005), or to cytosol and lipid droplets in *Medicago truncatula* (Domenico *et al.,* 2007).

The fact that HPL forms with specific expression patterns generate distinct patterns of green-leaf volatiles (Chehab *et al.,* 2006), suggests that the chemical complexity generated by these enzymes is of biological relevance. It is also clear that their role in defence is distinct from that of the AOS-derived jasmonates (Chehab *et al.,* 2008), but still the biological function of these enzymes remains far from being understood.

1.6 The Grapevine-*Plasmopara* interaction, an experimental model for grapevine volatiles

The oomycete *Plasmopara viticola,* which causes the downy mildew disease of grapevine, is an obligate biotroph. Downy mildew originated from North America and was introduced to Europe in 1878, where it still causes considerable losses in viticulture (reviewed in Gessler *et al.,* 2011; Kamoun *et al.,* 2015). *P. viticola* belongs to the family Peronosporaceae with both sexual and asexual life cycles (Figure 1.7) (Wong *et al.,* 2001). But the pathogen spreads extensively through the asexual cycle, (see Figure 1.11 highlighted in green) (Kiefer *et al.,* 2002).

The *P. viticola* sexually produced oospores spend the winter in fallen leaves or berries till the growing season (Figure 1.7). Upon favourable temperatue and rainfall conditions, these oospores germinate and produced macrosporangia that contain zoospores. These zoospores enter the stomata and cause primary infection. During the asexual cycle, sporangia are released from sporangiophores, that later produce zoospores (Gobbin *et al.,* 2005). In order to infect, both spores produced either from the sexual (oospores) or asexual cycle have to find stomata (Gobbin, 2004). When zoospores have landed on the stoma, they shed their flagella, encyst and form a germ tube in order to reach the substomatal cavity (Riemann *et al.,* 2002). In the substomatal cavity an infection vesicle is formed, which later forms hyphae. From primary hyphae, a mycelium develops that penetrates into the leaf tissues. Finally, haustoria develop into the host cells to gain the nutrients. After 4-6 days disease symptoms appear on leaves (Figure 1.8), inflorescences, berries and shoots (Kennelly *et al.,* 2007).

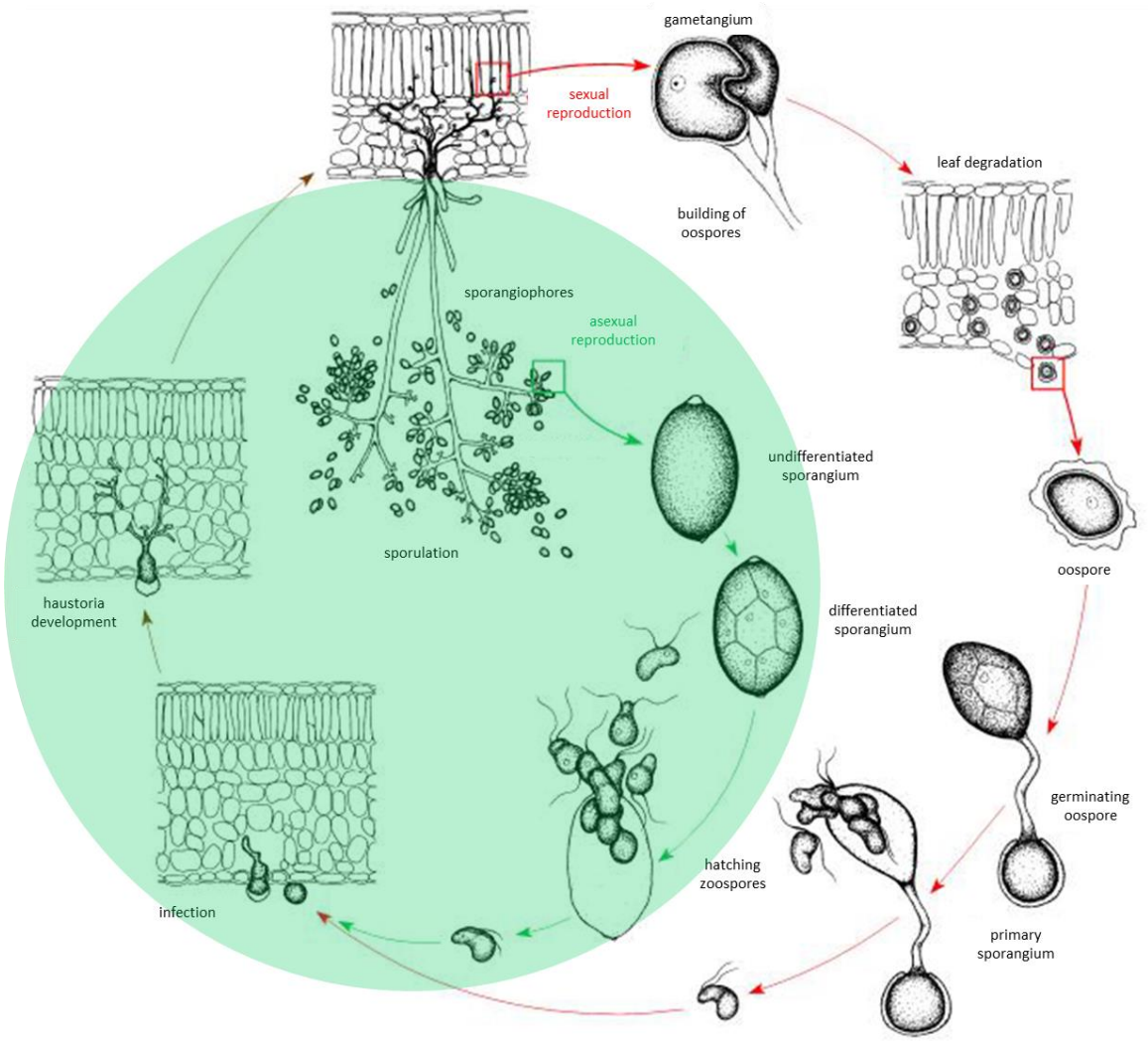

Figure 1.7 Developmental cycle of *Plasmopara viticola*. Sexual cycle marked with red arrows, asexual cycle with green arrows, also highlighted in green. Brown arrows mark the stages, which are shared by both cycles. Figure modified from (Gobbin, 2004).

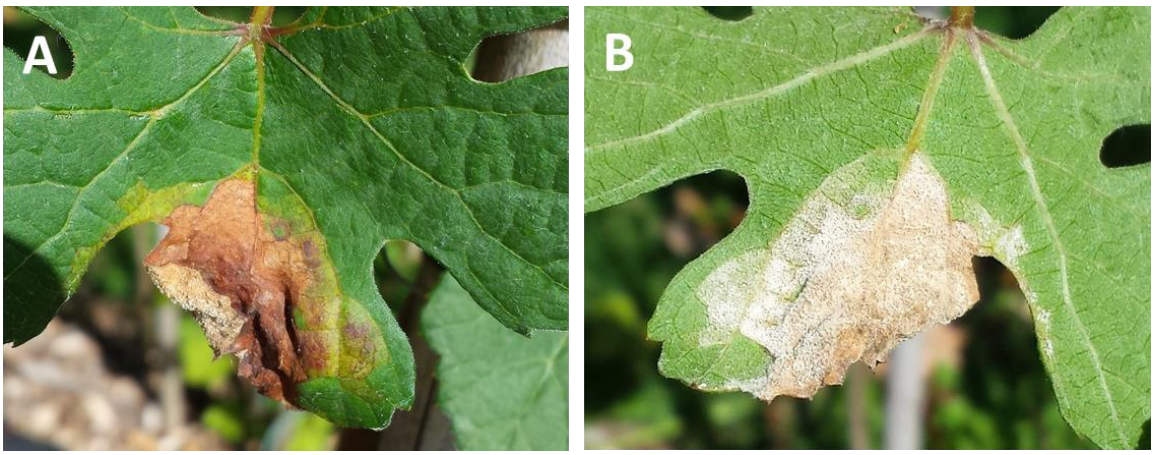

Figure 1.8 Downy mildew symptoms. A. Oilspots and necrosis on the adaxial leaf surface, B. Sporulation of *Plasmopara viticola* on the abaxial leaf surface (Pictures by Sahar Akaberi, Botanical Garden KIT, July 2016).

1.7 Scope of the Study

Defence responses in cell cultures from grapevine had been examined previously (Chang & Nick, 2012). In this system, PTI can be induced by a synthetic 22-amino-acid peptide (flg22) from a conserved flagellin domain, whereas the bacterial elicitor harpin induced an ETI-like immunity culminating in cell death. In the same system, it has been shown that flg22 induced the accumulation of jasmonic acid and its bioactive isoleucine conjugate JA-Ile, whereas harpin did not, assigning the activation of jasmonate synthesis clearly to basal, but not to cell-death related defence (Chang *et al.,* 2016). This led to the question, whether the bifurcation of the oxylipin pathway produced by the duplication into the CYP74A (AOS) jasmonate generating branch and the CYP74B (HPL) volatile generating branch might be linked with the bifurcation of defence signalling that either leads to basal immunity (AOS, jasmonate pathway) or a cell-death related immunity (HPL, volatile pathway). Therefore, in this study HPL was isolated from the *Vitis vinifera* cultivar Müller-Thurgau and overexpressed in the tobacco cell line BY-2 wanting to understand the swithch between basal and cell-death related defense.

1.7.1 Where is the grapevine HPL localised, and what is its enzymatic function?

HPLs from different plants show diverse subcellular localisation patterns. Therefore, in the first step of this study, subcellular localisation of the HPL was studied using fluorescent microscopy. Binary vectors with GFP fused both at the N- or the C-terminus of the enzyme were generated and transformed into tobacco cells. In addition to its diverse subcellular localisation patterns, HPLs from different plants also display substrate specificity. Hence, substrate preference of VvHPL has been determined subsequently by feeding potential substrates to the recombinantly expressed HPL and then analysed by Solid Phase Micro Extraction (SPME) coupled with gas chromatography mass spectrometry (GC-MS).

1.7.2 What is the function of grapevine HPL in defence signalling?

So far, two HPL genes (*VvHPL1* and *VvHPL2*) have been isolated from *Vitis vinifera* L. cv. 'Cabernet Sauvignon' berries and were characterised with respect to their molecular properties (Zhu *et al.,* 2012). The function of grapevine HPL in defence responses has not been addressed so far. A stable tobacco cell line overexpressing VvHPL1 was established to study its potentioal role in defence signalling.

Green Leaf Volatiles produced by the action of HPL are known to have antibacterial and antifungal activity. In the current work, the effects of HPL products, cis-3-hexenal and trans-2-hexenal on tobacco BY-2 cells have been followed.

1.7.3 How could volatiles affect Grapevine-*Plasmopara* interaction?

The cellular and molecular assay will be able to provide information about the characteristic about the enzyme. However, the information about its biological meaning is still missing. To further understand the fuction of volatile compounds, we introduced Grapevine-*Plasmopara* interaction as an experimental model. Most of the research on grapevine downy mildew has focused on the pathogen life cycle (Gessler *et al.,* 2011). However, it was suggested to study the key step in *P. viticola* life cycle, where the flagellate zoospores have to find their ways to the stoma. It has been shown that zoospores make use of chemical factors released from open stomata to target the host (Kiefer *et al.,* 2002). The role of volatile compounds that are emitted from stomata was therefore suggested as guiding signals in Grapevine-*Plasmopara* interaction. To achieve this answer, the volatiles emitted from leaves of *Vitis vinifera* cv. Müller-Thurgau and *Vitis rupestris* have been detected by SPME-GC-MS analysis. Later in this work, the effects of two interesting compounds on targeting behaviour of *P. viticola* zoospores have been investigated.

2. MATERIALS AND METHODS

2.1 Cell culture

Suspension cells of *Nicotiana tabacum* L. cv. 'Bright Yellow 2' (BY-2, Nagata *et al.,* 1992) were cultivated in Murashige and Skoog (MS) medium containing 4.3 $g \cdot l^{-1}$ Murashige and Skoog salts (Duchefa Biochemie, Haarlem, the Netherlands), 30 $g \cdot l^{-1}$ sucrose, 200 $mg \cdot l^{-1}$ KH_2PO_4, 100 $mg \cdot l^{-1}$ inositol, 1 $mg \cdot l^{-1}$ thiamine, and 0.2 $mg \cdot l^{-1}$ 2,4-dichlorophenoxyacetic acid (2,4-D), pH 5.8. Cells were subcultivated weekly by transferring 1.0 to 1.5 ml of stationary cells into 30 ml fresh medium in 100 ml Erlenmeyer flasks. The cells were then incubated on an orbital shaker (IKA Labortechnik, Staufen, Germany) at 150 rpm and 25°C in darkness. Transgenic suspension cells were subcultivated in the same medium as mentioned above, but supplemented with 45 $mg \cdot l^{-1}$ Hygromycin (for more details, see Appendix 5.1).

2.2 Cloning of *Vitis vinifera* HPL1

To over express *Vitis vinifera* HPL1 as a fusion with GFP either at the N- or the C-terminus, in tobacco BY-2 WT under control of the Cauliflower Mosaic Virus 35S promoter, a Gateway®-Cloning strategy was employed (Invitrogen Corporation, Paisley, UK). The insert was first amplified from the grapevine cultivar 'Müller-Thurgau' (Appendix 5.2) by RT-PCR based on the published sequence by Zhu *et al.,* (2012, accession HM627632) using specific primers extended by the specific flanks required for Gateway cloning (Appendix 5.3). The sequence has been deposited under KX379687 in GenBank. A complete overview of both constructs generated from this study can be found in (Appendix 5.4).

Leaves of *Vitis vinifera* cv. 'Müller-Thurgau' (voucher KIT-5585) were collected from plants in the greenhouse of the Botanical Garden of the Karlsruhe Institute of Technology, and immediately frozen in liquid nitrogen. Frozen tissues were ground to a fine powder in liquid nitrogen with a prechilled mortar and pestle. Total RNA was extracted from 50-70 mg of the powdered tissue using the Spectrum™ Plant Total RNA Kit (Sigma-Aldrich, Deisenhofen, Germany) following the protocol of the

manufacturer. Quality and yield of the RNA samples were determined by agarose gel electrophoresis and spectrophotometric measurement. For cDNA synthesis, 1 µg of RNA were used as a template for reverse transcription (M-MuLV reverse transcriptase, New England Biolabs, Frankfurt) and the reverse transcription was performed according to the protocol of the producer.

The HPL gene was amplified by PCR in a total volume of 20 µl with 0.4 mM of mixed dNTP, 0.4 µl of each primer, and 0.1 µl of Q5 DNA polymerase in the corresponding reaction buffer (New England Biolabs, Frankfurt) by 35 cycles of 94°C for 30 s, annealing at 58°C for 30 s, and synthesis at 68°C for 30 s, after initial denaturation at 94°C for 1 min, and a final extension at 68°C for 2 min. The size of the amplicons was analysed on 1.8% agarose gels stained with SyberSafe (Thermo Fisher, Frankfurt, Germany), and purified using the PCR Clean-up (Macherey-Nagel, Düren, Germany) kit according to the manufacturer instructions. The resulting coding sequences were inserted into the binary vector pH7WGF2,0 for the N-terminal fusion, and pH7FWG2,0 for the C-terminal fusion, respectively (Karimi *et al.,* 2002), using the Gateway technology (Invitrogen Corporation, Paisley, UK) according to the protocol of the manufacturer.

2.3 Transformation of tobacco BY-2 cells using *Agrobacterium*-mediated transformation

A BY-2 cell line overexpressing VvHPL1-GFP in a stable manner was generated according to Buschmann *et al.,* 2010 with some modifications: Cells from one flask cultivated under standard conditions were collected at day 3 after subcultivation and washed three times with 300 ml of Paul's medium (4.3 g l^{-1} Murashige and Skoog salts with 1% sucrose, but avoid of any hormones, pH 5.8) using sterile filtration (Nalgene filter holder, Thermo Scientific, Langenselbold, Germany) combined with an sterilised Nylon mesh (Eggert Mehlsiebe, Waldkirch, Germany) with a mesh size of 70 µm. The washed cells were then resuspended in 5 ml of Paul's medium yielding a 5-fold concentrated cell suspension. Five ml of this concentrated cell suspension were mixed with 180 µL of *Agrobacterium tumefaciens* prepared as follows.

This transgenic *Agrobacterium* suspension was prepared in the following way: 100 µl chemo-competent cells of the strain EHA105 were first thawed on ice, and then incubated with 100 ng of the binary expression vectors containing VvHPL1 for further 20 min. Bacteria were later spread onto LB (Lennox Broth, Roth, Karlsruhe, Germany) agar medium containing the appropriate antibiotics (50 $\mu g \cdot ml^{-1}$ rifampicin, 300 $\mu g \cdot ml^{-1}$ streptomycin, and 100 $\mu g \cdot ml^{-1}$ spectinomycin), and incubated for 3 days at 28°C in the dark. A single colony was inoculated into 5 ml of LB liquid medium supplied with the same antibiotics and incubated overnight at 28°C under vigorous agitation. The overnight culture was inoculated into 5 ml of fresh LB-medium (without antibiotics) at a starting OD_{600} of 0.15. After 4-5 h of cultivation at 28°C, when the OD_{600} had reached ~0.8, six ml of the suspension containing transformed *A. tumefaciens* bacteria were harvested and spun down at 8000 g (Heraeus Pico 17 Centrifuge, 600 Thermo Scientific, Langenselbold, Germany) for 7 min in a 50- ml Falcon tube at 28°C. The bacteria were then resuspended in 180 µl Paul's medium by mixing vigorously using a bench-top vortexer (Bender & Hobein, Zürich, Switzerland) to homogenize the suspension.

These bacterial suspensions were mixed with the BY-2 cells prepared as described above in a Falcon tube on an orbital shaker (100 rpm) for 5 min. Petri dishes (94 × 16 mm) were poured with Paul's agar (Paul's media with 0.5% Phytagel) without any antibiotics and allowed to solidify. The mixture of bacteria and cells was inoculated onto these plates placing the drops with sterile cut tips. The plates were then incubated for 3 days at 22°C in the dark.

Cells were subsequently transferred onto MS agar plates with 45 $\mu g \cdot ml^{-1}$ hygromycin to select transformed tobacco cells, and 300 $\mu g \cdot ml^{-1}$ cefotaxime to eliminate *Agrobacterium*. After incubation at 26°C in the dark for 3 weeks, calli had appeared and were transferred onto fresh MS agar plates (with corresponding antibiotics and cefotaxime) for further growth. Finally, a suspension culture was established from pooled calli that had sufficient size.

2.4 Stress and inhibitor treatments

To test for potential differences in the response of the transgenic line, different stress treatments were employed. As abiotic stressor, salinity was used, administering 50, 100, or 150 mM of NaCl at the time of subcultivation. To activate basal defence, the conserved bacterial flagellin fragment flg22 (antikoerper, Aachen, Germany) was dissolved in sterile water and used at 1 µM (Guan *et al.,* 2013). To activate cell-death related defence, the elicitor harpin derived from the phytopathogenic bacterium *Erwinia amylovora* was used at a final concentration of 18 or 27 $\mu g \cdot ml^{-1}$, respectively, after dilution from an aqueous stock solution of 300 $mg \cdot ml^{-1}$ (Pflanzenhilfsmittel, ProAct, Starnberg, Germany). Again, these elicitors were added at the time of subcultivation. In some experiments, cells were treated with 100 µM of (±)-Jasmonic acid ((±)-JA) (Sigma-Aldrich, Germany), or with 200 nM of the inhibitor of NADPH oxidase, diphenyleneiodonium (DPI) (Cayman, USA) dissolved from a stock of 20 mM in DMSO.

2.5 Microscopy and phenotyping of the VvHPL1 overexpressor

Fluorescent proteins were observed using the AxioObserver Z1 (Zeiss, Jena, Germany) inverted microscope equipped with a laser dual spinning disk scan head from Yokogawa (Yokogawa CSU-X1 Spinning Disk Unit, Yokogawa Electric Corporation, Tokyo, Japan), a cooled digital CCD camera (AxioCamMRm; Zeiss), and two laser lines (488 and 561 nm, Zeiss, Jena, Germany) attached to the spinning disk confocal scan head. Images were recorded using a Plan-Apochromat 63x/1.44 DIC oil objective operated via the Zen 2012 (Blue edition) software platform. To test for a potential colocalisation of the fusion protein with plastids, the tpFNR-mEosFP (Schattat *et al.,* 2012, kind gift of Prof. Dr. Jaideep Mathur, Guelph University, Canada) was transiently transformed into the VvHPL1-GFP overexpressors based on the *Agrobacterium*-based protocol (Buschmann *et al.,* 2010) described above.

After subcultivation under control conditions, or treatment for 24 h with the different stress factors or inhibitors described in the previous section, 500 µl of each sample were transferred into custom-made staining chambers (Nick *et al.,* 2000) to remove

the medium and to determine mortality by the Evans Blue exclusion test (Gaff & Okong'O-Ogola, 1971): The cells were incubated for 3-5 min in 2.5% (w/v) Evans Blue (Sigma-Aldrich) dissolved in Millipore water, and then washed with MS medium three times. The membrane-impermeable dye can penetrate only into dead cells, such that the frequency of blue cells was scored under AxioImager Z.1 microscope (Zeiss, Jena, Germany) using differential interference contrast, and mortality was calculated as the ratio of dead cells over the total number of cells. Results represent mean values obtained from at least three independent experimental series with 500 cells per individual data point. The results were tested for significance using Student's *t*-test at 95% and 99% confidence level.

To determine mitotic index, 500 µl of BY-2 wild type and HPLox cell lines collected from day 1 through day 7 were transferred into a 2- ml reaction tube (Eppendorf). After addition of one drop of 10% (v/v) Triton X-100 (Roth), cells were stained for 2 min with the fluorescent dye Hoechst 22358 (Sigma-Aldrich, Neu-Ulm, Germany) at a final concentration of 1 $\mu g \cdot ml^{-1}$. The frequency of cells in mitosis was scored under the AxioImager Z.1 microscope (Zeiss, Jena, Germany), using a 20x objective (Plan-Apochromat 20x/0.75) and DAPI filter. Results represent mean values obtained from at least three independent experimental series with 500 cells per individual data point.

To quantify cell width and cell length, aliquots of 500 µl were collected on a daily base from day 1 to day 7 after subcultivation and viewed under AxioImager Z.1 microscope (Zeiss, Jena, Germany) equipped with an ApoTome microscope slider in differential interference contrast (DIC) using a 20x objective (Plan-Apochromat 20x/0.75). To ensure unbiased sampling, the MosaiX module of the imaging software (Zeiss) was used. Images were processed and analysed using the AxioVision software. Cell length and width were measured from the image of the central section of the cells using the length measurement function of the AxioVision software according to Maisch and Nick (2007). Each data point represents mean and standard error from at least 1500 individual cells obtained from three independent experimental series. The results were tested for significance using Student's *t*-test at 95 % and 99% confidence level.

2.6 Verification of the expression of the HPL1-GFP fusion

The overexpression of the VvHPL1-GFP fusion was verified on two levels. First, the expression level and correct size of the VvHPL1-domain was tested for the transcript by RT-PCR as described above. Second, the presence of fusion proteins in the correct size was verified by Western Blot using monoclonal antibodies against the GFP reporter. Cells from the non-transformed tobacco BY-2 wild type (WT) and HPL overexpressing (HPLox) cells were collected at day 3 after subcultivation, at the peak of proliferation activity. Extracts of soluble and microsomal proteins were obtained according to Jovanovic *et al.,* 2010. After removing the medium by centrifugation for 10 minutes at 4°C with 13000 g (Heraeus Pico 17 Centrifuge, 600 Thermo Scientific, Langenselbold, Germany), cells were homogenized according to Nick *et al.,* (1995), with some modifications, in the same volume of extraction buffer containing 25 mM morpholine ethanesulfonic acid, 5 mM EGTA, 5 mM $MgCl_2$, pH 6.9, supplemented with 1 mM dithiothreitol (DTT), and 1 mM phenylmethylsulphonyl fluoride (PMSF) by using a glass potter with narrow gap for 15 minutes on ice. Cell lysates were first centrifuged at 13000 g for 5 minutes. The supernatant was then ultracentrifuged at 100000 g, 4°C for 15 minutes (rotor TLA 100.2, Beckman, Munich, Germany) to yield a soluble fraction (containing cytosolic proteins), and a microsomal fraction (containing plasma membrane, endomembrane, mitochondrial, and plastidic proteins).

The microsomal and cytosolic fractions were dissolved in sample loading buffer (containing 50 mM Tris/HCl (pH 6.8), 30% glycerol (v/v), 300 mM DTT, 6% SDS, 0.01% bromophenol blue) and denatured at 95°C for 5 min. Samples were then subjected to SDS-PAGE on 10% (w/v) polyacrylamide gels and subsequently probed by Western blotting according to Nick *et al.,* (1995) in parallel with a prestained molecular weight marker (Broad Range 11-245 kDa, New England Biolabs, Frankfurt). The fusion of VvHPL1 was detected by monoclonal mouse antibodies against the GFP reporter (Anti-Green Fluorescent Protein antibody, Sigma-Aldrich, Deisenhofen) in a dilution of 1:1000 in Tris buffered saline Tween (TBST) containing 20 mM Tris/HCl, 300 mM NaCl, 1% Tween, pH 7.4. For signal development, a goat polyclonal anti-mouse IgG conjugated to alkaline

phosphatase (Sigma-Aldrich, Deisenhofen) in a dilution of 1:2500 in TBST was employed. Equal loading was verified by running a replicate gel that was stained with Coomassie Brilliant Blue.

2.7 Recombinant expression of VvHPL1

The coding sequence of the *VvHPL1* cloned from 'Müller-Thurgau' was inserted into the pET-DEST42 Gateway vector (Appendix 5.5) using the Gateway recombinase reaction. The resulting construct encoding the VvHPL1 protein fused with a tag comprising 6 histidine residues was expressed in *E. coli* (ER2566) cells following heat-shock transformation. A single positive colony of freshly transformed bacteria was inoculated into 60 ml of LB liquid medium containing ampicillin (100 $\mu g \cdot ml^{-1}$) and grown at 37°C overnight. The entire volume of the preculture was inoculated into 3 L of LB medium supplemented with 100 $mg \cdot L^{-1}$ of ampicillin and cultivated at 37 °C. When an OD_{600} of 0.8-1.0 had been reached, 500 µM isopropyl-β-D-thiogalactopyranoside (IPTG) were added to induce gene expression. The culture was subsequently incubated at 18°C for 20 h. Cells were harvested by centrifugation at 10000 g for 20 min at 4°C, and proteins were extracted according to Mu *et al.,* (2012) with minor modification The procedure is as follows: The sedimented cells were washed with 50 mM sodium phosphate buffer pH 7.0, spun down again, and subsequently suspended in 20 ml of lysis buffer (50 mM Tris-HCl, 500 mM NaCl, 0.5% Triton X-100, 0.5 mM PMSF pH 8.0), and lysed twice using a French Press at 1000 bar. Cell debris was removed by centrifugation (15000 g, 4°C for 30 min), and the supernatant fraction containing the soluble recombinant VvHPL1 was applied onto Ni-NTA agarose, previously equilibrated with binding buffer (50 mM Tris-HCl, 500 mM NaCl and 0.5% Triton X-100 pH 8.0). Unbound proteins were washed out from the column with washing buffer (50 mM sodium phosphate buffer, 500 mM NaCl, 0.5% Triton X-100 and 150 mM imidazole, pH 7.0), and the His-tagged recombinant HPL was eluted with elution buffer (50 mM sodium phosphate buffer, 500 mM NaCl, 0.5% Triton X-100 and 500 mM imidazole, pH 7.0). The eluted fractions were concentrated and desalted by Amicon Ultra 15-ml centrifugal filters (Merck Millipore, Darmstadt, Germany) with an exclusion size of 30 kDa, and stored in 50 mM sodium phosphate buffer pH 7.0, at 4°C. The

concentrated eluates were then separated by SDS-PAGE on 10% acrylamide gels and the size of the fusion protein was verified by Western Blot using a monoclonal mouse anti-histidine antibody 1:2000 (Penta.His Antibody, BSA-free, Qiagen) diluted in Tris Buffered Saline (TBS), based on the prestained molecular weight marker (Broad Range 11-245 kDa, New England Biolabs, Frankfurt). Protein concentration was determined using the amidoblack assay (Popov *et al.,* 1975) and quantified against a calibration curve of bovine serum albumin.

2.8 Identification of HPL products:

2.8.1 Identification of HPL products by SPME analysis

Solid Phase Microextraction (SPME) was employed to find out the product of HPL. For SPME, approximate 20 µg of purified recombinant VvHPL1 were mixed with 2 ml of 50 mM sodium phosphate buffer, pH 7, containing 40 µM of either 9-HPOD/T or 13-HPOD/T (Larodan, Sweden) in SPME vials, and analysed by SPME-GC-MS carried out on an Agilent 6890 gas chromatograph equipped with a Gerstel MP2 autosampler and an Agilent 5973N mass spectrometer for peak detection and compound identification. The autosampler was operated in SPME mode with a fitted polydimethylsiloxanefibre (1 cm, 23-gauge, 100 µm PDMS, Supelco, Bellefonte, PA) for extraction. The sample was incubated for 10 min at 40°C, and the volatile compounds were extracted under agitation (250 rpm) at 40°C for 10 min. The GC was fitted with a DB-Wax column (30 m× 0.32 mm in diameter, 0.5 µm film thickness). Helium was used as carrier gas with a column flow rate of 1.5 $ml \cdot min^{-1}$. Volatiles were desorbed from the fiber in the GC inlet (220°C) for 6 min and separated using the following temperature program: 40°C for 5 min, increasing at $10°C \cdot min^{-1}$ to 200°C, which was held for further 5 min. The MS transfer line and ion source temperatures were set to 270°C and 230°C, respectively. The MS was operated in EI mode and positive ions at 70 eV were recorded with a scan range from *m*/*z* 30 to *m*/*z* 300.

The identity of detected volatiles was determined by comparing mass spectra with those of authentic standards and spectral libraries. The U.S. National Institute of Standards and Technology (NIST-05a) and the Wiley Registry 7^{th} edition mass

spectral libraries were used for identification. Compounds were considered to be positively identified after matching of both mass spectra and linear retention indices (LRI) with that of authentic samples. LRI was calculated from a compound retention time relative to the retention of a series of n-alkanes (C_8-C_{28}).

2.8.2 Identification of HPL products by SBSE analysis

For analysis by Stir Bar Sorptive Extraction (SBSE), a stir bar (0.5 mm film thickness, 10 mm length, Gerstel GmbH, Mülheim an der Ruhr, Germany) coated with PDMS was used. The stir bar was placed in a 20- ml glass headspace vial along with the reaction medium (2 ml containing 20 µg of purified recombinant VvHPL1 mixed with 2 ml of 50 mM sodium phosphate buffer, pH 7, and 40 µM of either 9-HPOD/T or 13-HPOD/T) and 2 ml of a concentrated NaCl solution (5 M). SBSE was performed at ambient temperature for 2 h whilst stirring at 260 rpm. After extraction, the stir bar was removed with magnetic tweezers, washed with MilliQ water, gently dried with a lint-free tissue and then transferred into a glass thermal desorption tube for GC-MS analysis. The system consisted of a Gerstel TDU thermodesorption system (Gerstel GmbH, Mülheim an der Ruhr, Germany), mounted on an Agilent 7890B gas chromatograph system coupled to a quadrupole Agilent 5977B electron ionisation (70 eV) mass spectrometer (Agilent Technologies, Palo Alto, CA, USA).

The glass thermal desorption tube was introduced into the thermodesorption unit, where the stir bar was heated to release and transfer the volatiles into a Gerstel programmed temperature vaporization (PTV) inlet (CIS-4) via a baffled glass liner (Gerstel GmbH, Mülheiman an der Ruhr, Germany). The thermal desorption was carried out with a temperature program from 30°C held for 1 min, ramped at 60°C·min^{-1} to 250 °C and held for further 6 min with a helium flow rate of 70 ml·min^{-1}. The CIS injector was held at -20°C for the total desorption time and then ramped at 10°C·s^{-1} in the splitless mode to 300°C, and then held for additional 5 min to transfer the trapped volatiles onto the analytical column. The TDU was operated in the solvent vent mode, whereas the CIS-4 was operated in splitless mode.

The GC was fitted with an HP-5MS capillary column (30 m × 0.25 mm in diameter, 0.25 µm film thickness, Agilent Technologies). Helium was used as carrier gas with a column flow rate of 1 ml·min^{-1}. The MS transfer line and ion source temperatures were set at 270°C and 230°C, respectively. The MS was operated in EI mode and positive ions at 70 eV were recorded with a scan range from *m*/*z* 30 to *m*/*z* 450. The GC oven temperature was programmed as follows: 40°C for 10 min, ramped at 4°C·min^{-1} to 300°C, and held for further 10 min.

Detected volatiles were identified by comparing mass spectra with those of authentic standards and spectral libraries. The NIST-14 mass spectral libraries were used for identification. Compounds were considered to be positively identified after matching of both mass spectra and linear retention indices (LRI) with that of authentic samples. LRI was calculated from a compound retention time relative to the retention of a series of n-alkanes (C_8-C_{28}).

2.9 Quantification of JA-Ile content

For hormonal analysis, non-transformed BY-2 wild type as well as HPLox cells were harvested after treatment with 27 µg· ml^{-1} harpin for either 30 min or 3 h, respectively, or with equal volume of water as solvent control. The culture medium was removed by vacuum by using a Büchner funnel, fresh weight was determined, and the drained cells were frozen in liquid nitrogen. Contents of the isoleucine conjugate of jasmonic acid (JA-Ile), were quantified using a standardized ultraperformance liquid chromatography – tandem mass spectrometry (UPLC-MS/MS)-based method and [$^2H_2$] JA-Ile as internal standard according to (Balcke *et al.,* 2012). Values represent mean and standard errors from six independent biological repeats.

2.10 Effect of C_6-volatiles on plant cells

The cellular effect of VvHPL1 products were examined in cell cultures expressing a fluorescent actin marker (fimbrin actin-binding domain 2 in fusion with GFP, Sano *et al.,* 2005). Both cis-3-hexenal (50% purified in triacetine, Sigma-Aldrich), and trans-2-hexenal (98% purified, Sigma-Aldrich) were tested for their putative role in

signalling and defence responses. Cells were collected at day 3 after subcultivation on 0.8% MS-agar, and 1 µL of cis-3-hexenal, trans-2-hexenal, or the solvent control (Triacetin) were placed on 10 mm sterile filter paper discs in the centre of the MS-agar plate and incubated for 10 minutes. After incubation, cells were transferred to MS-medium. Cells were then observed by spinning-disc microscopy as described above.

2.11 Effect of mechanical wounding on *VvHPL1* transcripts

The detached forth leaf from the shoot apex of *Vitis vinifera* cv. 'Müller-Thurgau' plants from the greenhouse of the Botanical Garden of the Karlsruhe Institute of Technology were wounded 20 times using a 5mm cork borer to simulate herbivore damage. Leaves were frozen after 2, 4 and 6 hours treatment along with the non-wounded control in liquid nitrogen and kept in a -80 °C freezer till RNA extraction. The transcript level of the *VvHPL1* in response to mechanical wounding in grapevine leaf was determined by quantitative RT-PCR. mRNA was extracted from treated leaves using the same approach as described in 2.2 The quality and integrity of RNA was controlled as described above using spectrophotometry. cDNA synthesis was carried out using 1µg total RNA as described above. For detection of the expression levels of HPL specific primers for the *VvHPL1* were designed (see Appendix 5.6). According to Reid *et al.,* (2006) ubiquitin conjugating enzyme (UBC) was selected as internal standards. qPCR analysis was carried out in 20 µl reactions containing 200 nM of each primer, 200 nM of each dNTP, 1X GoTaq colourless buffer, 2.5 mM additional $MgCl_2$, 0.5 U GoTaq polymerase (Promega, Mannheim, Germany), 1x SYBR green I (Invitrogen, Darmstadt,Germany) and 1 µl of a 1:10 cDNA dilution according to (Gutjahr *et al.,* 2008). Three technical replicates were performed for each sample. The relative expression level of *VvHPL1* was calculated with the delta delta C_t method (Livak & Schmittgen, 2001) using the UBC as endogenous control for normalization. The experiment was repeated for three biological replicates and the mean fold change was calculated and plotted along with corresponding standard errors. This protocol was adapted from (Svyatyna et al., 2014).

2.12 Analysis of volatiles emitted from grapevine leaves

Volatile organic compounds emitted form grapevine leaves of *Vitis vinifera* cv. 'Müller-Thurgau' and *Vitis rupestris* were analysed. The healthy third or fourth leaf from the shoot apex was harvested from plants of the Botanical Garden of the Karlsruhe Institute of Technology and placed in SPME vials. From each grapevine plant, five leaves were sampled. VOCs were extracted by SPME and analysed by GC-MS as explained in (2.8.1).

2.13 Propagation of *Plasmopara viticola*

Vitis vinifera cv. 'Müller-Thurgau' is highly susceptible to *Plasmopara viticola*, thus used for propagation in the laboratory. Detached leaves of 'Müller-Thurgau' plants from the greenhouse of the Botanical Garden of the Karlsruhe Institute of Technology were washed with deionized water and used for the pathogen propagation in petri dishes. *Plasmopara viticola* (Berk. & Curtis) Berl. & De Toni was isolated from the field from the host cultivar Gutedel in Pfaffenweiler in Germany and selected into single sporangial strains (Gómez-Zeledón *et al.,* 2013). In this study the single sporangial strain 1137_C20 was used, that infect 'Müller-Thurgau' intensively. Leaves were placed with the abaxial surface on an aqueous suspension of sporangia in a 14 cm petri dish and incubated overnight in the dark while covered with black foil at 16 °C in a Percival plant incubator. The incubator was equipped with full spectrum lamps (Philips Master TL-D Super 80 18W/840, Cool White, Eindhoven). Light intensity was adjusted to 25 $\mu mol \cdot m^{-2} \cdot s^{-1}$ (Williams *et al.,* 2007) during day cycles of 14 hours and 0 $\mu mol \cdot m^{-2} \cdot s^{-1}$ during night cycles of 10 hours, by constant temperature of 16 °C. At the following day the leaf was removed from the suspension and placed with the inoculated abaxial side up on a wet tissue paper in another petri dish. Sporangia appeared after 4-7 days. Successful infection was shown (Figure 2.1) as a dense white sporulation layer containing sporangiophores and many sporangia. Freshly harvested sporangia were used for stomatal targeting experiments.

Figure 2.1 *Vitis vinifera* cv. 'Müller-Thurgau' leaf infected successfully with *P.viticola* (Picture by Sahar Akaberi, June 2016).

To release sporangia, infected 'Müller-Thurgau' leaves were cut into small pieces and immersed in water in a Schott flask and shaken gently. Leaf pieces were removed afterwards. To adjust the solution of sporangia to a concentration of approximately 60.000 cells per ml to ensure optimal germination rate (Kiefer *et al.,* 2002), a hemacytometer (Fuchs-Rosenthal, Thoma, Freiburg) was used. The solution was then incubated at 16°C in a climate chamber in dark for 1.5 - 2 hours to let zoospores emerge. Targeting of zoospores was observed with 100 µL zoospore suspension (6.000 sporangia per leaf disc).

2.14 Effect of volatiles on zoospores targeting behaviour

Vitis rupestris leaves were used to study the stomatal targeting. The forth or fifth leaf from the shoot apex was harvested and washed with water. Leaf discs of 13 mm diameter were prepared and placed in 14 cm petri dishes. Leaf discs were infected with *P. viticola*. Targeting of zoospores to the stomata was followed upon exogenous application of 2 µL β-caryophyllene (≥80% purified, Sigma-Aldrich) or 2 µL farnesene (mixture of isomers, Sigma-Aldrich) along with a water control on a small paper disc. The petri dish was closed and incubated for 20 min at room temperature. Infection was stopped by incubation of the leaf discs in double distilled water. After drying with a tissue paper, leaf discs were placed on object slides for staining of the infected area with a 30 µl droplet of Blankophor (Bayer, Leverkusen, Germany; 0.1% w/v in 10% ethanol). Leaf discs were observed with

a fluorescence microscope (DM750, Leica, Switzerland), equipped with a camera (DFC400, Leica, Switzerland), under UV-light excitation using a DAPI filter set (filterblock A, excitation filter BP 340-380 nm and suppression filter LP 425). For each time point three leaf discs were used. Pictures were taken at 10x magnification and were recorded using the software Leica Application Suite V3.3.1. Numbers of targeted and non-targeted zoospores per treatment were evaluated. This experiment was repeated for at least five biological replicas.

The effects of β-caryophyllene or farnesene on the frequency of targeted zoospores have been tested in the above explained conditions. Numbers of targeted zoospores were evaluated in five categories ranging continuously from one zoospore per stoma up to four zoospores per stoma. Category five includes infected stomata with more than 4 zoospores. The sum of infected stomata was calculated.

3. RESULTS

3.1 HPL1 from *Vitis vinifera* cv. 'Müller-Thurgau' shows all features of a canonical CYP74B

Based on primers bordering the full-length of *VvHPL1* coding sequence, a cDNA of the predicted size (1464 bp) was amplified from *Vitis vinifera* cv. 'Müller-Thurgau' leaves and sequenced. This sequence is predicted to encode a polypeptide of 487 amino acids with a calculated molecular mass of 55 kDa. The predicted protein sequence was aligned with other CYP74 sequences obtained through a BLAST search of the Swissprot database (www.expasy.org) using the ClustalW algorithm and a Neighbor Joining tree was constructed and subjected to a bootstrap test based on 500 replicates (Figure 3.1). The VvMTh-HPL1 protein grouped closely with a protein which has been isolated from the *vinifera* cultivar 'Cabernet Sauvignon' and shown experimentally to be a canonical CYP74B accepting 13-HPOD/T as substrates (Zhu *et al.,* 2012). Also other members of this clade were experimentally confirmed as 13-HPLs (Figure 3.1). We were able to recover numerous sequence homologues from both, monocot and dicot plants by a BLAST search. Further members could be found in gymnosperms, pteridophytes and mosses. However, despite intensive searching and lowering of stringency levels, it was not possible to identify any putative relative from algae. The CYP74 enzymes, thus, seem to be confined to terrestrial plants (including the Bryophytes). The recovered sequences clustered into several clades that were mostly clearly delineated: one clade comprised members, for which AOS activity had either been shown experimentally (Figure 3.1, green circles), or, for which at least the molecular signature qualifying these members as *bona-fide* AOS (Appendix 5.7) was found (Figure 3.1, blue circles). It seems that this clade is confined to the Angiosperms, since sequences from the moss *Physcomitrella* that are registered as AOS neither have been tested experimentally, nor by their molecular signature show features of 9/13-HPLs activity. Also, the CYP74B enzymes grouped into a clearly delineated clade, comprising also the HPL1 from 'Müller-Thurgau' (Figure 3.1, red circle). Again, the members of this clade had been neither experimentally shown to confer 13-HPL activity, nor the presence of this activity could be inferred

from the molecular signature in their active center (Appendix 5.7). In addition to sequences from Angiosperms, two members of the heterosporic fern *Selaginella* could be found in this group.

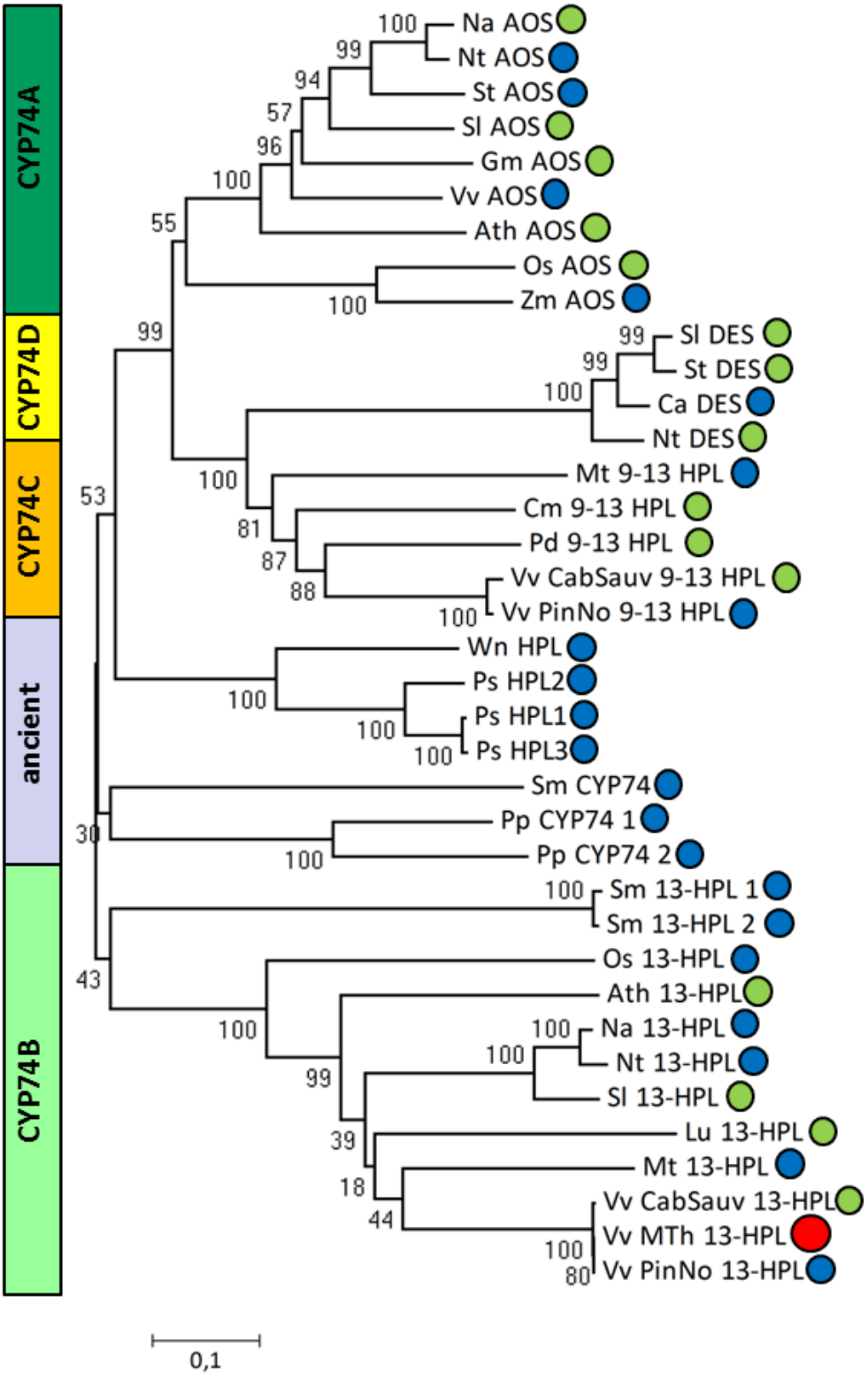

Figure 3.1 Molecular phylogeny constructed by the neighbor-joining algorithm on selected members of the CYP74 family. The position of the HPL sequence from 'Müller-Thurgau' is indicated by a red circle. Green circles indicate proteins, where the respective enzymatic activity has been demonstrated experimentally, blue circles indicate proteins, where the respective enzymatic activity has been inferred from the presence of the respective specificity signatures in the sequence. Values next to the branches represent the percentage of replicate trees in which the associated taxa clustered together in the bootstrap test (based on 500 replicates). The Swissprot accessions of the shown sequences are: CYP74A (AOS): *Na* AOS *Nicotiana attenuata* Q8W4X8 (Ziegler *et al.,* 2001); *Nt* AOS *Nicotiana tabacum* L8B431; *St* AOS *Solanum tuberosum* Q8H1X6 (Farmaki *et al.,* 2006); *Sl* AOS *Solanum lycopersicum* Q9M464, *Gm* AOS *Glycine max* A0MAV6 (Wu *et al.,* 2008); *Vv* AOS *Vitis vinifera* F6H025, *At* AOS *Arabidopsis thaliana* Q96242 (Lee *et al.,* 2008); *Os* AOS *Oryza sativa* Q7XYS3 (HA *et al.,* 2002); *Zm* AOS *Zea mays* Q6RW10. CYP74B (13-HPL): *Sm* 13-HPL 1 *Selaginella moellendorffi* D8RA26, *Sm* 13-HPL 2 *Selaginella moellendorffi* D8QZ31, *Os* 13-HPL *Oryza sativa* Q7X9C2, *At*13-HPL *Arabidopsis thaliana* Q9ZSY9 (Bate *et al.,* 1998); *Na* 13-HPL *Nicotiana attenuata* Q93YF8, *Nt* 13-HPL *Nicotiana tabacum* Q45KF8, *Sl* 13-HPL *Solanum lycopersicum* Q9ARH8 (Matsui *et al.,* 2000); *Lu* 13-HPL *Linum usitatissimum* E3VWA8 (Gogolev *et al.,* 2012); *Mt* 13-HPL *Medicago truncatulata* Q4ZGM9, VvCabSauv 13-HPL *Vitis vinifera* cv. 'Cabernet Sauvignon' HPL1 E5FXI7 (Zhu *et al.,* 2012); Vv MTh 13-HPL *Vitis vinifera* cv. 'Müller-Thurgau' this work; KX379687. VvPinNo 13-HPL. Ancient HPL: *Wn HPL Wollemia nobilis* A0A0C9QM15, no plastid localisation sequence; *Ps* HPL1 *Picea sitchensis* A9NX03, no plastid localisation sequence; *Ps* HPL2 *Picea sitchensis* B8LKD1, no plastid localisation sequence; *Ps* HPL3 *Picea sitchensis* B8LK69, no plastid localisation sequence; *Sm* CYP74 *Selaginella moellendorfii* D8T6U4, plastid localisation sequence verified; *Pp* CYP74 1 *Physcomitrella patens* A9SNA2, plastid localisation sequence verified; *Pp* CYP74 1 *Physcomitrella patens* A9S014, plastid localisation sequence verified. CYP74C (9/13- HPL): *Mt* 9/13-HPL *Medicago truncatulata* Q7X9B3, *Cm* 9/13-HPL *Cucumis melo* Q93XR3 (Tijet *et al.,* 2001); *Pd* 9/13-HPL *Prunus dulcis* Q7XB42 (Mita *et al.,* 2005); *VvCabSauv* 9/13-HPL *Vitis vinifera* cv. 'Cabernet Sauvignon' HPL 2 E5FXI8 (Zhu *et al.,* 2012); *VvPinNo* 9/13-HPL *Vitis vinifera* cv. 'Pinot Noir' F6HQI4. CYP74D (DES): *Sl* DES *Solanum lycopersicum* Q9FPM6 (Itoh & Howe, 2001); *St* DES *Solanum tuberosum* Q9AVQ1 (Stumpe *et al.,* 2001); *Ca* DES *Capsicum annuum* Q0PHS9, Nt DES *Nicotiana tabacum* Q8W2N5 (Fammartino *et al.,* 2007).

Furthermore, the still limited number of DES sequences formed a well-defined cluster. The enzymatic activity of these proteins had mostly been already experimentally shown, for one member, the *bona-fide* DES from *Capsicum annuum*, a specific phenylalanine in the ERR-domain (Appendix 5.7), which is crucial to delineate DES from 9/13-HPLs activity (Toporkova *et al.,* 2013) predicts a DES activity for this member as well.

Neighbouring to the DES clade, there a similarly well delineated clade can be inferred that harbours 9/13-HPLs. Again, this activity has been either already validated experimentally or it is at least predicted, for instance by a specific WV dyade in the substrate binding I-loop that has been shown to switch from DES to 9/13-HPLs activity (Hughes *et al.,* 2009). Also, the other HPL member known from *Vitis vinifera*, VvHPL2, belongs to this group (Zhu *et al.,* 2012).

In addition to the four well delineated CYP74 clades found in the Angiosperms, the recovered homologues from mosses, ferns, or the living fossile gymnosperm *Wollemia nobilis* formed lineages that stood at the basal of the tree and were not clustering with any of the four clades. The enyzmatic activity has not been tested for any of these sequences, and it was also not possible to infer their activity from the above-mentioned molecular signatures in the active center because they deviated from the patterns seen in the Angiosperm. This group was also not forming a clear cluster but was intermediate between the CYP74B and the CYP74C clade, whereby for the moss *Physcomitrella patens* and the heterosporic fern *Selaginella moellendorffii* several members are found that partially are closer to the CYP74B, whereas other members of the same species are closer to CYP74C. As mentioned above, the classification of some members of this basal CYP74 group as AOS is to be questioned, since these proteins have not been tested for their enzymatic activity, and lack the molecular signatures that would qualify them as *bona-fide* AOS.

Moreover, the VvMTh-HPL1 sequence displays all molecular features characteristic of a canonical CYP74B (Figure 3.2): (i) a putative N-terminal plastid transit peptide comprising amino-acid residues 1 to 31 as predicted by two algorithms, targetP (www.cbs.dtu.dk/services/TargetP/), and ChloroP (www.cbs.dtu.dk/services/ChloroP/), (ii) a cysteine triade signature relevant for heme binding at positions 111, 142, and 146, (iii) a substrate-binding I-loop correspond to the oxygen-binding domain in other cytochrome P_{450} proteins, (iv) the ERR triade domain characteristic for the CYP74 family, known to modulate substrate specificity, and (v) a highly conserved iron-binding cysteine at residue 438. The different subclades of the CYP74 family carry specific molecular features related to substrate specificity (Appendix 5.7).

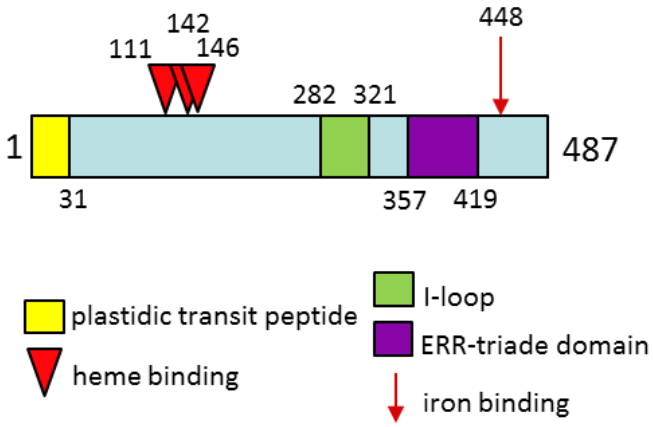

Figure 3.2 Molecular features of the HPL isolated from *Vitis vinifera* cv. 'Müller-Thurgau' according to (Toporkova *et al.,* 2013). Substrate binding is located in the I-loop (corresponding to the oxygen-binding domain in other cytochrome P_{450} proteins), the ERR triade domain is characteristic for the CYP74 family and modulates substrate specificity. A full alignment of the HPL isolated from *Vitis vinifera* cv. 'Müller-Thurgau' along with representative of the different CYP74 subclades and the subclade-specific signatures is given in Appendix 5.6.

Based on these features, the VvMTh-HPL1 clearly qualifies as a canonical member of the CYP74B clade, confirming the position in the phylogenetic tree. Specifically, the VvMTh-HPL1 harbours a leucine in position 115 in contrast to the grapevine AOS which carries a phenylalanine at this position. The mutation of this crucial leucine to phenyalanine has been shown to convert HPL activity into an AOS activity (Lee *et al.,* 2008). Likewise, the second feature of this HPL signature, an alanine in position 133 (contrasting with a serine in AOS) is present as well, showing that VvMTh-HPL1 displays the molecular signature for a 13-HPL (Lee *et al.,* 2008).

3.1.1 Grapevine HPL showed plastid localisation

To verify the subcellular localisation of the *Vv*HPL1, N- or C-terminal fusions of VvHPL1 with green fluorescent protein (GFP) were expressed under the control of the cauliflower mosaic virus *35S* promoter in tobacco BY-2 cells (Figure 3.3). The C-terminal fusion appeared in small ovoid organelles (Figure 3.3.B). Co-expression with the N-terminal fragment of ferredoxin NADPH oxidoreductase including the transit peptide, tpFNR-mEosFP, a stroma marker (Schattat *et al.,* 2012), identified the VvHPL1 containing organelles as proplastids (Figure 3.4). When GFP was fused to the N-terminus of HPL1, such that the reporter masked the transit peptide, the pattern was different: GFP was visible in long filaments that by their morphology and localisation in cytoplasmic strands were identified as transvacuolar ER tubules (Figure 3.3 A).

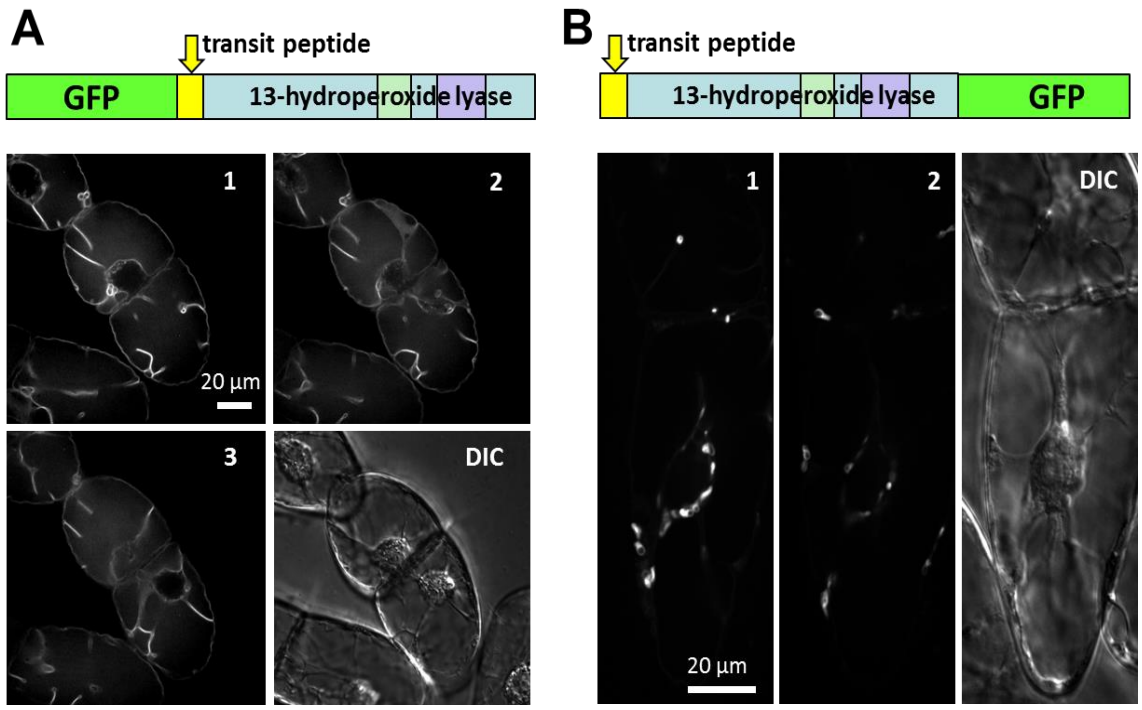

Figure 3.3 Localisation of the HPL isolated from *Vitis vinifera* cv. 'Müller-Thurgau'. **A** Stable expression of GFP fused N-terminally of HPL in tobacco BY-2. Three representative confocal sections from a z-stack along with a differential-interference contrast (DIC) image of the same cell are shown. **B** Stable expression of GFP fused C-terminal of HPL in tobacco BY-2. Two representative confocal sections from a z-stack along with a differential-interference contrast (DIC) image of the same cell are shown.

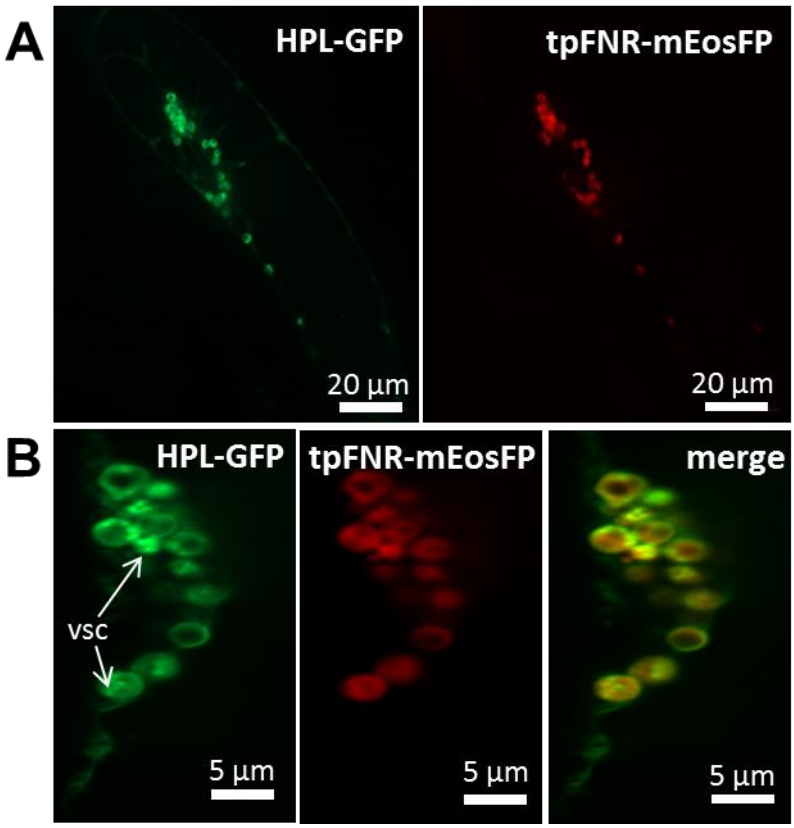

Figure 3.4 Localisation of the HPL isolated from *Vitis vinifera* cv. 'Müller-Thurgau' Duplex visualisation of GFP fused C-terminal of HPL and the stroma marker tpFNR-mEosFP shown as overview **A**, and as zoom-in of the nuclear region **B**, respectively. White arrows in **B** indicate vesicular structures (vsc) in the proplastid interior, where the HPL-GFP signal accumulates.

3.1.2 Recombinant VvHPL1 prefers 13-hydroperoxy-fatty acids as substrate

To characterise the substrate specificity, the full-length coding sequence of *HPL1* isolated from *Vitis vinifera* cv. 'Müller-Thurgau' was cloned into the pET-DEST42 vector for recombinant expression in fusion with a 6x histidine tag at the C-terminus of the protein. The destination vector was expressed in *E.coli* cells and induced with 500 µM IPTG at 18°C. The recombinant VvHPL1 protein purified using Ni-NTA agarose was soluble and showed the predicted molecular weight of 59 kDa. The purified recombinant VvHPL1 was confronted with all four potential hydroperoxy-fatty acid substrates (13-HPOD, 13-HPOT, 9-HPOD and 9-HPOT), and the respective reactions were analysed with two extraction methods, SPME and SBSE, coupled with GC-MS.

Table 3.1 Survey about substrate preference of recombinant VvHPL1 tested with different fatty acid hydroperoxides and identified products.

Substrate	Products							
	n-hexanal	trans-2-hexenal	cis-3-hexenal	trans-2-hexenol	cis-3-hexenol	nonanal	2-nonenal	(*Z*,*Z*)-3,6-nonadienal
13-HPOT	-	+	+	-	-	-	-	-
13-HPOD	+	-	-	-	-	-	-	-
9-HPOD	-	-	-	-	-	-	-	-
9-HPOT	-	-	-	-	-	-	-	-

The results (Table 3.1) show that recombinant VvHPL1 was able to catalyse the cleavage of either 13-HPOD or 13-HPOT into C_6-volatiles. In contrast, the recombinant VvHPL1 showed no activity towards 9-HPOD or 9-HPOT. The major product from 13-HPOD was hexanal (Figure 3.5), while 13-HPOT as substrate yielded cis-3-hexenal and trans-2-hexenal (Figure 3.6). These compounds were verified by comparing mass spectra with those of authentic standards and spectral libraries. We could not produce any C_9-volatiles such as nonanal, 2-nonenal or (z,z)-3,6-nonadienal, neither with 9-HPOD, nor with 9-HPOT. Moreover, none volatile compounds were detected in control samples using substrates and sodium phosphate buffer in the absence of recombinant protein. Based on these results, the *HPL1* gene isolated from *Vitis vinifera* cv. 'Müller-Thurgau' is concluded to encode a functional 13-HPL, which is able to catalyse the cleavage of 13-hydroperoxy-fatty acids into C_6-aldehydes and therefore can also functionally be categorized as a member of the CYP74B subfamily.

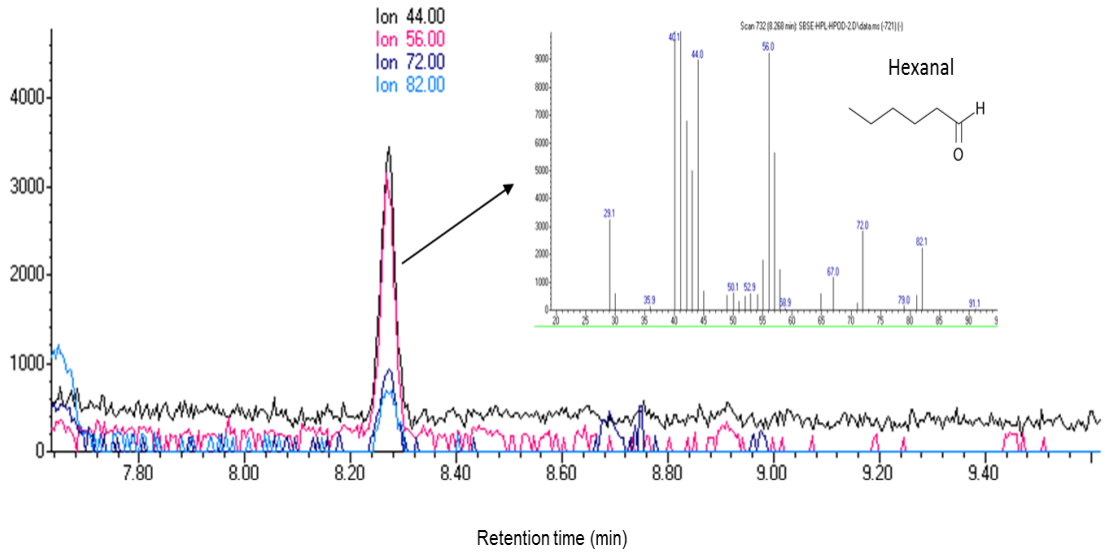

Figure 3.5 VvHPL1 substrate specificity assay performed with the recombinant enzyme. Extracted ion chromatograms and spectra of hexanal showed that the recombinant VvHPL1 catalyse the cleavage of 13-HPOD into hexanal.

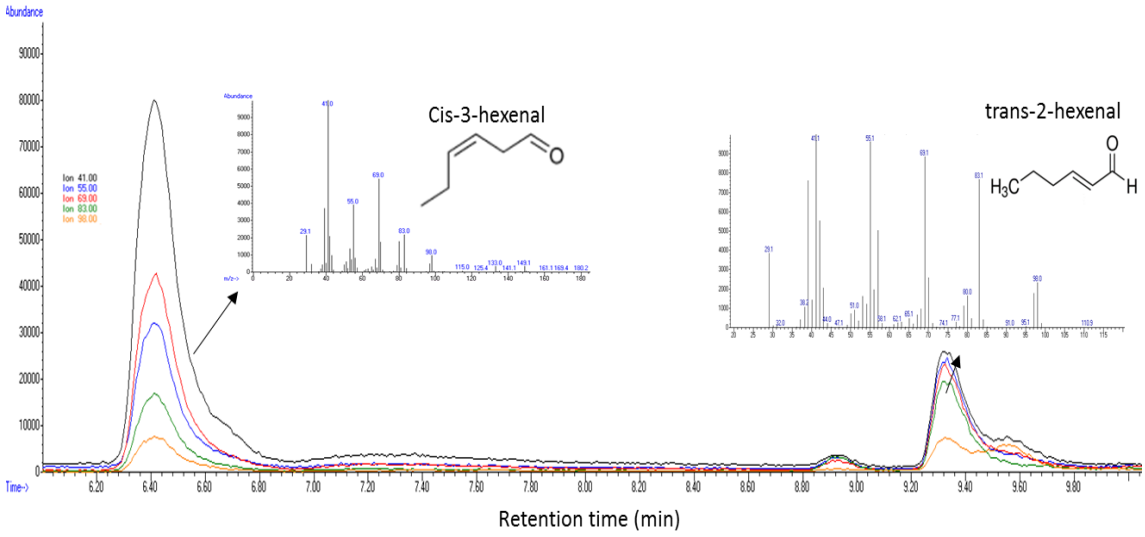

Figure 3.6 VvHPL1 substrate specificity assay performed with the recombinant enzyme. Extracted ion chromatograms and spectra of cis-3-hexenal and trans-2-hexenal showed that the recombinant VvHPL1 catalyse the cleavage of 13-HPOT into cis-3-hexenal and trans-2-hexenal.

3.2 Overexpression of the HPL1-GFP fusion caused no phenotypic effect

Since the C-terminal fusion of GFP to HPL1 was found to preserve a correct subcellular localisation, it was asked further, whether overexpression of this apparently functional fusion could cause any phenotypic effects. However, when the phenotype of the HLP1ox line was followed through a cultivation cycle under normal conditions, we could not detect any deviation from the non-transformed wild type, neither with respect to viability (which was invariably high and close to 100%, Figure 3.7 A), nor with respect to the amplitude, nor the temporal pattern of the mitotic index (Figure 3.7 B). Even subtle details of physiology, such as cell elongation were preserved in the overexpressor line (Figure 3.8).

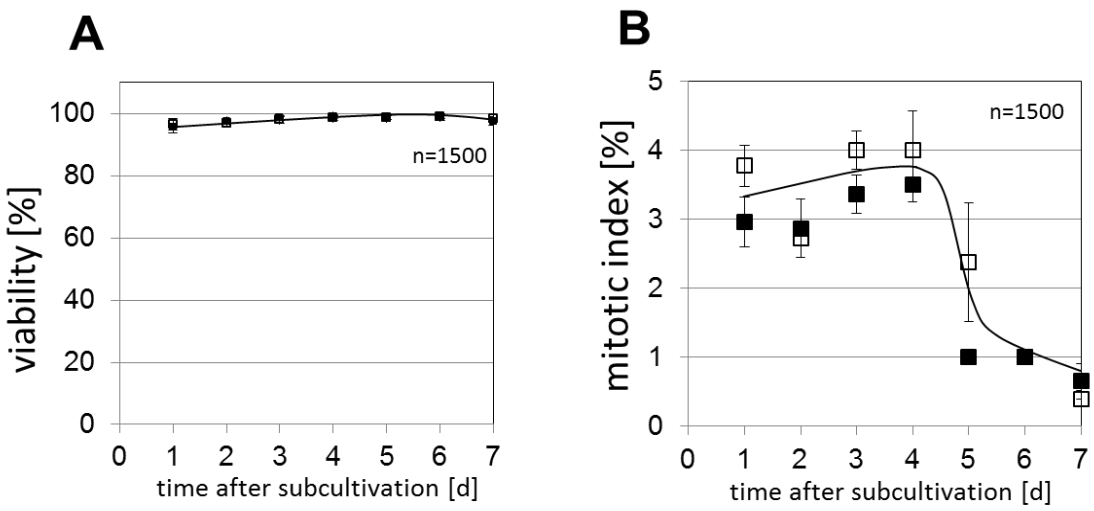

Figure 3.7 Physiological parameters of the HPL1-GFP overexpressor (black) compared to non-transformed BY-2 (white): viability (**A**), and mitotic index (**B**) over the cultivation cycle. Values represent mean and standard errors from a population of 1500 cells per measurement.

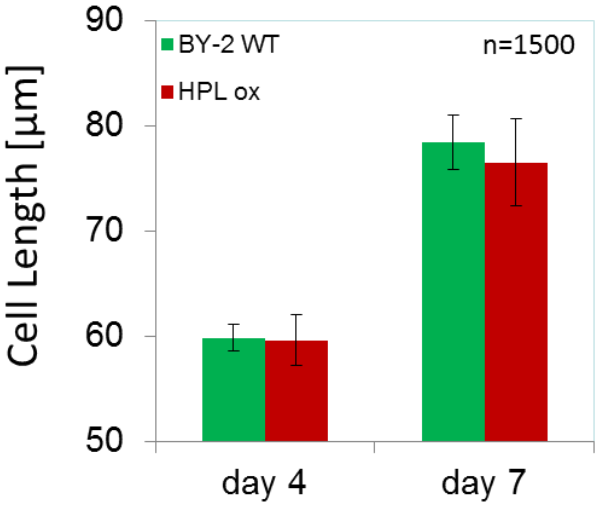

Figure 3.8 Physiological parameters of the HPL1-GFP overexpressor (red bar) compared to non-transformed BY-2 (green bar): cell length at the end of proliferation phase (day 4) and the end of expansion phase (day 7). Values represent mean and standard errors from a population of 1500 cells per measurement.

Therefore it was verified, to what extent the transgene was overexpressed. However, when the presence of the foreign transcripts was probed, high-steady state levels for the VvHPL1 transcript were found in all of the probed transgenic lines. This transcript was of the predicted size, whereas it was completely absent from the non-transformed controls (Figure 3.9).

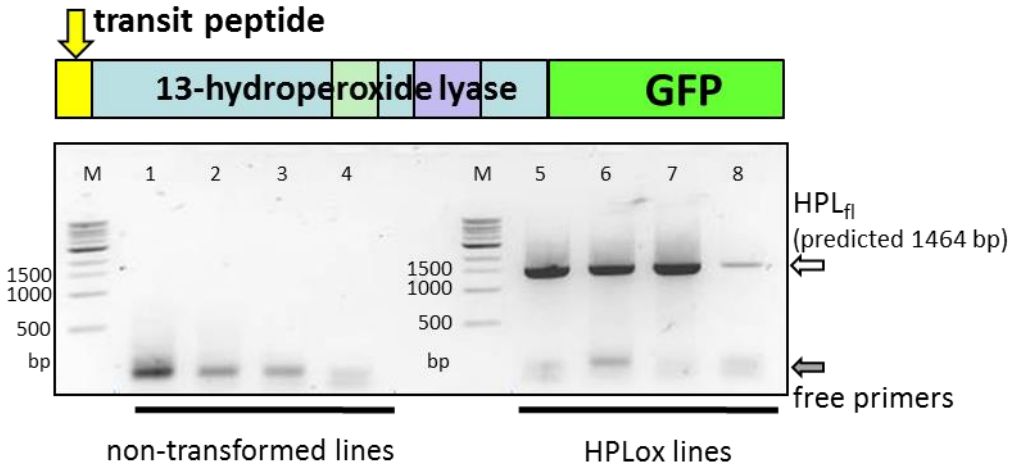

Figure 3.9 High-steady state levels of the *VvHPL1* transcript. Steady-state levels of the *HPL1* transcript in four samples from non-transformed BY-2 (left) and in four samples from tobacco BY-2 overexpressing the *HPL1* isolated from *Vitis vinifera* cv. 'Müller-Thurgau' in fusion with GFP at the C-terminus (right) under physiological conditions probed by RT-PCR with primers spanning full-length *HPL1* predicted to produce an amplificate of 1464 bp in length. White arrow: putative full-length *HPL1* transcript, grey arrow: free primer pairs.

Moreover, the presence of the HPL1-GFP fusion protein in the microsomal fraction of the transformed cells was also confirmed by using a monoclonal anti-GFP antibody (Figure 3.10). The fusion protein was of the predicted size and was not detected in extracts from non-transformed cells. Thus, although HPL1-GFP is properly expressed, accumulates to well detectable levels, and is correctly localised in the plastidic stroma, no phenotypic effect under normal conditions has been observed, indicating that the enzyme is not active, possibly due to a lack of substrate.

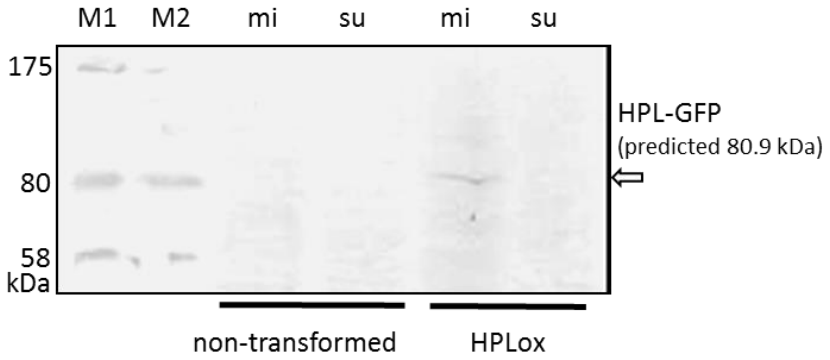

Figure 3.10 Immunodetection of VvHPL1 in tobacco lines overexpressing HPL1 isolated from *Vitis vinifera* cv. 'Müller-Thurgau' in fusion with GFP at the C-terminus. The putative HPL1-GFP fusion protein is exclusively detected by Western Blotting (using a monoclonal antibody against the GFP tag) in microsomal (mi) fractions from cells overexpressing HPL1-GFP, but not in the cytosolic supernatant of the same cells (su), nor in any fraction from non-transformed BY-2 cells. M1 and M2 are two size markers from different commercial products. The size of the predicted HPL1-GFP fusion is 80.9 kDa.

3.3 The function of VvHPL1 / volatiles in stress signalling

3.3.1 The HPL1-GFP overexpressor is more sensitive to salt stress

It was asked therefore, whether a phenotype could be uncovered, when the substrate is provided by activation of lipid peroxidation. In suspension cells, lipid peroxidation can be efficiently triggered by salt stress (Ismail *et al.,* 2012). HPLox and non-transformed wild type BY-2 cells were subcultivated in the presence of 0, 50, 100, or 150 mM NaCl, respectively. Salt-induced mortality of both cell lines was evaluated 24 h after onset of the treatment. Whereas in absence of salt mortality was very low (below 5%) in both lines, it increased progressively with increasing salinity (Figure 3.11). Irrespective of the NaCl concentration, the mortality of the HPLox cells was significantly higher compared with the non-transformed wild type. This increase of mortality (around 15%) was not dependent on the concentration of salt, but remained constant, although the overall mortality increased strongly from 40% for 50 mM NaCl to around 90% for 150 mM NaCl. The effect of HPL1 overexpression on mortality was therefore additive.

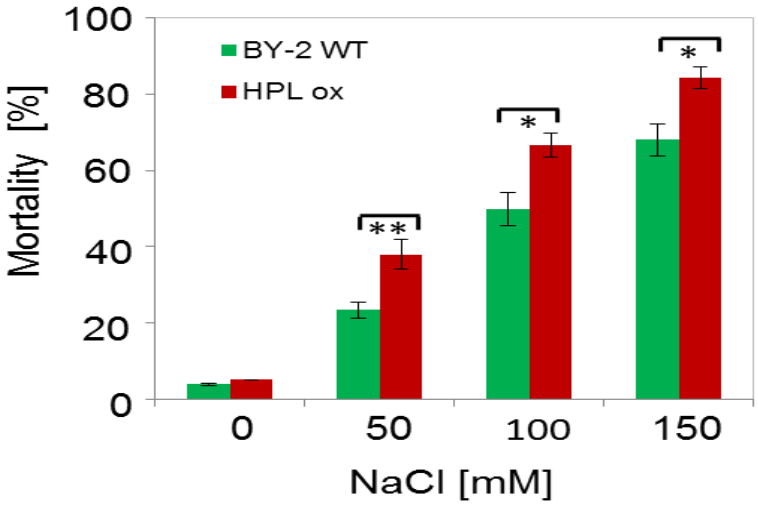

Figure 3.11 Elevated inducibility of signal-dependent cell death in tobacco BY-2 overexpressing the HPL isolated from *Vitis vinifera* cv. 'Müller-Thurgau' in fusion with GFP at the C-terminus under physiological conditions. Mortality after addition of NaCl in the non-transformed BY-2 (green bars) versus the HPL overexpressor (red bars). Mortality was scored after 24 h of treatment. Values represent mean and standard errors from a population of 1500 cells per measurement and at least three independent experimental series. Brackets indicate differences that are significant at $P < 0.05$ (*) or $P < 0.01$ (**), Student's *t*-test.

3.3.2 HPL1 overexpression specifically elevates cell-death related, but not basal defence

Since a phenotype in the HPL1 overexpressor can be induced by activating lipid peroxidation through salinity as abiotic stress, which leads to a further question: whether similar phenomena in the context of defence could be seen. In grapevine cells, basal defence (PTI) can be efficiently triggered by the bacterial PAMP flg22, whereas the bacterial elicitor harpin activates a cell-death related form of defence (Chang & Nick, 2012). The same pattern is also observed in tobacco BY-2 (Guan *et al.,* 2013). Therefore the responses of HPLox and non-transformed wild type to flg22 (10 µM) and harpin (27µg· ml $^{-1}$) were followed. As in the salt-stress experiment, mortality was determined 24 hours later using the Evan's Blue assay (Figure 3.11). While flg22 induced only a slight increase of mortality, the effect of harpin was strong, dose-dependent, and specific for the genotype (Figure 3.12): in the non-transformed wild type, mortality hardly exceeded 10%. In contrast, harpin enhanced cell mortality in a dose-dependent manner, reaching up to 30% after 24 hours for 27 µg· ml $^{-1}$ harpin (Figure 3.13).

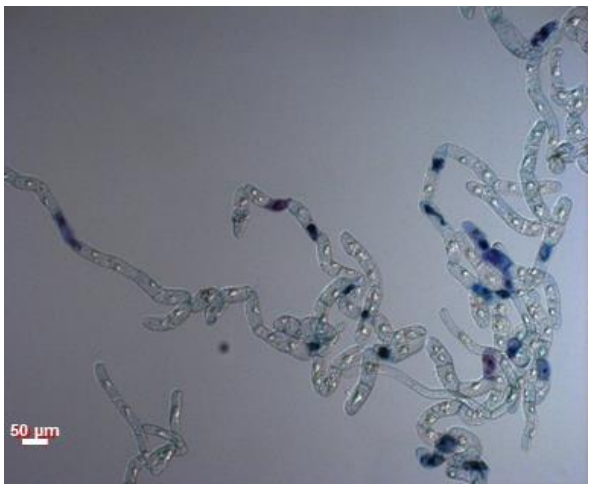

Figure 3.12 Representative image of an Evans Blue assay after treatment of tobacco BY-2 cells overexpressing the HPL isolated from *Vitis vinifera* cv. 'Müller-Thurgau' with 27 µg·ml^{-1} of the bacterial elicitor harpin.

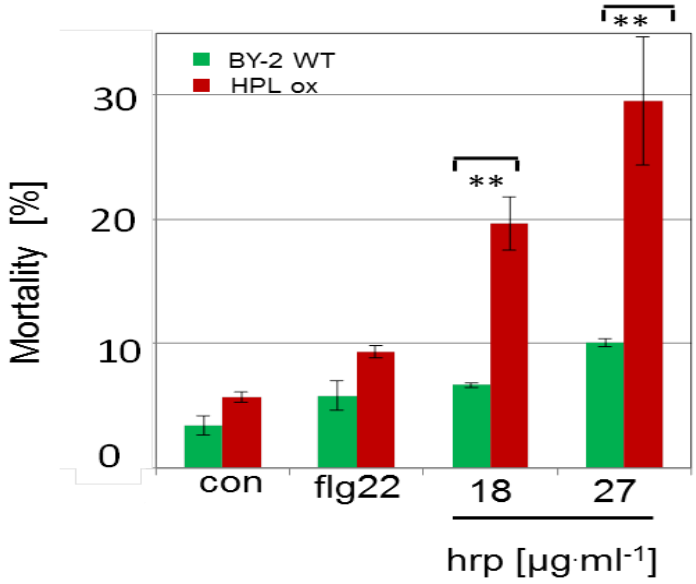

Figure 3.13 Elevated inducibility of signal-dependent cell death in tobacco BY-2 overexpressing the HPL isolated from *Vitis vinifera* cv. 'Müller-Thurgau' in fusion with GFP at the C-terminus. Mortality after addition of the PAMP flg22 (10 µM), compared to 18 µg·ml^{-1} or 27 µg·ml^{-1} of harpin (hrp). Mortality was scored after 24 h of treatment in the non-transformed BY-2 (green bars) versus the HPL overexpressor (red bars). Values represent mean and standard errors from a population of 1500 cells per measurement and at least three independent experimental series. Brackets indicate differences that are significant at P <0.05 (*) or P <0.01 (**), Student's t-test.

Jasmonic acid (JA) is known to activate basal immunity, and it was asked, whether activation of JA signalling can mitigate the harpin-triggered cell-death response observed in the HPLox line. In fact, 100 µM of racemic JA administered prior to harpin treatment was able to prevent the otherwise strong activation of cell death by 27 µg· ml^{-1} harpin (Figure 3.14). In the non-transformed wild type, this JA pretreatment could reduce harpin-induced mortality to even lower levels. Thus, exogenous JA acted antagonistically to the HPL1 overexpression with respect to the harpin response.

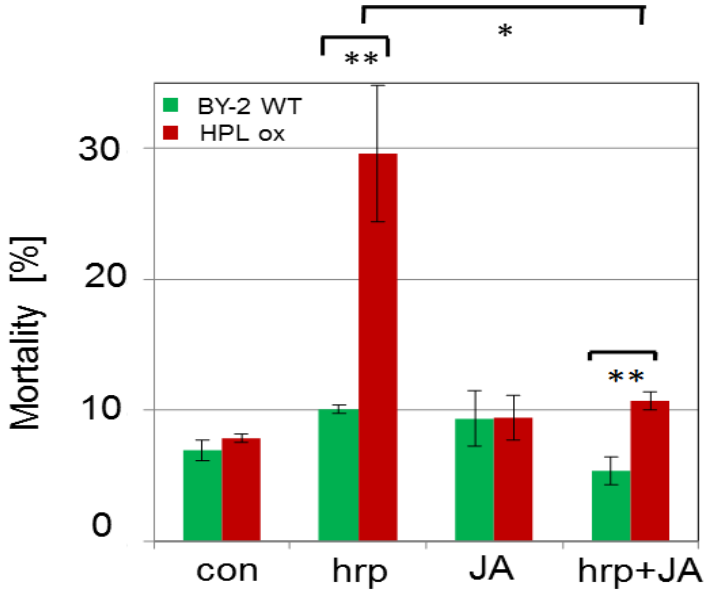

Figure 3.14 Effect of jasmonic acid (JA, 100 µM) on cell death induced by harpin (hrp, 27 µg·ml^{-1}). Mortality was scored after 24 h of treatment in the non-transformed BY-2 (green bars) versus the HPL overexpressor (red bars). Treatment was launched 2 hours after subcultivation. Values represent mean and standard errors from a population of 1500 cells per measurement and at least three independent experimental series. Brackets indicate differences that are significant at P <0.05 (*) or P <0.01 (**), Student's t-test.

The activation of cell-death by harpin treatment is correlated with oxidative burst, which is triggered by the NADPH oxidase located in the plasma membrane. This NADPH oxidase, Respiratory burst oxidase Homolog (RboH) can be inhibited by the specific inhibitor diphenyleneiodonium (DPI) (Chang *et al.,* 2011). In fact, pre-treatment of cell cultures for 30 min with 200 nM DPI could significantly reduce the mortality induced by 27 µg·ml^{-1} harpin (Figure 3.15). It should be noted, however, that this rescue of viability remained partial (contrasting with the effect of JA, where

the rescue was complete). Nevertheless, these data indicate that the NADPH oxidase participates in the mechanism responsible for the HPL1-dependent stimulation of harpin-triggered cell death.

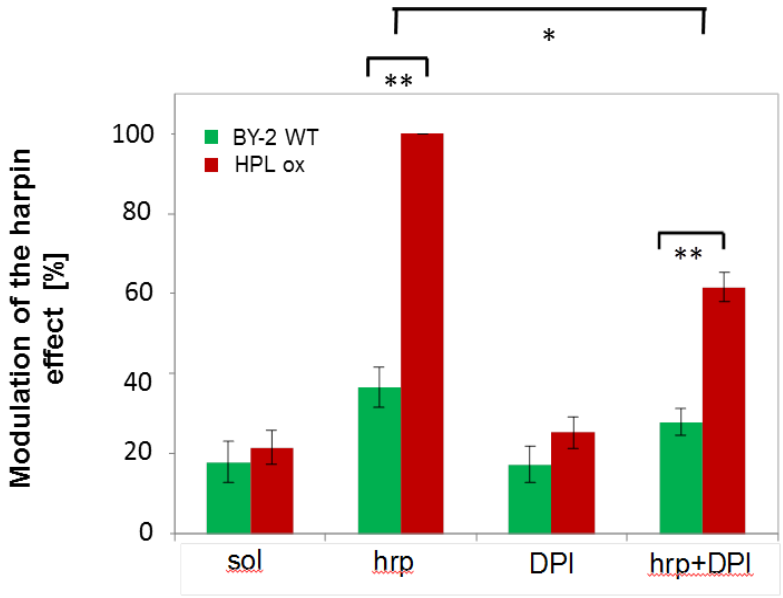

Figure 3.15 Effect of the NADPH oxidase inhibitor Diphenyleneiodonium (DPI, 0,2 µM) on cell death induced by harpin (hrp, 27 µg·ml^{-1}). Mortality was scored after 24 h of treatment in the non-transformed BY-2 (green bars) versus the HPL overexpressor (red bars).Treatment was launched 30 minutes after subcultivation. Values represent mean and standard errors from a population of 1500 cells per measurement and at least three independent experimental series. Brackets indicate differences that are significant at P <0.05 (*) or P<0.01 (**), Student's t-test.

Since activation of JA signalling mitigated harpin-induced cell death in the HPLox line, it was intriguing whether this antagonism should be mirrored in a transient modulation of the bioactive jasmonate conjugate JA-Ile. In fact, a transient reduction of JA-Ile levels by almost 50% at 30 min after treatment with 27 µg·ml^{-1} harpin were observed in the non-transformed wild type (Figure 3.16). This reduction was not stable 3 h after the treatment, the JA-Ile had recovered to its original level. This transient reduction of JA-Ile was not seen in the HPLox line. Here, the initial level (which was equal to that seen in the non-transformed wild type) was maintained (Figure 3.16) indicating that the overexpression of HPL had rendered the jasmonate-synthesis pathway insensitive to harpin-triggered signalling.

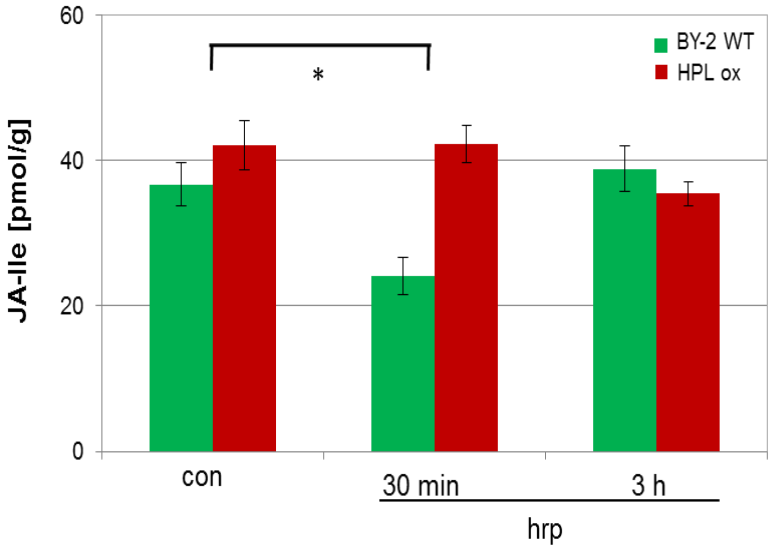

Figure 3.16 Quantification of Jasmonoyl-Isoleucine (JA-Ile) in tobacco BY-2 overexpressing the HPL isolated from *Vitis vinifera* cv. 'Müller-Thurgau' in fusion with GFP at the C-terminus. Effect of harpin (hrp, 27 µg·ml^{-1}) in the non-transformed BY-2 (green bars) versus the HPL overexpressor (red bars) on Jasmonoyl-Isoleucine (JA-Ile) level. The JA-Ile levels were quantified after 30 minutes and 3 hour of treatment along with control samples without harpin. Values represent mean and standard errors per measurement and at least three independent experimental series. Brackets indicate differences that are significant at P <0.05 (*) or P <0.01 (**), Student's t-test.

3.4 Cis-3-hexenal but not trans-2-hexenal evokes a specific actin response on BY-2 cells

The potential cellular effect of the two cognate VvHPL1 products, cis-3-hexenal and trans-2-hexenal were examined in suspension cells. Since cell-death related immunity as elicited by harpin causes a rapid disassembly of the cortical actin filaments subtending the membrane, which is one of the earliest cellular hallmarks of ensuing cell death (Guan *et al.,* 2013). Actin responses to these two C_6-volatiles were investigated along with the appropriate solvent control using a transgenic BY-2 tobacco cell line, where actin was visualised by the second actin-binding domain of plant fimbrin in fusion with GFP (Sano *et al.* 2005). In the solvent control, a rich meshwork of cortical actin filaments was observed by spinning-disc microscopy (Figure 3.17 A). After treatment with trans-2-hexenal, no significant differences in comparison to the solvent control were detected (Figure 3.17 C). In contrast, a

treatment with cis-3-hexenal caused a rapid and strong disintegration of the meshwork which was already fully developed at the earliest time point (10 min after start of the treatment) (Figure 3.17 B). Thus, there is a stereospecific, rapid and drastic response of cortical actin to C_6-volatiles.

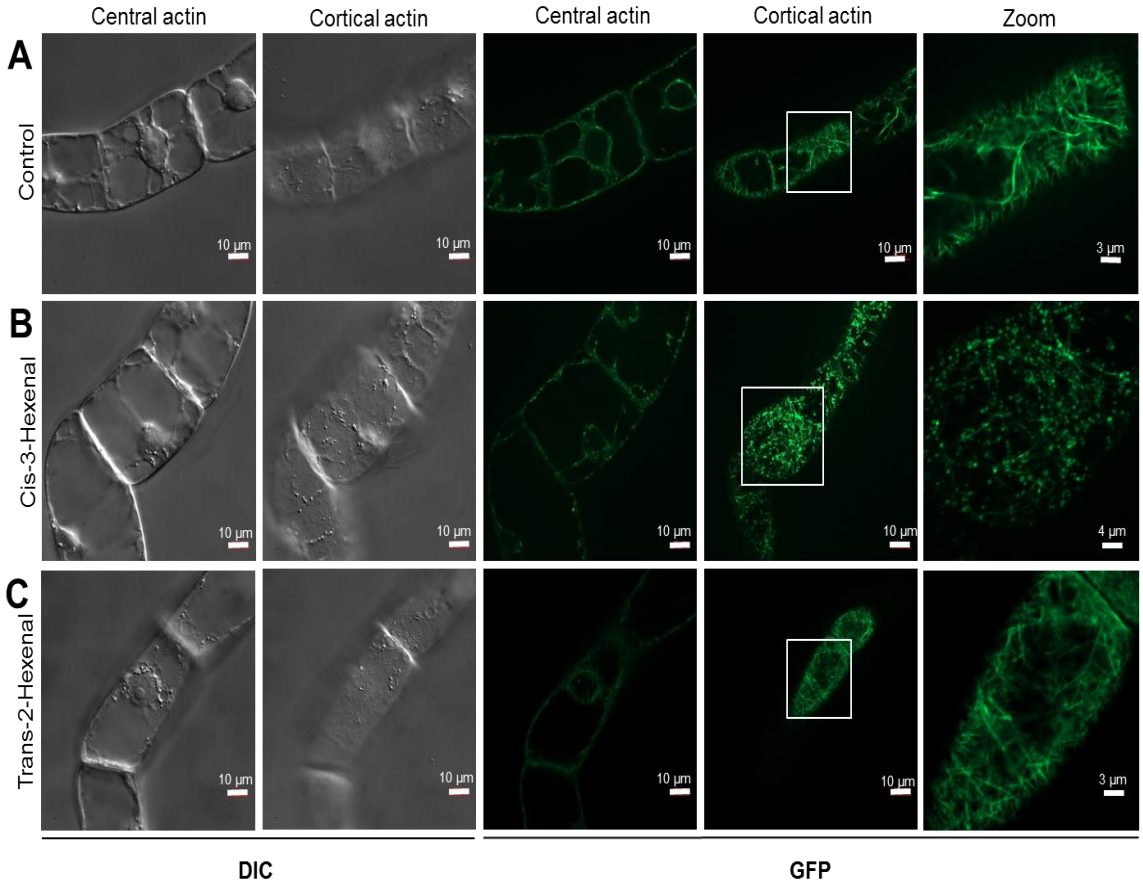

Figure 3.17 Effect of the two VvHPL1 products on transgenic BY-2 tobacco cell line overexpressing actin-binding domain 2 of plant fimbrin in fusion with GFP. **A**, Responses of BY-2 cells to the solvent control (Triacetin). **B**, Treatment with cis-3-hexenal, and **C**, Treatment with trans-2-hexenal. For each treatment, representative confocal sections from a z-stack along with the differential-interference contrast (DIC) image of the same cell, visualisation of GFP fused with actin and zoom-in of cortical actin are shown, respectively.

3.5 Exploring whole plant functions of volatiles

In order to address a potential role of volatiles on the organismic level, the response of HPL to herbivor attack was simulated by wounding experiment.

3.5.1 Mechanical wounding of *Vitis vinifera* cv. Müller-Thurgau leaves induced accumulation of *HPL1* transcripts

In response to mechanical wounding, GLVs are released in plants by the action of HPL. Therefore the transcript level of *VvHPL1* in response to wounding was examed. As shown in (Figure 3.18), mechanical wounding increased the accumulation of *HPL1* transcripts in *Vitis vinifera* cv. 'Müller-Thurgau' leaves. Transcripts increased 2 hours after wounding attaining the maximum levels. Quantitative real-time PCR analysis showed that HPL1 is highly expressed in all wounded samples compared to non-wounded samples, suggesting its possible role in wound induced response in grapevine leaves.

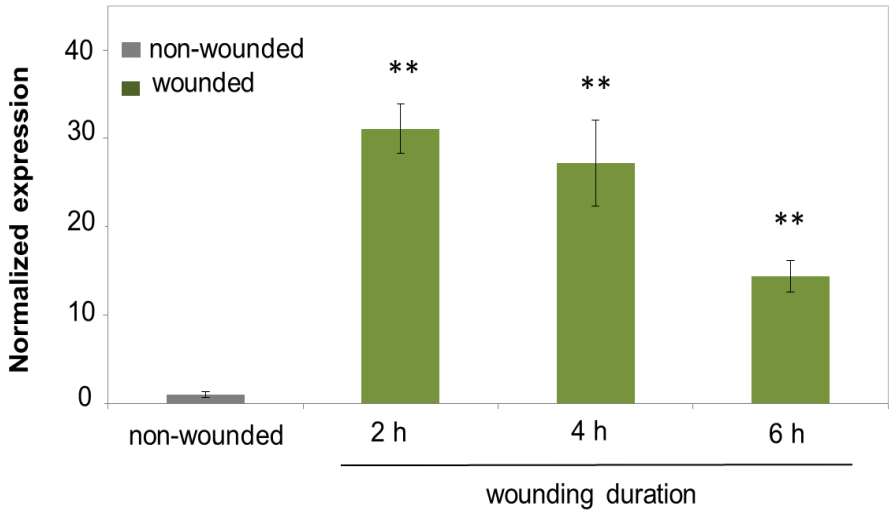

Figure 3.18 Expression of *VvHPL1* in response to mechanical wounding. Quantification of *HPL1* transcripts in *Vitis vinifera* cv. 'Müller-Thurgau' leaf by quantitative real-time PCR normalized to the expression of ubiquitin conjugating enzyme (UBC). Data represent mean values from three independent experimental series, error bars represent standard errors. Brackets indicate differences that are significant at P <0.01 (**), Student's t-test.

3.5.2 Grapevine leaves emit a variety of volatile compounds

To find out volatile candidates that affect zoospore targeting behaviour, leaves of two grapevine species were analysed by SPME-GC-MS. Quantification results of the main volatiles obtained from fresh leaves of *Vitis vinifera* cv. 'Müller-Thurgau' and *Vitis rupestris* are shown in Table 3.2. A total of 12 compounds were identified. The composition of volatiles varied strongly according to the grapevine species (Appendix 5.8). Leaves of *Vitis vinifera* cv. 'Müller-Thurgau' had a larger variety of VOCs compared to *Vitis rupestris.* Monoterpenes, sesquiterpenes and esters were the most volatiles identified. Regarding monoterpenes, ocimene was the major compound detected in both grapevine leaves. Caryophyllene and farnesene were the main sesquiterpenes detected mainly in leaves of *Vitis vinifera* cv. 'Müller-Thurgau' (Table 3.2, highlighted). These two compounds were further studied for their potential roles in zoospores targeting.

Table 3.2 Content of volatiles obtained by SPME-GC-MS analysis in leaves of *Vitis vinifera* cv. 'Müller-Thurgau' and *Vitis rupestris*. Numbers indicate mean values of peak areas obtained from six measurements. 0, indicate compound that has not detected from the samples.

Compounds	*Vitis vinifera* cv. 'Müller-Thurgau'	*Vitis rupestris*
cis-3-hexenyl acetate	12343839	0
cis-3-hexenyl butyrate	7036280	0
Z-3-hexenyl 2-methylbutanoate	520917	0
3-hexenyl hexanoate	220972	0
dimethyl 1-hexadecanamine	559969	0
caryophyllene	65410	22626
N,N-dimethyl 1-hexadecanamine, N,N-dimethyl	155575	0
cis-3-hexenyl propanoate	18821	0
trans-β-ocimene	90787	1015276
(Z,E)-α-farnesene	63755	0
(E,E)-α-farnesene	21104788	2014096
(E)-4,8-Dimethyl-1,3,7-nonatriene	0	3980713

3.5.3 Exogenous farnesene mistargeted *Plasmopara* zoospores

In order to verify the effect of volatiles on zoospores in sensing stomata, by an exogenous source of β-caryophyllene or farnesene, a leaf disc assay was set up. Zoospores of the single sporangial strain 1137_C20 (Gómez-Zeledón *et al.,* 2013),

were hatched *in vitro*, inoculated on *Vitis rupestris* leaf discs in the presence of a small volume of volatile placed on a filter paper in the center of the petridish. Zoospores targeting were evaluated microscopically after 20 minutes by blankophor staining. The effects of exogenous sources of β-caryophyllene or farnesene on the targeting behaviour of *P. viticola* zoospores from a leaf-disc assay were plotted in (Figure 3.19). In the presence of β-caryophyllene, the targeting of zoospores to the stomata was moderately affected as compared to the control assay. Under this condition 92% of zoospores were successful in finding their way to the stomata. In contrast, an exogenous source of farnesene could affect zoospore targeting negatively. In the presence of an exogenous farnesene around 60% of the zoospores were targeted to the stomata successfully, whereas the rest of them either formed germ tubes or were found on leaf veins (Figure 3.20). The results of this assay demonstrated reduced targeting of zoospores by an exogenous source of farnesene.

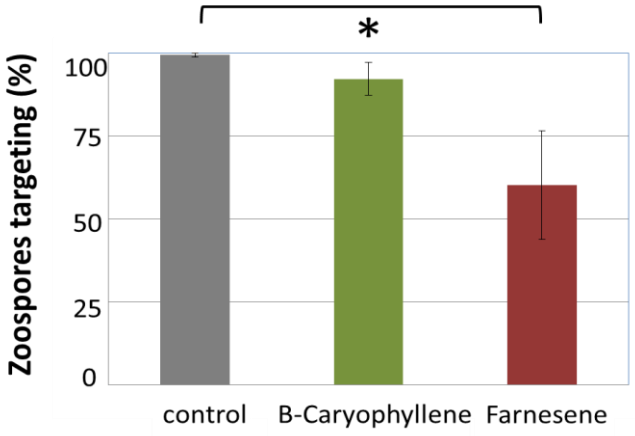

Figure 3.19 Effects of an exogenous source of β-caryophyllene or farnesene on the targeting behaviour of *Plasmopara viticola* zoospores in relation to water control. Data represent mean values from three independent experimental series, error bars represent standard errors. Brackets indicate differences that are significant at $P < 0.05$ (*), Student's *t*-test.

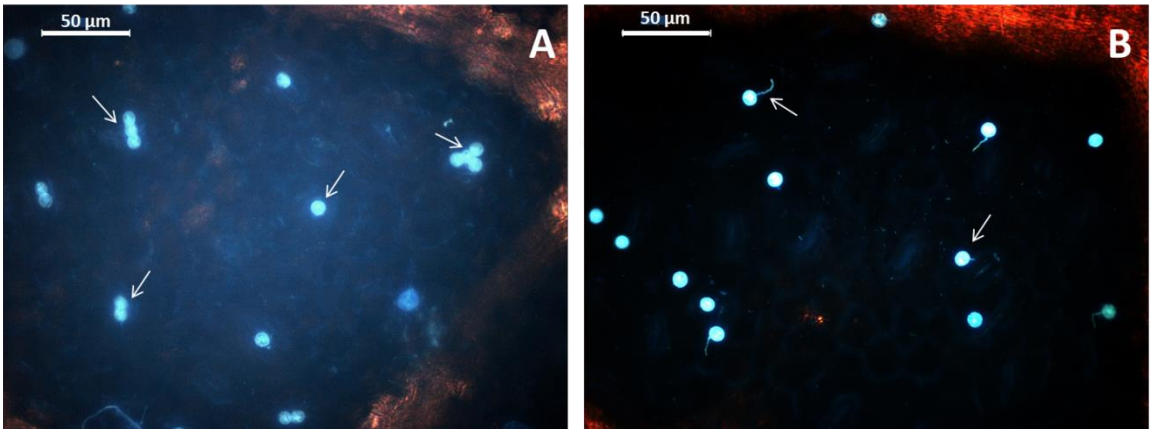

Figure 3.20 Stomatal targeting of *Plasmopara viticola* zoospores under exogenous source of volatiles **A**. Control condition: several zoospores targeted successfully to the stomata. Infected stomata with cysts and germinated cysts 20 minutes after inoculation of a *Vitis rupestris* leaf disc. Arrows indicate encysted gathered zoospores on stomata of *Vitis rupestris* **B.** Zoospore targeting under application of an exogenous source of farnesene. Arrows indicate zoospores that produced germ tubes before targeting to the stomata.

3.5.4 Exogenous β-caryophyllene and farnesene affect frequency of targeted zoospores

To find out if the exogenous source of volatile compound could affect the frequency of targeted zoospores. The number of zoospores per stomata has been evaluated from a leaf disc assay. The frequency of targeted zoospores under exogenous sources of β-caryophyllene or farnesene in relation to water control has been plotted (Figure 3.21). In the presence of an exogenous source of β-caryophyllene or farnesene the frequency of targeted zoospores were affected as compared to the control assay without a volatile source. β-caryophyllene and farnesene significantly reduced the number of stomata with one zoospore. In contrast, an exogenous source of β-caryophyllene or farnesene could not affect the frequency of targeted zoospores with two or more zoospores per stomata. These results correlate with the “gathering effect” of zoospores, where several zoospores infect one single stoma.

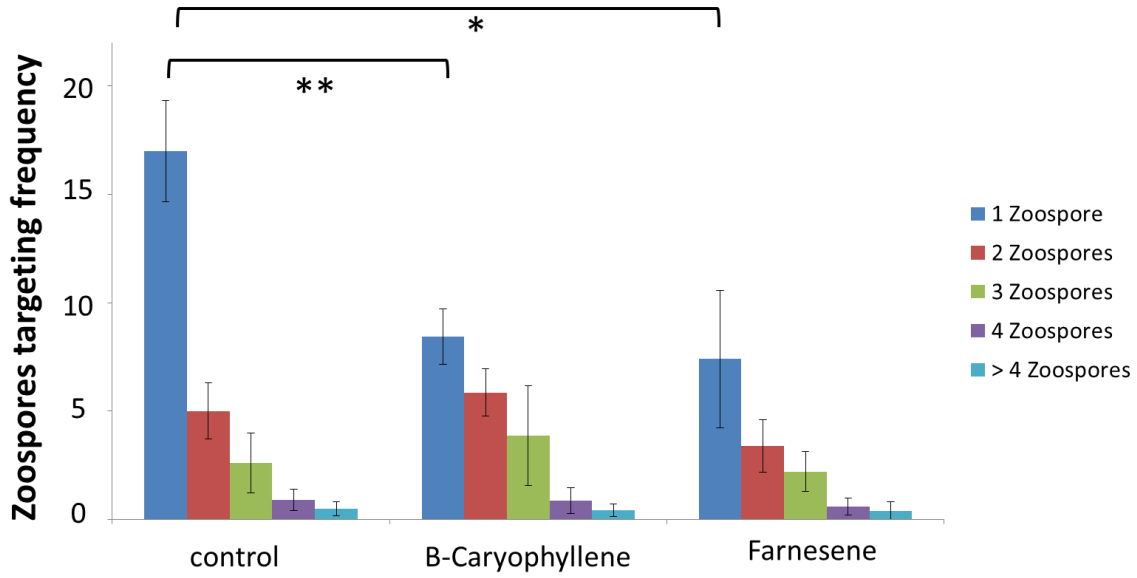

Figure 3.21 Effects of an exogenous source of β-caryophyllene or farnesene on the frequency of targeted *Plasmopara viticola* zoospores. Numbers of targeted zoospores were evaluated in five categories ranging continuously from one zoospore per stoma up to four zoospores per stoma. Category "more than 4" includes infected stomata with more than 4 zoospores. Data represent mean values from three independent experimental series, error bars represent standard errors. Brackets indicate differences that are significant at $P < 0.05$ (*) or $P < 0.01$ (**), Student's *t*-test.

3.6 Summary of results

Plants emit volatile compounds to respond efficiently to various biotic and abiotic stress conditions. Green Leaf Volatiles as one important group of volatile compounds are produced through the cleavage action of hydroperoxide lyase (HPL). In this study, the HPL1 was isolated from the *Vitis vinifera* cultivar 'Müller-Thurgau' and overexpressed in the tobacco BY-2 cells. Co-expression of VvHPL1-GFP fusion with a stroma marker (tpFNR-mEosFP) verified its plastid localisation.

The substrate specificity of the VvHPL1 was tested by feeding 9-HPOD/T and 13-HPOD/T to the recombinantly expressed enzyme. Assays using Solid Phase Micro Extraction (SPME) coupled with gas chromatography mass spectrometry (GC-MS) showed that recombinant VvHPL1 was able to catalyse the cleavage of 13-HPOD/T into C_6-volatiles. In contrast, the recombinant HPL showed no activity towards 9-HPOD/T. The major product from 13-HPOD was hexanal, while 13-HPOT as substrate yielded cis-3-hexenal and trans-2-hexenal. These results confirmed VvHPL1 as 13-HPL (CYP74B), which consistent with the prediction derived from sequence comparisons.

Overexpression of the HPL1-GFP fusion in tobacco suspension caused no phenotypic effect in comparison to the non-transformed wild type under standard conditions. The overexpression of HPL conferred elevated cell motality in response to salinity. The HPLox cell line also showed higher mortality in response to harpin elicitor. This harpin-triggered cell-death response was mitigated by activation of JA signalling in the HPLox line.

The cellular effect of VvHPL1 products (cis-3-hexenal and trans-2-hexenal) were examined on BY-2 cell expressing a fluorescent actin marker. Cis-3-hexenal, but not its isomer trans-2-hexenal, elicited a rapid response of actin filaments indicative of a receptor-mediated programmed cell-death response.

The role of volatiles was studied on the whole plant by using Grapevine-*Plasmopara* interaction as an experimental model. The effects of two volatile compounds, β-caryophyllene and farnesene released from the leaves of the

grapevine were studied with respect to the targeting behaviour of *P. viticola* zoospores. An exogenous source of farnesene affects the targeting of *P. viticola* zoospores, whereas they could still target to the stomata in the presence of an exogenous source of β-caryophyllene.

4. DISCUSSION

Plants make use of Volatile Organic Compounds to interact with their continuously changing environment. Although during the last decades various studies revealed different aspects of plant volatile compounds, there are still many questions that remain unclear. Green Leaf Volatiles, as one important group of volatile organic compounds, not only contribute to flavour aromas in fruits and vegetables, but are also considered to participate in plant defence responses to pathogens or herbivors (Matsui *et al.,* 2000). The aim of this study was to explore the molecular mechanisms underpinning the role of Green Leaf Volatiles in defence signalling.

Green Leaf Volatiles are generated from fatty acid hydroperoxides by the cleavage reaction of fatty acid hydroperoxide lyase (HPL). To get insights into the cellular functions of HPL, Hydroperoxide Lyase from *Vitis vinifera* cv. 'Müller-Thurgau' (VvHPL1) has been investigated. This study focused on cellular functions of Hydroperoxide Lyase 1 from *Vitis vinifera* cv. 'Müller-Thurgau' (VvHPL1). Where is this enzyme localised, what is its enzymatic function and how does it function in response to different biotic and abiotic stress factors?

On the other hand, volatiles can be hijacked as cues, by which pathogens locate entrance gates into the host, such as stomata (reviewed in Melotto *et al.,* 2008). For a better understanding of the volatile roles on the organismic level, the Grapevine-*Plasmopara* interaction was included as a unique experimental model in this study. It is known that *P. viticola* uses the chemical signals released from host plants to target the stomata (Kiefer *et al.,* 2002). But still the host factors that guide *P. viticola* zoospores are unknown. Are there specific volatile compounds used by *P. viticola* zoospores as cues to find their ways to the stomata? How could these host factors affect the pathogen development?

4.1 The VvHPL1 from 'Müller-Thurgau' is a CYP74B using 13-HPOT to generate 2-hexenal

Based on sequence similarity and the presence of specific molecular signatures, the VvHPL1 is a member of the plant CYP74 enzymes. VvHPL1 was predicted to be a member of the CYP74B clade favouring 13-hydroperoxy fatty acids and generating C_6-volatiles.

In this study, the enzymatic activity was confirmed using purified recombinant protein. It was found that the VvHPL1 from cv. 'Müller-Thurgau', similar to its homologue from cv. 'Cabernet Sauvignon' (Zhu *et al.,* 2012) was indeed a true CYP74B specifically accepting 13-hydroperoxy fatty acids (and not 9-hydroperoxy fatty acids) as substrate, giving rise to the cis- and the trans-isomer of the C_6-volatile 2-hexenal (cis-3-hexenal and trans-2-hexenal). Further analysis showed that recombinant VvHPL1 from 'Müller-Thurgau' preferred 13-HPOT as substrate. When 13-HPOD was offered, no hexanal was detected using SPME analysis. This might be because the potential levels of hexanal in the head space did not reach the threshold for detection and therefore SBSE as an alternative analytical approach was employed. In fact, here, it was possible, to detect hexanal as product from the enyzmatic conversion of 13-HPOD. However, similar to the HPL homologue from tomato (Howe *et al.,* 2000), the substrate preference of VvHPL1 is clearly on the site of the 13-HPOT, channelling the metabolic pathway towards cis-3-hexenal and trans-2-hexenal.

4.2 The VvHPL1 from 'Müller-Thurgau' is located in the plastid

The oxylipin pathway is strongly compartmentalised, and this subcellular partitioning has been studied in great detail for jasmonate biosynthesis (reviewed in Wasternack & Hause, 2013), whereby the initial steps proceed in the plastid, followed by further processing in the peroxisome, and final activation in the cytoplasm. For the concurrent oxylipin branches, this compartmentalisation is less clear and there has been some controversy about the localisation of HPLs: Whereas all three HPL versions of rice were shown to be imported into plastids

using an in-vitro import assay (Chehab *et al.,* 2006) as well as the HPL of tomato (Froehlich *et al.,* 2001), a HPL of almond was reported to accumulate in lipid droplets upon transient transformation into tobacco protoplasts (Mita *et al.,* 2005), and for alfalfa, specific 9-HPL isoforms were reported to be located in the cytosol and in lipid droplets, again using transient transformation in protoplasts or leaves (Domenico *et al.,* 2007). Due to different localisation patterns, the subcellular localisation of VvHPL1 needs to be studied in more detail. Since all previous studies had either relied on in-vitro assays (Froehlich *et al.,* 2001; Chehab *et al.,* 2006), or on transient expression (Mita *et al.,* 2005; Domenico *et al.,* 2007), stable cell line expressing VvHPL1 in tobacco BY-2 was generated in this study. Since the N-terminus of HPL1 harbours a predicted transit peptide for chloroplast targeting, but chloroplast targeting was reported to occur in some cases even in absence of the chloroplast transit peptide (Froehlich *et al.,* 2001), as a result, both C- and N-terminal fusions of HPL with GFP were constructed. As expected from the prediction of an N-terminal plastid targeting sequence, a qualitatively different localisation pattern for these two constructs was observed: when GFP was fused at the C-terminus, the VvHPL1 localised in ovoid organelles that by transient transformation with the stroma marker tpFNR-mEosFP were shown to be proplastids (Figure 3.4). In contrast, when the GFP was fused to the N-terminus, thus masking the putative plastid import sequence, the VvHPL1 was not seen in the proplastids but in filamentous structures that by morphology and localisation seem to be transvacuolar strands of the ER (Figure 3.3 A). Since stable expression of the C-terminal HPL-GFP fusion produced a localisation consistent for a canonical 13-HPL (Froehlich *et al.,* 2001; Chehab *et al.,* 2006), It was, therefore, promising to use this overexpressor line to address potential cellular functions of this enzyme.

Quantitative phenotyping of this line with respect to viability, mitotic index, and cell length under normal physiological conditions did not reveal any difference between the overexpressor and the non-transformed wild type (Figure 3.7 & Figure 3.8). However, the overexpression seen by spinning disk microscopy could be confirmed both on the transcript level (Figure 3.9), as well as by detection of the fusion protein on the protein level (Figure 3.10). This led to the question, whether

the cryptic function of VvHPL1 can be rendered manifest, when lipoxygenation is stimulated by exposing this transgenic line to stress conditions, thus providing the substrates for this enzyme.

4.3 VvHPL1 functions in cell-death related stress signalling

In response to salt stress, higher levels of reactive oxygen species are formed in cells (Ismail *et al.,* 2012). In cell culture, oxidative burst can be conveniently induced by imposing salinity stress (grapevine cells: Ismail *et al.,* 2012; tobacco BY-2 cells: Monetti *et al.,* 2014), and this will activate lipid peroxidation (Hazman *et al.,* 2015). While the HPL1 overexpressor did not exhibit any phenotype under normal conditions, it was significantly more sensitive to sodium stress consistent with the prediction that salinity induced activation of lipoxygenation will provide the substrate for the ectopic HPL1 (Figure 3.11). The enzymatic product apparently stimulates salinity-induced cell death. At first sight, it would appear counterintuitive, why an enzyme producing a stress-induced toxic compound should confer an evolutionary advantage, but it should be kept in mind that on the organismic level, elimination of imbalanced cells can help to adapt to salinity (Shabala, 2009).

A vigorous oxidative burst can also be evoked by activation of defence through chemical elicitors. However, the timing of this oxidative burst differs between the two layers of innate immunity (Chang & Nick, 2012) correlated with a difference in mortality: The bacterial PAMP flg22 induces a late oxidative burst (that follows the defence-related rapid apoplastic alkalinisation reporting calcium influx) and does not evoke a cell-death response. In contrast, the bacterial elicitor harpin activates a rapid oxidative burst whereas calcium influx is delayed, which is followed by induced cell death (grapevine cells: Chang & Nick, 2012; tobacco BY-2 cells: Guan *et al.,* 2013). It was observed that the HPL overexpressor line showed only a mildly elevated mortality in response to flg22, which remained below the threshold for significance and was generally hardly detectable in both cell lines, consistent with the results published by Guan *et al.,* 2013. In contrast, the mortality in response to harpin was strongly promoted in a dose-dependent manner in the HPL overexpressor (Figure 3.13), consistent with a mechanism, where lipid peroxidation

triggered by the early oxidative burst will generate the substrate required for the ectopic HPL to act and thus disclose an otherwise cryptic phenotype. Similar to salinity stress, the cell-death response to harpin has to be seen as adaptive, corresponding to a hypersensitive response (HR) as an efficient strategy against invasion by biotrophic pathogens.

The reactive oxygen species (ROS) inducing the elevated cell-death response in the overexpressor line, are released in response to a signal. If a molecule acts as a signal, its release and dissipation must be regulated, which differs from a situation, where this molecule is just produced as byproduct of cellular damage. In fact, ROS are employed as common signals to induce and regulate the response to different stress factors (Baxter *et al.,* 2014). A central player for this regulated oxidative burst is the NADPH oxidase RboH in the plasma membrane (Marino *et al.,* 2012). To address the role of this NADPH oxidase, the activity of this signal was inhibited by diphenyleneiodonium (DPI). Since this inhibitor at low concentrations (200 nM) could mitigate the elevated harpin-induced mortality seen in the HPL overexpressor (Figure 3.15), it is straightforward to assume that RboH is responsible for the release of the lipoxygenation. There is an interesting cell biological aspect in this context, though: RboH is located in the plasma membrane, but the lipoxygenation takes place in the plastid. Thus, the signal released by RboH has to travel which might speak against superoxide as direct cause for the lipoxygenation and calling for a scenario with a second messenger. A second messenger known to be relevant for lipid peroxidation is peroxynitrite, the reaction product of nitric oxide and superoxide (Farmer & Mueller, 2013). In this context, it is worth mentioning that DPI inhibits NADPH-dependent flavoproteins, which in mammalian cells includes the nitric oxide synthases (Stuehr *et al.,* 1991). Although the major source of NO in plants seems to be the nitrate reductase (Meyer *et al.,* 2005), which is a soluble enzyme, a plasma membrane bound enzymatic activity producing nitric oxide from nitrite has been reported for tobacco roots (Stöhr *et al.,* 2001). Thus, a role of NO in the genesis of the products generated by HPL is worth to be investigated in future experiments. The involvement of a second factor (in addition to the superoxide generated by RboH) is also indicated by the fact that

DPI could not completely eliminate the harpin-induced induction of mortality, but only reduce it by about 40% (Figure 3.15).

Irrespective of the molecular details leading to the stress induced lipoxygenation, the data from this study support an explanation where the absence of a phenotype in the HPL overexpressor under normal conditions is caused by a lack of substrate.

If HPL acts in cell-death related signalling, activation of the concurrent pathway (jasmonate signalling) should produce an antagonistic effect. JA is known to induce the expression of various defence-related genes, when applied exogenously (Creelman & Mullet, 1997; Wasternack & Parthier, 1997). As a consequence, activation of the JA pathway will trigger various defence responses such as induction of phytoalexins, proteinase inhibitors, pathogenesis-related proteins or cell wall modification (Wasternack & Parthier, 1997). For instance, exogenous application of JA in tomato plants enhanced defence responses by inducing proteinase inhibitors (Thaler *et al.,* 1996). In fact, jasmonate has been shown to mitigate the effect of salinity stress in wheat seedlings linked with reduced lipid peroxidation (Qiu *et al.,* 2014), and is known to promote the resistance to necrotrophic pathogens, whereas the hypersensitive response (HR) to biotrophic pathogens is often suppressed by jasmonate (Yan & Xie, 2015). If the activation of cell death by harpin is a manifestation of a signalling pathway acting in HR-related defence, it should be quelled by exogenous jasmonate. This implication has been experimentally shown previously for the same experimental model, tobacco BY-2 (Andi *et al.,* 2001). If HPL acts in cell-death related signalling, jasmonate should mitigate cell death in the HPL overexpressor and it should do so to a larger extent as compared to the non-transformed wild type. This was exactly, what has been observed: jasmonic acid pretreatment could completely eliminate the harpin-induced mortality in the overexpressor (Figure 3.14), which means that the effect of jasmonic acid was more pronounced than that of DPI.

There are different possible mechanisms for this antagonistic signalling. Since the effect was seen in a line, where HPL was overexpressed under control of the constitutive CaMV-35S promoter, a transcriptional repression as mechanism is very unlikely. The most straightforward mechanism would be competition of

(ectopic) VvHPL1 and (endogenous) AOS for a common substrate (Figure 4.1). When jasmonate increases either abundance or enzymatic activity of AOS, this would account for the observed mitigation. The self-activation of jasmonate biosynthesis by jasmonate signalling has been discussed extensively (Sasaki *et al.,* 2001) and also confirmed for *Nicotiana* (Paschold *et al.,* 2008). Specifically, the transcription of AOS by different jasmonates has been well investigated in classical studies (Laudert & Weiler, 1998). However, this jasmonate-dependent transcriptional activation is accompanied by considerable posttranslational control (Scholz *et al.,* 2015). It should also be kept in mind that the abundance of the bioactive JA-Ile observed in a cell result from a dynamic equilibrium between synthesis and catabolism (Heitz *et al.,* 2012).

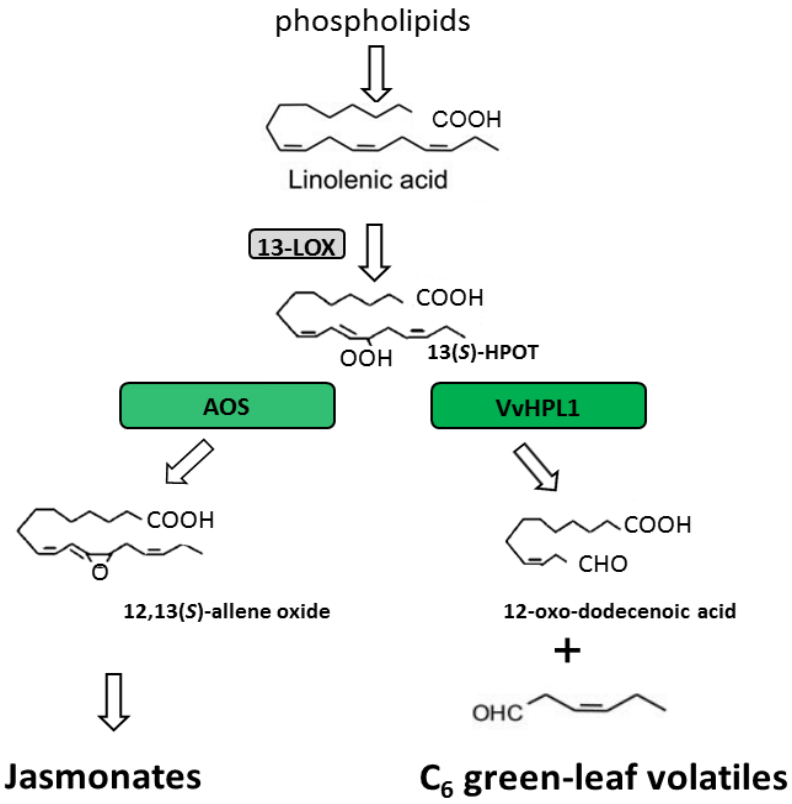

Figure 4.1 Simplified scheme for the metabolic pathways driven by the two CYP74 subclades, where (ectopic) VvHPL1 and (endogenous) AOS compete for a common substrate (13-HPOT), adapted from (Hughes et al., 2009). LOX, lipoxygenase; HPOT, hydroperoxy octadecatrienoic acid; AOS, allene oxide synthase; VvHPL1, hydroperoxide lyase isolated from *Vitis vinifera* cv. 'Müller-Thurgau' (Akaberi *et al.* 2016 in preparation).

Competition between AOS and HPL for a common substrate can account for the rapid decrease in the steady-state levels of JA-Ile observed 30 min after elicitation in the wild type (Figure 3.16) and is consistent with the rapid and transient activation of oxidative burst induced by harpin (Chang & Nick, 2012). However, the subsequent (relatively swift) recovery to the initial JA-Ile levels cannot be explained by biosynthesis alone. There is clearly a missing link. This missing link might be the catabolic conversion of JA-Ile that has been shown to modulate JA-Ile levels very rapidly, in a time frame of less than one hour (Heitz *et al.,* 2012). The fact that the HPL overexpressor does not show this transient drop, although substrate competition is expected to be even harsher points into the same direction. There will be no real understanding of jasmonate dynamics without a closer look on catabolism.

Irrespective of these open points on jasmonate dynamics that are worth to be pursued in future studies, findings of this study lead to the conclusion that HPL acts in a signalling pathway that acts in signal-dependent (programmed) cell death, for instance as a strategy against pathogens. This pathway is regulated in a dynamic way by the availability of substrate-triggered by signal-dependent oxidative burst (involving the NADPH oxidase RboH). If this model holds true, the enzymatic products generated by HPL should be able to activate programmed cell death.

4.4 Is the product of VvHPL1 activating cell-death signalling?

The biological effect of C_6-volatiles could be a chronic or acute toxicity - for instance, aphid fecundity was doubled on potato plants that had been genetically engineered for reduced HPL activity, which was explained by a general toxicity of green leaf volatiles (Vancanneyt *et al.,* 2001).

Also, the effect of short-chained aldehydes as "volatile phytoalexins" (Zeringue & McCormick, 1989) is explained in terms of unspecific cytotoxicity. Alternatively, C_6-volatiles might act as specific signals. The regulatory specificities discussed above such as the link with signal-dependent oxidative burst and the antagonism with jasmonate signalling support a scenario, where the products of HPL act as cellular signals rather than as toxic executors of cell death (Figure 4.2). Whether a molecule is a signal, mainly depends on the presence of a receptor interpreting this molecule as a signal. When the cellular effect of the enzymatic products of the VvHPL1 on a BY-2 cell line expressing a GFP actin marker was tested, a rapid disintegration of cortical actin for cis-3-hexenal was observed (Figure 3.17 B), a hallmark for programmed cell death (Smertenko & Franklin-Tong, 2011). This actin response was not seen for its isomer, trans-2-hexenal. When a biological response is elicited by a molecule, but not by its isomer, the effect cannot be caused by a general chemical effect, but by interaction with a different molecule that is isomer-specific. In other words: the isomer specificity of the actin response indicates that this response must be activated by a "receptor". *Nota bene*: the presence of a "receptor"-based signalling chain for a specific green leaf volatile isomer in the plant itself does not exclude that green leaf volatiles also act as toxins in the

interaction with other organisms. However, a plant-based signal chain must be linked with a plant-specific cellular response (programmed cell death). Future work will therefore be dedicated to understand the biological function and the molecular and cellular events underlying this response.

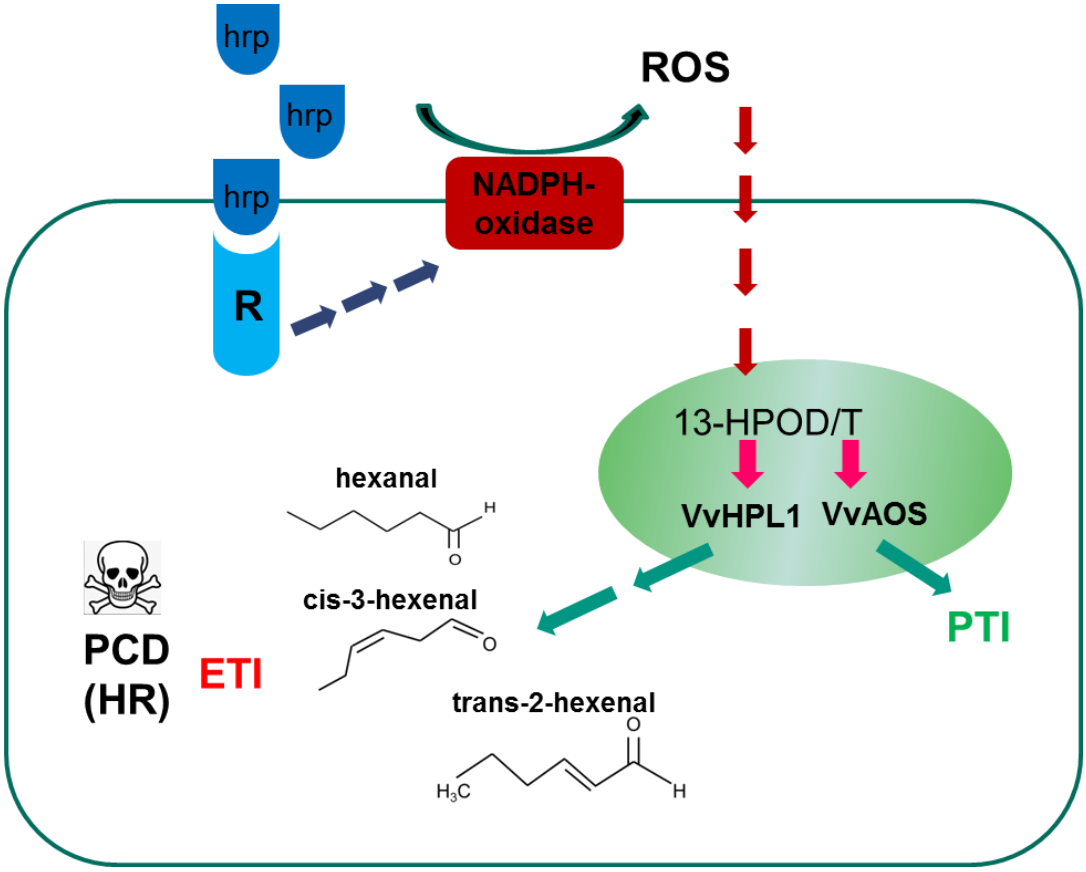

Figure 4.2 Model for VvHPL1-mediated cell-death related signaling as strategy against pathogens. Recognition of the bacterial elicitor harpin (hrp) by the resistance (R) receptors will result in the stimulation of the membrane-bound NADPH oxidase, leading to the production of heigher levels of ROS (reactive oxygen species). Lipid peroxidation triggered by the oxidative burst will then generate the substrate 13-HPOD/T required for the (ectopic) VvHPL1. Both enzymes, (ectopic) VvHPL1 and (endogenous) VvAOS compete for the common substrate. As a consequence, the VvHPL1 products act as cellular signals of ETI-like cell death. Whereas, increasing the activity of VvAOS by exogenous jasmonate application mitigated the harpin-induced cell death. The duplication into the CYP74A (AOS) jasmonate generating branch and the CYP74B (HPL) volatile generating branch is linked with the bifurcation of defence signalling that either leads to basal immunity (AOS, jasmonate pathway) or a cell-death related immunity (HPL, volatile pathway). HPOD/T, hydroperoxy octadecadienoic/octadecatrienoic acid; AOS, allene oxide synthase; VvHPL1, *Vitis vinifera* hydroperoxide lyase 1; PTI, PAMP-triggered immunity; ETI, effector-triggered immunity; PCD, programmed cell death; HR, hypersensitive response.

4.5 Conclusion

The results from this study support the above proposed model in context to: firstly, the hydroperoxide lyase isolated from *Vitis vinifera* cv. 'Müller-Thurgau' (VvHPL1) is a CYP74B using 13-HPOD/T to generate C_6-volatile and therefore, classified as 13-HPL. Secondly, the stable expression of the C-terminal HPL-GFP fusion showed plastid localisation, consistent for a canonical 13-HPL. Thirdly, overexpression of VvHPL1 in BY-2 cells causes higher mortality in response to bacterial elicitor harpin, as well as to salinity. Under applied stress conditions, NADPH oxidase in the plasma membrane will generate higher levels of ROS. This oxidative burst will then trigger lipid peroxidation that generates the substrate required for the ectopic VvHPL1. Lastly, the products of VvHPL1 could activate cell-death signaling. This cell-death response to harpin, corresponding to a hypersensitive response (HR) would be an efficient strategy against biotrophic pathogens. Finally, the activation of the cell death by harpin is quelled by exogenous jasmonate, due to the competition between AOS and VvHPL1 for a common substrate. Exogenous application of jasmonate increases the enzymatic activity of AOS, which shift the pathway toward basal immunity.

4.6 Outlook: Towards understanding the organismic functions of volatiles in grapevine

The role of volatiles on the whole plant, as one of the targets for future research.

4.6.1 Green Leaf Volatiles / HPL induction in response to wounding in grapevine

Green Leaf Volatiles as they are termed so, are released instantly from leaves after wounding. GLVs are mainly produced by the action of HPL during defence responses especially against herbivores and pathogens (Liu *et al.,* 2012). The rapid and strong induction of *VvHPL1* expression after mechanical wounding in grapevine leaves may be related to the production of volatile compounds that serve

as protection against herbivores. As this VvHPL1 is confirmed to be 13-HPL, its induction could lead to the production of C_6-volatiles in response to wounding in grapevine. Consistent with observation from this work, HPL induction upon wounding has been observed in various plants such as, *Arabidopsis* (Bate *et al.,* 1998), *Citrus jambhiri* (Gomi *et al.,* 2003), *Lycopersicon esculentum* (Howe *et al.,* 2000). HPL-derived volatiles are known to have different roles in plant defence responses. HPL-derived volatiles have antimicrobial activity (Croft *et al.,* 1993). They could affect insect feeding during herbivory (Halitschke *et al.,* 2004). In addition, HPL-derived volatiles also play roles in signalling within and between plants. Upon wounding, damaged leaves could form GLVs and send them to the leaves of the same plant, as well as the leaves of neighbouring plants in order to induce defence responses (Matsui, 2006).

4.6.2 Volatile signals affect targeting behaviour of *Plasmopara viticola*

Some pathogens such as oomycetes are able to find their host by developing motile zoospores (Hardham, 1992). Zoospores of *P. viticola* use stomata as an entrance gate to the host plant. Therefore, this early step of zoospore targeting plays a pivotal role to begin the infection process in grapevine plants.

One possible strategy that most of oomycetes zoospores use to enter the host is chemotaxis, in which zoospores are chemotactically attracted to the specific host signals. For instance, zoospores of *Phytophthora palmivora* showed chemotaxis towards isovaleraldehyde (Cameron & Carlile, 1981). Zoospores of *Phytophthora sojae* are attracted chemotactically by isoflavones released from roots of the host plant (Tyler *et al.,* 1996). Chemotaxis has been shown in another oomycetes, *Aphanomyces cochlioides*, where zoospores are attracted to the specific host attractant called cochliophilin A (Takayama *et al.,* 1998).

As shown previously (Kiefer *et al.,* 2002), in Grapevine-*Plasmopara* interaction, stomatal closure induced by abscisic acid (ABA) application inhibited targeting of zoospores. These observations suggested the involvement of host volatile compounds that were released from the open stomata as guiding signals for

zoospore targeting (Kiefer *et al.,* 2002). To get insight into the potential roles of host volatile compounds as factors that might guide zoospores, the role of two sesquiterpenes (β-caryophyllene and farnesene), detected when analyzing leaf volatiles from two different grapevine species, have been investigated with respect to their susceptibility to *P. viticola* (Table 3.2).

This study showed that zoospores of *P. viticola* were mistargeted in the presence of an exogenous source of farnesene (Figure 3.19). They were encysted and germinated before targeting to the stomata (Figure 3.20 B). Whereas, encystment and germination of zoospores should happen after targeting to the stomata to reach the substomatal cavity (Kiefer *et al.,* 2002). While the whole gas phase in the petri dish was filled with farnesene molecules, zoospores were attracted and swam everywhere. At the end, the attracted zoospores failed in targeting to the stomata and encysted. By contrast, β-caryophyllene has not induced significant chemotactic response in zoospores of *P. viticola* (Figure 3.19). Most of the zoospores were targeted to the stomata in the presence of β-caryophyllene. It is known that environmental signals that affect zoospores behaviour are detected by receptors presents on the surface of zoospores (Bishop-Hurley *et al.,* 2002). This might indicate that zoospores of *P.viticola* have specific receptors to sense farnesene. Since, β-caryophyllene has not induced encystment and germination of zoospores. It has been shown that both farnesene and β-caryophyllene are functioning as attractants for natural enemies in alfalfa plants damaged by insect feeding (Blackmer *et al.,* 2004). However, the roles of farnesene and β-caryophyllene in the targeting behaviour of *P. viticola* zoospores have not yet been reported, although the biological function of these volatile compounds has been investigated.

The frequency of targeted zoospores in case of one zoospore per stomata has been reduced in the presence of an exogenous source of volatiles. Whereas, the number of stomata occupied with two or more zoospores have not been changed significantly. These observations are similar to adelphotaxis reported in the oomycete *Achlya*, where attracted zoospores amplify host signals and attract other zoospores (Thomas & Peterson, 1990). In this study, the zoospores were not able

to find the stomata easily in the presence of an exogenous source of volatiles. Whereas, the ones which have found the stomata and targeted successfully might have sent signals to the others and show them the way to the stomata. For future research, a deeper understanding of the *Plasmopara* zoospore chemotaxis will be required to test the effect of different volatile compounds on their targeting behaviour.

5. APPENDIX

5.1 Suspension cultures used in this study and its cultivation conditions

Name of the cell line	Volume for Subcultivation	Antibiotics	Sources
BY-2 Wild Type	1 ml	none	(Nagata *et al.*, 1992)
BY-2 GF-11	1.5 ml	Hygromycin 30 $\mu g \cdot ml^{-1}$	(Sano *et al.*, 2005)
VvHPL1	1.5 ml	Hygromycin 45 $\mu g \cdot ml^{-1}$	This work

5.2 Coding sequence of the Hydroperoxide Lyase gene under investigation

VvHPL1 (GenBank: KX379687)

MLSSTVMSVSPGVPTPSSLTPPSPPSSSPVRAIPGSYGWPVLGPIADRLDYFWFQGPETF
FRKRIDKYKSTVFRTNVPPSFPFFVGVNPNVIAVLDCKSFSFLFDMDVVEKKNVLVGDFM
PSVKYTGDIRVCAYLDTAETQHARVKSFAMDILKRSSSIWASEVVASLDTMWDTIDAGVA
KSNSASYIKPLQRFIFHFLTKCLVGADPAVSPEIAESGYVMLDKWVFLQLLPTISVNFLQ
PLEEIFLHSFAYPFFLVKGDYRKLYDFVEQHGQAVLQRGETEFNLSKEETIHNLLFVLGF
NAFGGFTIFFPSLLSALSGKPELQAKLREEVRSKIKPGTNLTFESVKDLELVHSVVYETL
RLNPPVPLQYARARKDFQLSSHDSVFEIKKGDLLCGFQKVAMTDPKIFDDPETFVPDRFT
KEKGRELLNYLFWSNGPQTGSPSDRNKQCAAKDYVTMTAVLFVTHMFQRYDSVTASGSSI
TAVEKAN-

5.3 Primers used for Gateway® cloning

Primers	Sequences (5'- 3')
VvHPL1 Fw	GGGG ACA AGT TTG TAC AAA AAA GCA GGC TTCATG TTG TCT TCC ACG GTC ATG
VvHPL1 Re N-terminal	GGGG AC CAC TTT GTA CAA GAA AGC TGG GTC TCA GTT AGC TTT CTC AAC GGC GGTG
VvHPL1 Re C-terminal	GGGG AC CAC TTT GTA CAA GAA AGC TGG GTC GTT AGC TTT CTC AACGGC GGTG

5.4 Gateway® destination vectors constructed

Overview of the constructs generated from this study:

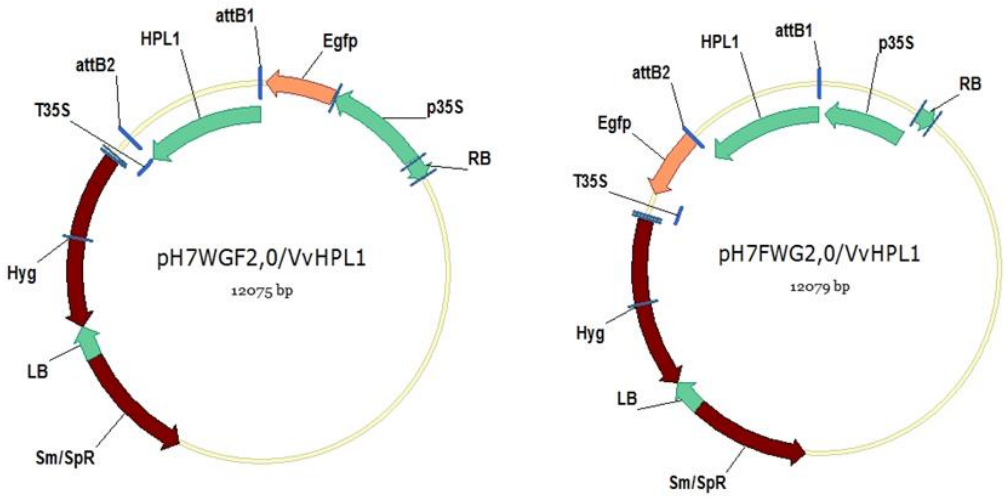

5.5 Gateway® destination vector used for recombinant expression of VvHPL1

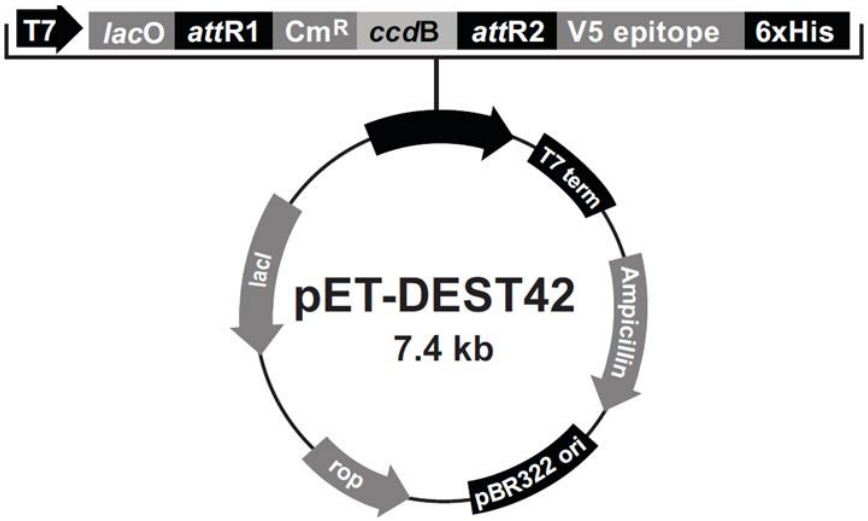

5.6 Primers used for real-time qPCR analysis

Primers	Sequences (5'- 3')
HPL Fw	AGCCGGGAACAAATCTAACC
HPL Re	TTTCTGGCTCGAGCGTATTG
UBC Fw	GAGGGTCGTCAGGATTTGGA
UBC Re	GCCCTGCACTTACCATCTTTAAG

5.7 Alignment: Alignment of the HPL isolated from *Vitis vinifera* cv. 'Müller-Thurgau' along with the two published HPL sequences VvHLP1 and VvHLP2 (Zhu *et al.,* 2012), and representative members of CYP74A (AOS from *Arabidopsis thaliana*, UniProt accession Q96242, predicted AOS from *Vitis vinifera*, UniProt accession F6H025), CYP74B (HPL from *Arabidopsis thaliana*, UniProt accession Q96242), CYP74C (HPL from *Medicago truncatulata*, UniProt accession Q7X9B3), and CYP74D (DES from *Solanum tuberosum*, UniProt accession Q9AVQ1. The following features are indicated in the sequences:

- Interaction sites with haem propionate marked as
- Highly conserved cysteine residue (iron binding) at C-terminus marked as
- The CYP74 characteristic signature FXXG-9 gaps – XXXCXG
- Specificity defining F in AOS that mutated to L converts AOS to HPL (Lee *et al.,* 2008)
- Specificity defining L in AOS that is converted to V(Lee *et al.,* 2008)
- Specificity defining S in AOS that is converted to A(Lee *et al.,* 2008)
- Specificity defining NAFGG in 74C (substrate binding pocket, Toporkova *et al.,* 2013)
- Specificity defining WV in 74C (substrate binding pocket, Hughes *et al.,* 2009)
- Substrate recognition site (I-helix) is indicated by ____ (corresponds to oxygen binding in canonical cytochrome-P450, Toporkova *et al.,* 2013)
- ERR triade domain (interaction with the I-helix and important for substrate specificity) with a 74B specific C and a DES specific F (mutation of this V to F will generate AOS activity, Toporkova *et al.,* 2013)

CLUSTAL W (1.83) multiple sequence alignment
Parameters
-matrix=blosum -gapopen=10 -gapext=0.05 -endgaps=10 -gapdist=0.05

```
Predicted plastidic transit peptides   ____________________________________________________

HPL_MTh                                  ----------------------------MLSSTVMSVSPGVPTPSSLT
vHPL1_Cabernet_Sauvignon                 ----------------------------MLSSTVMSVSPGVPTPSSLT--
VvHPL2_Cabernet_Sauvignon                ---------------------------------MSSSSSSLPLNFVN--
AOS_Vitis_F6H025_predicted               MASPSLTFPSLQLQFPTHTKSSKPSNHKLIVRPIFASVSEKPSVPVSQ--
Arabidopsis_C74A_AOS_Q96242              MASISTPFP---ISLHPKTVRSKPLKFRVLTRPIKASGSETPDLTVAT--
Arabidopsis_C74B2_HPL_Q9ZSY9             ----------------------------MLLRTMAATSPRPPPSTSLTSQ
Medicago_C74C_HPL_ Q7X9B3                ------------------------------------------MASSS--
Solanum_tuberosum__C74D_DES_Q9AVQ1       ---------------------------------------------MSS--


                                                                                  ___________

HPL_MTh                                  -PPSPPSSSPVRAIPGSYGWPVLGPIADRLDYFWFQGPETFFRKRIDKYK
VvHPL1_Cabernet_Sauvignon                -PPSPPSSSPVRAIPGSYGWPVLGPIADRLDYFWFQGPETFFRKRIDKYK
VvHPL2_Cabernet_Sauvignon                --SSSSSKLPLRSIPGDCGSPFFGPIKDRFDYFYNEGRDPFFRTRMQKYQ
AOS_Vitis_F6H025_predicted               --SQVTPPGPIRKIPGDYGLPFIGPIKDRLDYFYNQGREEFFRSRAQKHQ
Arabidopsis_C74A_AOS_Q96242              --RTGSKDLPIRNIPGNYGLPIVGPIKDRWDYFYDQGAEEFFKSRIRKYN
Arabidopsis_C74B2_HPL_Q9ZSY9             QPPSPPSQLPLRTMPGSYGWPLVGPLSDRLDYFWFQGPDKFFRTRAEKYK
Medicago_C74C_HPL_ Q7X9B3                --ETSSTNLPLKPIPGSYGLPIIGPLHDRHDYFYNQGRDKYFQTRIEKYN
Solanum_tuberosum__C74D_DES_Q9AVQ1       --YSELSNLPIREIPGDYGFPIISAIKDRYDYFYNQGEDAWFHNKAEKYK
                                                  *:: :**. * *....: ** ***: :* : :*:.:  *::


HPL_MTh                                  STVFRTNVPPSFPFFVGVNPNVIAVLDCKSFSFLFDMDVVEKKNVLVGDF
VvHPL1_Cabernet_Sauvignon                STVFRTNVPPSFPFFVGVNPNVIAVLDCKSFSFLFDMDVVEKKNVLVGDF
VvHPL2_Cabernet_Sauvignon                STVFRANMPPGP--FMALNPNVVVLLDAISFPILFDTSRIEKRNVLDGTY
AOS_Vitis_F6H025_predicted               STVFRSNMPPGP--FISSNSKVIVLLDGKSFPVLFDVSKVEKKDVFTGTF
Arabidopsis_C74A_AOS_Q96242              STVYRVNMPPGA--FIAENPQVVALLDGKSFPVLFDVDKVEKKDLFTGTY
Arabidopsis_C74B2_HPL_Q9ZSY9             STVFRTNIPPTFPFFGNVNPNIVAVLDVKSFSHLFDMDLVDKRDVLIGDF
Medicago_C74C_HPL_ Q7X9B3                STVLKLNMPPGG--FIAPDPKVIALLDGASFPILFDNAKVEKRDVLDGTF
Solanum_tuberosum__C74D_DES_Q9AVQ1       STVVKINMAPGP--FTSNDYKLVAFLDANSFVCMFDNSLIDKTDTLGGTF
                                         *** : *:.*    *   : ::::..**  **  :**   ::* : : * :


HPL_MTh                                  MPSVKYTGDIRVCAYLDTAETQHARVKSFAMDILKRSSSIWASEVVASLD
VvHPL1_Cabernet_Sauvignon                MPSVKYTGDIRVCAYLDTAETQHARVKSFAMDILKRSSSIWASEVVASLD
VvHPL2_Cabernet_Sauvignon                MPSTAFTGGYRVCAYLDPSEPNHALLKRLFTSSLAARHHNFIPVFRSCLT
AOS_Vitis_F6H025_predicted               MPSTEFTGGFRVLSYLDPSEPDHTKLKRLLFFLLQSSRDRVIPEFHSCFS
Arabidopsis_C74A_AOS_Q96242              MPSTELTGGYRILSYLDPSEPKHEKLKNLLFFLLKSSRNRIFPEFQATYS
Arabidopsis_C74B2_HPL_Q9ZSY9             RPSLGFYGGVCVGVNLDTTEPKHAKIKGFAMETLKRSSKVWLQELRSNLN
Medicago_C74C_HPL_ Q7X9B3                MPSTDFFGGYRTCAFQDTAEPSHSLLKRFIFHILSSKHDTFIPLFQTNLT
Solanum_tuberosum__C74D_DES_Q9AVQ1       KPGKEYYSGYRPVAFIDTKDPNHAALKGYILSAFAKRHNLFIPLFRNSLS
                                          *.    ..       *. :..*  :*      :          .


HPL_MTh                                  TMWDTIDAGVA-KSNSASYIKPLQRFIFHFLTKCLVGADPAVSPEIAESG
VvHPL1_Cabernet_Sauvignon                TMWDTIDAGVA-KSNSASYIKPLQRFIFHFLTKCLVGADPAVSPEIAESG
VvHPL2_Cabernet_Sauvignon                ELFTTLEDDVS-RKGKADFNGISDNMSFNFVFKLFCDKH-PSETKLGSNG
AOS_Vitis_F6H025_predicted               ELSETLESELAAKG-KASFADPNDQASFNFLARALYGTK-PADTKLGTDG
Arabidopsis_C74A_AOS_Q96242              ELFDSLEKELSLKG-KADFGGSSDGTAFNFLARAFYGTN-PADTKLKADA
Arabidopsis_C74B2_HPL_Q9ZSY9             IFWGTIESEIS-KNGAASYIFPLQRCIFSFLCASLAGVDASVSPDIAENG
Medicago_C74C_HPL_ Q7X9B3                EHFTDLEKELAGKHQKASFNTSIGGITFNFLFKLITDKN-PSETKIGDSG
Solanum_tuberosum__C74D_DES_Q9AVQ1       DHLFNNLEKQVTEQGKSDFNALLPTMTFNFIFRLLCDQTNPSDTVLGAQG
                                                    .   :.:        * *:   : .   . .. :  ..


HPL_MTh                                  YVMLDKWVFLQLLPTISVN--FL-QPLEEIFLHSFAYPFFLVKGDYRKLY
VvHPL1_Cabernet_Sauvignon                YVMLDKWVFLQLLPTISVN--FL-QPLEEIFLHSFAYPFFLVKGDYRKLY
VvHPL2_Cabernet_Sauvignon                PNLVTKWLFLQLAPFITLGLSMLPNVVEDLLLHTFPLPSLFVKSDYKKLY
AOS_Vitis_F6H025_predicted               PGLITTWVVFQLSPILTLG---LPKFIEEPLIHTFPLPAFLAKSSYQKLY
Arabidopsis_C74A_AOS_Q96242              PGLITKWVLFNLHPLLSIG---LPRVIEEPLIHTFSLPPALVKSDYQRLY
Arabidopsis_C74B2_HPL_Q9ZSY9             WKTINTWLALQVIPTAKLG--VVPQPLEEILLHTWPYPSLLIAGNYKKLY
Medicago_C74C_HPL_ Q7X9B3                PTLVQTWLAAQLAPLATAGLPKIFNYLEDVLIRTIPIPAWTVKSSYNKLY
Solanum_tuberosum__C74D_DES_Q9AVQ1       PEHLRKWLFPQLIPSLSA--KKLPNIIEDTLFHNFLIPFGFIKSDYNKLV
                                            : .*:  :: *  .     : . :*: :::.   *     ..*.:*
```

I-Helix

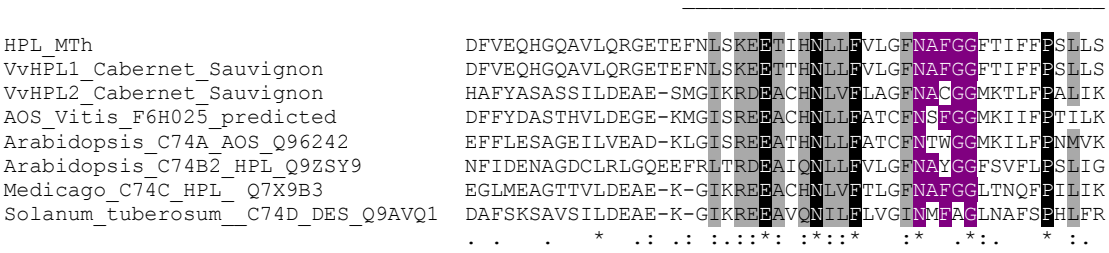

ERR-triade

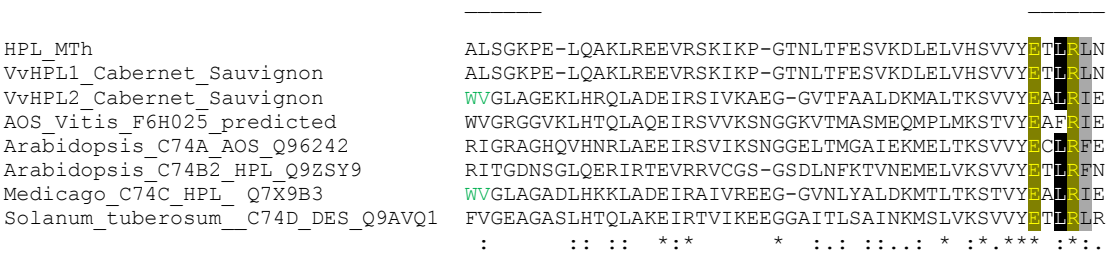

ERR-triade

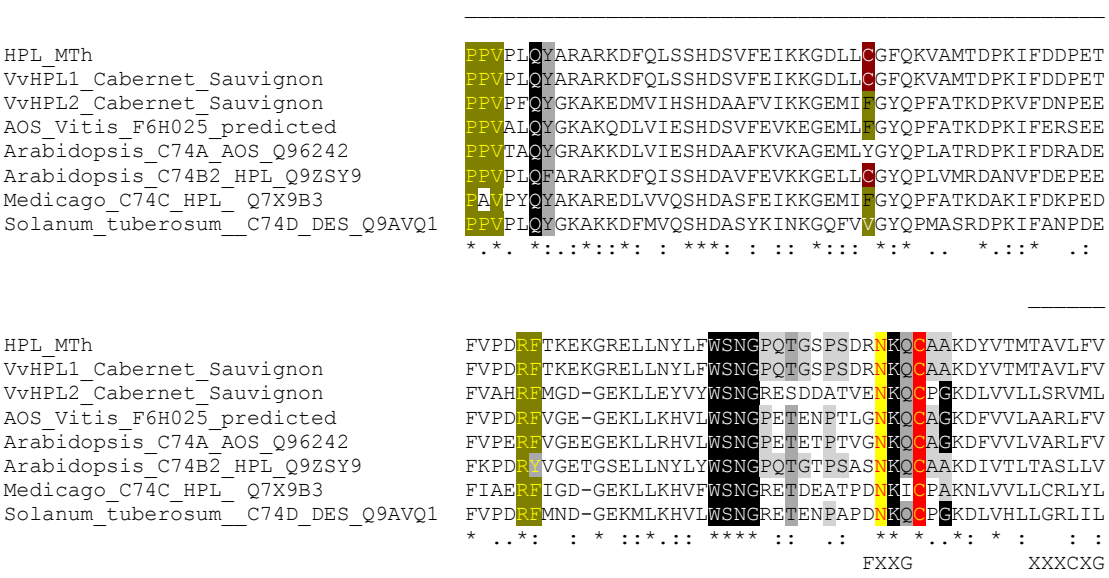

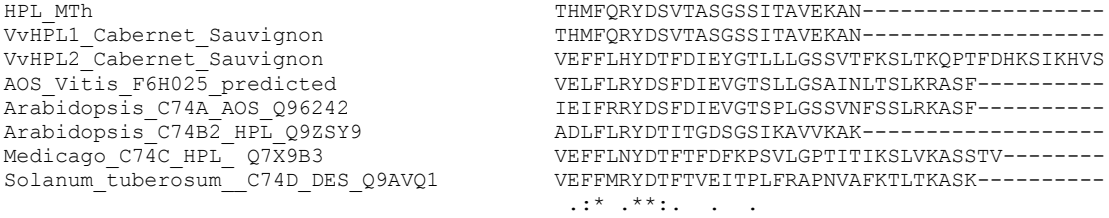

5.8 Three different volatiles emitted from leaves of *Vitis vinifera* cv. Müller-Thurgau and *Vitis rupestris.*

Ratios of the three different volatile compounds (caryophyllene, trans-β-ocimene and (E,E)-α-farnesene)) emitted from leaves of the *Vitis vinifera* cv. Müller-Thurgau (MTh) over *Vitis rupestris* (Rup) plotted as log_{10}.

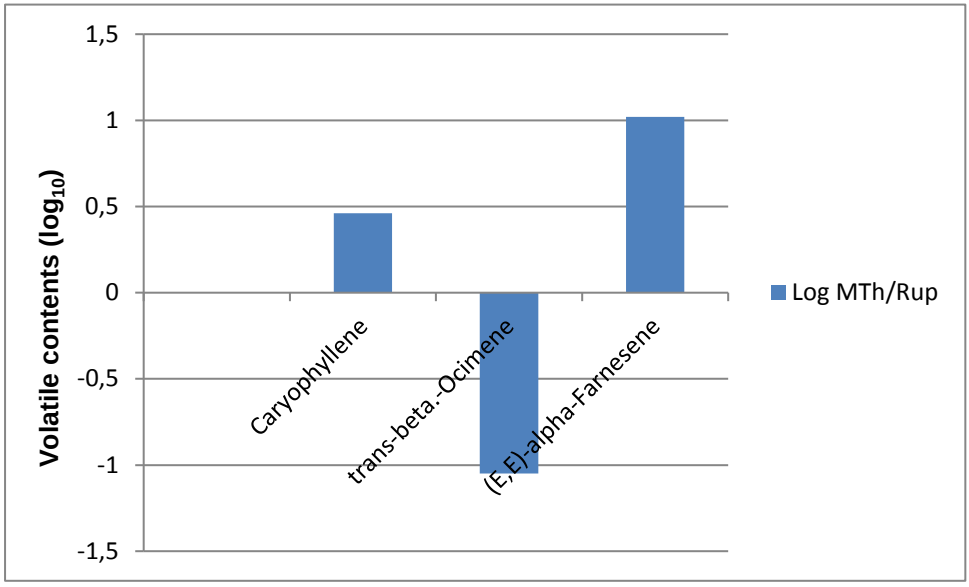

REFERENCES

Almagro, L., Gomez Ros, L. V., Belchi-Navarro, S., Bru, R., Ros Barcelo, A., Pedreno, M. A. (2009). Class III peroxidases in plant defence reactions. *Journal of Experimental Botany* **60** (2), 377–390.

Andi, S., Taguchi, F., Toyoda, K., Shiraishi, T., Ichinose, Y. (2001). Effect of Methyl Jasmonate on Harpin-Induced Hypersensitive Cell Death, Generation of Hydrogen Peroxide and Expression of PAL mRNA in Tobacco Suspension Cultured BY-2 Cells. *Plant and Cell Physiology* **42** (4), 446–449.

Arimura, G., Matsui, K., Takabayashi, J. (2009). Chemical and molecular ecology of herbivore-induced plant volatiles: proximate factors and their ultimate functions. *Plant & cell physiology* **50** (5), 911–923.

Arimura, G., Ozawa, R., Kugimiya, S., Takabayashi, J., Bohlmann, J. (2004). Herbivore-induced defense response in a model legume. Two-spotted spider mites induce emission of (E)-beta-ocimene and transcript accumulation of (E)-beta-ocimene synthase in Lotus japonicus. *PLANT PHYSIOLOGY* **135** (4), 1976–1983.

Armijo, G., Schlechter, R., Agurto, M., Munoz, D., Nunez, C., Arce-Johnson, P. (2016). Grapevine Pathogenic Microorganisms: Understanding Infection Strategies and Host Response Scenarios. *Frontiers in plant science* 7, 382.

Balcke, G. U., Handrick, V., Bergau, N., Fichtner, M., Henning, A., Stellmach, H. (2012). An UPLC-MS/MS method for highly sensitive high-throughput analysis of phytohormones in plant tissues. *Plant methods* **8** (1), 47.

Baldwin, I. T., Halitschke, R., Paschold, A., Dahl, C., Preston, C. A. (2006). Volatile signaling in plant-plant interactions: "talking trees" in the genomics era. *Science (New York, N.Y.)* **311** (5762), 812–815.

Bate, N. J., Sivasankar, S., Moxon, C., Riley, J. M., Thompson, J. E., Rothstein, S. J. (1998). Molecular characterization of an Arabidopsis gene encoding hydroperoxide lyase, a cytochrome P-450 that is wound inducible. *PLANT PHYSIOLOGY* **117** (4), 1393–1400.

Bate, N. J. & Rothstein, S. J. (1998). C6-volatiles derived from the lipoxygenase pathway induce a subset of defense-related genes. *Plant J* **16** (5), 561–569.

Baxter, A., Mittler, R., Suzuki, N. (2014). ROS as key players in plant stress signalling. *Journal of Experimental Botany* **65** (5), 1229–1240.

Beauchamp, J., Wisthaler, A., Hansel, A., Kleist, E., Miebach, M., Niinemets, U. L.O. (2005). Ozone induced emissions of biogenic VOC from tobacco. Relationships between ozone uptake and emission of LOX products. *Plant Cell Environ* **28** (10), 1334–1343.

Bindschedler, L. V., Dewdney, J., Blee, K., A., Stone, J. M., Asai, T., Plotnikov, J. (2006). Peroxidase-dependent apoplastic oxidative burst in Arabidopsis required for pathogen resistance. *The Plant Journal* **47** (6), 851–863.

Bishop-Hurley, S. L., Mounter, S. A., Laskey, J., Morris, R. O., Elder, J., Roop, P. (2002). Phage-Displayed Peptides as Developmental Agonists for Phytophthora capsici Zoospores. *Applied and environmental microbiology* **68** (7), 3315–3320.

Blackmer, J. L. Rodriguez-Saona, C., Byers, J. A., Shope, K. L., Smith, J. P. (2004). Behavioral Response of Lygus hesperus to Conspecifics and Headspace Volatiles of Alfalfa in a Y-Tube Olfactometer. *J Chem Ecol* **30** (8), 1547–1564.

Blee, K. A., Jupe, S. C., Richard, G., Zimmerlin, A., Davies, D. R., Bolwell, G. P. (2001). Molecular identification and expression of the peroxidase responsible for the oxidative burst in French bean (Phaseolus vulgaris L.) and related members of the gene family. *Plant molecular biology* **47** (5), 607–620.

Bolwell, G. P. (1998). Comparative Biochemistry of the Oxidative Burst Produced by Rose and French Bean Cells Reveals Two Distinct Mechanisms. *PLANT PHYSIOLOGY* **116** (4), 1379–1385.

Bostock, R. M. (2005). Signal Crosstalk and Induced Resistance. Straddling the Line Between Cost and Benefit. *Annu. Rev. Phytopathol.* **43** (1), 545–580.

Buschmann, H., Green, P., Sambade, A., Doonan, J. H., Lloyd, C. W. (2011). Cytoskeletal dynamics in interphase, mitosis and cytokinesis analysed through Agrobacterium-mediated transient transformation of tobacco BY-2 cells. *New Phytologist* **190** (1), 258–267.

Cameron, J. N.; Carlile, M. J. (1981): Binding of isovaleraldehyde, an attractant, to zoospores of the fungus Phytophthora palmivora in relation to zoospore chemotaxis. *Journal of cell science* **49**, 273–281.

Casey, R. & Hughes, R. K. (2007). Recombinant Lipoxygenases and Oxylipin Metabolism in Relation to Food Quality. *Food Biotechnology* **18** (2), 135–170.

Chang, X., Heene, E., Qiao, F., Nick, P. (2011). The phytoalexin resveratrol regulates the initiation of hypersensitive cell death in Vitis cell. *PloS one* **6** (10), e26405.

Chang, X., Nick, P., Yang, C. (2012). Defence Signalling Triggered by Flg22 and Harpin Is Integrated into a Different Stilbene Output in Vitis Cells. *PloS one* **7** (7), e40446.

Chang, X., Riemann, M., Liu, Q., Nick, P., Wang, G. (2015). Actin as Deathly Switch? How Auxin Can Suppress Cell-Death Related Defence. *PLoS ONE* 10 (5), e0125498.

Chang, X., Seo, M., Takebayashi, Y., Kamiya, Y., Riemann, M., Nick, P. (2016). Jasmonates are induced by the PAMP flg22 but not the cell death-inducing elicitor Harpin in Vitis rupestris. *Protoplasma.*

Chehab, E. W., Raman, G., Walley, J. W., Perea, J. V., Banu, G., Theg, S., Dehesh, K. (2006). Rice Hydroperoxide Lyases with unique expression patterns generate distinct aldehyde signatures in Arabidopsis. *PLANT PHYSIOLOGY* **141** (1), 121–134.

Chehab, E. W., Kaspi, R., Savchenko, T., Rowe, H., Negre-Zakharov, F., Kliebenstein, D. (2008). Distinct Roles of Jasmonates and Aldehydes in Plant-Defense Responses. *PloS one* 3 (4), e1904.

Conrath, U. (2011). Molecular aspects of defence priming. *Trends in Plant Science* **16** (10), 524–531.

Creelman, R. A. & Mullet, J. E. (1997). Biosynthesis and action of Jasmonates in plants. *Annual review of plant physiology and plant molecular biology* **48**, 355–381.

Croft, K. P.C., Juttner, F., Slusarenko, A. J. (1993). Volatile Products of the Lipoxygenase Pathway Evolved from Phaseolus vulgaris (L.) Leaves Inoculated with Pseudomonas syringae pv phaseolicola. *PLANT PHYSIOLOGY* **101** (1), 13–24.

Dangl, J. L., Horvath, D. M., Staskawicz, B. J. (2013). Pivoting the plant immune system from dissection to deployment. *Science (New York, N.Y.)* **341** (6147), 746–751.

Dat, J., Vandenabeele, S., Vranová, E., van Montagu, M., Inzé, D., van Breusegem, F. (2000). Dual action of the active oxygen species during plant stress responses. *Cellular and molecular life sciences : CMLS* **57** (5), 779–795.

Dodds, P. N. & Rathjen, J. P. (2010). Plant immunity: towards an integrated view of plant-pathogen interactions. *Nature reviews. Genetics* **11** (8), 539–548.

Domenico, S., Tsesmetzis, N., Di Sansebastiano, G. P., Hughes, R. K., Casey, R., Santino, A. (2007). Subcellular localisation of Medicago truncatula 9/13-hydroperoxide lyase reveals a new localisation pattern and activation mechanism for CYP74C enzymes. *BMC plant biology* 7, 58.

Duan, D., Fischer, S., Merz, P., Bogs, J., Riemann, M., Nick, P. (2016). An ancestral allele of grapevine transcription factor MYB14 promotes plant defence. *EXBOTJ* **67** (6), 1795–1804.

Dudareva, N., Murfitt, L. M., Mann, C. J., Gorenstein, N., Kolosova, N., Kish, C. M. (2000). Developmental regulation of methyl benzoate biosynthesis and emission in snapdragon flowers. *The Plant cell* **12** (6), 949–961.

Dudareva, N., Klempien, A., Muhlemann, J. K., Kaplan, I. (2013). Biosynthesis, function and metabolic engineering of plant volatile organic compounds. *The New phytologist* **198** (1), 16–32.

Durrant, W. E. & Dong, X. (2004). Systemic Acquired Resistance. *Annu. Rev. Phytopathol.* **42** (1), 185–209.

Elstner, E. F. (1982). Oxygen Activation and Oxygen Toxicity. *Annu. Rev. Plant. Physiol.* **33** (1), 73–96.

Engelberth, J., Alborn, H. T., Schmelz, E. A., Tumlinson, J. H. (2004). Airborne signals prime plants against insect herbivore attack. *Proceedings of the National Academy of Sciences of the United States of America* **101** (6), 1781–1785.

Eurostat (2007). The use of plant protection products in the European Union. Data 1992-2003. 3rd ed. Luxembourg: EUR-OP.

Fammartino, A., Cardinale, F., Göbel, C., Mène-Saffrané, L., Fournier, J., Feussner, I., Esquerré-Tugayé, M. (2007). Characterization of a divinyl ether biosynthetic pathway specifically associated with pathogenesis in tobacco. *PLANT PHYSIOLOGY* **143** (1), 378–388.

Farag, M. A., Fokar, M., Abd, H., Zhang, H., Allen, R. D., Par, P. W. (2005). (Z)-3-Hexenol induces defense genes and downstream metabolites in maize. *Planta* **220** (6), 900–909.

Farmaki, T., Sanmartin, M., Jimenez, P., Paneque, M., Sanz, C., Vancanneyt, G. (2006). Differential distribution of the lipoxygenase pathway enzymes within potato chloroplasts. *Journal of Experimental Botany* **58** (3), 555–568.

Farmer, E. E. & Mueller, M. J. (2013). ROS-Mediated Lipid Peroxidation and RES-Activated Signaling. *Annu. Rev. Plant Biol.* **64** (1), 429–450.

Fauconnier, M. L. & Marlier, M. (1997). Fatty acid hydroperoxides pathways in plants. A review. *Grasas y Aceites* **48** (1), 30–37.

Feussner, I. & Wasternack, C. (2002). The lipoxygenase pathway. *Annual review of plant biology* **53**, 275–297.

Froehlich, J. E., Itoh, A., Howe, G. A. (2001). Tomato allene oxide synthase and fatty acid hydroperoxide lyase, two cytochrome P450s involved in oxylipin metabolism, are targeted to different membranes of chloroplast envelope. *PLANT PHYSIOLOGY* **125** (1), 306–317.

Frost, C. J., Mescher, M. C., Dervinis, C., Davis, J. M., Carlson, J. E., Moraes, C. M. (2008). Priming defense genes and metabolites in hybrid poplar by the green leaf volatile cis -3-hexenyl acetate. *New Phytologist* **180** (3), 722–734.

Fu, Z. Q., Dong, X. (2013). Systemic Acquired Resistance. Turning Local Infection into Global Defense. *Annu. Rev. Plant Biol.* **64** (1), S. 839–863.

GAFF, D. F. & OKONG'O-OGOLA, O. (1971). The Use of Non-permeating Pigments for Testing the Survival of Cells. *J Exp Bot* **22** (3), 756–758.

Garcia-Brugger, A., Lamotte, O., Vandelle, E., Bourque, S., Lecourieux, D., Poinssot, B. (2006). Early signaling events induced by elicitors of plant defenses. *Molecular plant-microbe interactions : MPMI* **19** (7), 711–724.

Gershenzon, J. (2007). Plant volatiles carry both public and private messages. *Proceedings of the National Academy of Sciences* **104** (13), 5257–5258.

Gessler, C., Pertot, I., Perazzolli, M. (2011). Plasmopara viticola: a review of knowledge on downy mildew of grapevine and effective disease management. *Phytopathologia Mediterranea* **50** (1), 3–44.

Gobbin, D., Jermini, M., Loskill, B., Pertot, I., Raynal, M., Gessler, C. (2005). Importance of secondary inoculum of Plasmopara viticola to epidemics of grapevine downy mildew. *Plant Pathology* **54** (4), 522–534.

Gobbin, D. (2004). Redefining Plasmopara viticola epidemiological cycle by molecular genetics. Dissertation, Zürich. Swiss Federal Institute of Technology,

Gogolev, Y. V., Gorina, S. S., Gogoleva, N. E., Toporkova, Y. Y., Chechetkin, I. R., Grechkin, A. N. (2012). Green leaf divinyl ether synthase. Gene detection, molecular cloning and identification of a unique CYP74B subfamily member. In: *Biochimica et Biophysica Acta (BBA) - Molecular and Cell Biology of Lipids* 1821 (2), 287–294.

Gómez-Zeledón, J., Zipper, R., Spring, O. (2013). Assessment of phenotypic diversity of Plasmopara viticola on Vitis genotypes with different resistance. In: *Crop Protection* 54, 221–228.

Gomi, K., Yamasaki, Y., Yamamoto, H., Akimitsu, K. (2003). Characterization of a hydroperoxide lyase gene and effect of C6-volatiles on expression of genes of the oxylipin metabolism in Citrus. In: *Journal of plant physiology* **160** (10), 1219–1231.

Guan, X., Buchholz, G., Nick, P. (2013). The cytoskeleton is disrupted by the bacterial effector HrpZ, but not by the bacterial PAMP flg22, in tobacco BY-2 cells. *Journal of Experimental Botany* **64** (7), 1805–1816.

Gutjahr, C., Banba, M., Croset, V., An, K., Miyao, A., An, G. (2008). Arbuscular mycorrhiza-specific signaling in rice transcends the common symbiosis signaling pathway. *The Plant cell* **20** (11), 2989–3005.

HA, S., LEE, B., LEE, D., KUK, Y. I., LEE, A., HAN, O., BACK, K. (2002). Molecular characterization of the gene encoding rice allene oxide synthase and its expression. *Bioscience, biotechnology, and biochemistry* **66** (12), 2719–2722.

Halitschke, R., Ziegler, J., Keinanen, M., Baldwin, I. T. (2004). Silencing of hydroperoxide lyase and allene oxide synthase reveals substrate and defense

signaling crosstalk in Nicotiana attenuata. *The Plant journal : for cell and molecular biology* **40** (1), 35–46.

Hamilton-Kemp, T. R., McCracken, C. T., J., Loughrin, J. H., Andersen, R. A., Hildebrand, D. F. (1992). Effects of some natural volatile compounds on the pathogenic fungiAlternaria alternata andBotrytis cinerea. *Journal of chemical ecology* **18** (7), 1083–1091.

Hardham, A. R. (1992). Cell Biology of Pathogenesis. *Annu. Rev. Plant. Physiol. Plant. Mol. Biol.* **43** (1), 491–526.

Hazman, M., Hause, B., Eiche, E., Nick, P., Riemann, M. (2015). Increased tolerance to salt stress in OPDA-deficient rice Allene Oxide Cyclase mutants is linked to an increased ROS-scavenging activity. *Journal of Experimental Botany* **66** (11), 3339–3352.

Heitz, T., Widemann, E., Lugan, R., Miesch, L., Ullmann, P., Desaubry, L. (2012). Cytochromes P450 CYP94C1 and CYP94B3 catalyze two successive oxidation steps of plant hormone Jasmonoyl-isoleucine for catabolic turnover. *The Journal of biological chemistry* **287** (9), 6296–6306.

Holopainen, J. K., Gershenzon, J. (2010). Multiple stress factors and the emission of plant VOCs. *Trends in Plant Science* **15** (3), 176–184.

Howe, G. A., Lee, G. I., Itoh, A., Li, L., DeRocher, A. E. (2000). Cytochrome P450-dependent metabolism of oxylipins in tomato. Cloning and expression of allene oxide synthase and fatty acid hydroperoxide lyase. *PLANT PHYSIOLOGY* **123** (2), 711–724.

Huang, M., Sanchez-Moreiras, A. M., Abel, C., Sohrabi, R., Lee, S., Gershenzon, J., Tholl, Dorothea (2012). The major volatile organic compound emitted from *Arabidopsis thaliana* flowers, the sesquiterpene (E)-beta-caryophyllene, is a defense against a bacterial pathogen. *The New phytologist* **193** (4), 997–1008.

Hughes, R. K., Domenico, S., Santino, A. (2009). Plant Cytochrome CYP74 Family. Biochemical Features, Endocellular Localisation, Activation Mechanism in Plant Defence and Improvements for Industrial Applications. *ChemBioChem* **10** (7), 1122–1133.

Ismail, A., Takeda, S., Nick, P. (2014). Life and death under salt stress. Same players, different timing? *Journal of Experimental Botany* **65** (12), 2963–2979.

Ismail, A., Riemann, M., Nick, P. (2012). The jasmonate pathway mediates salt tolerance in grapevines. *Journal of Experimental Botany* **63** (5), 2127–2139.

Itoh, A. & Howe, G. A. (2001). Molecular Cloning of a Divinyl Ether Synthase. Identification as a CYP74 cytochrome P-450. *Journal of Biological Chemistry* **276** (5), 3620–3627.

Jones, J. D G. & Dangl, J. L. (2006). The plant immune system. *Nature* **444** (7117), 323–329.

Jovanovic, A. M., Durst, S., Nick, P. (2010). Plant cell division is specifically affected by nitrotyrosine. *Journal of Experimental Botany* **61** (3), 901–909.

Kamoun, S., Furzer, O., Jones, J. D. G., Judelson, H. S., Ali, G.S., Dalio, R. J. D. (2015). The Top 10 oomycete pathogens in molecular plant pathology. In: *Molecular plant pathology* **16** (4), 413–434.

Karimi, M., Inzé, D., Depicker, A. (2002). GATEWAY™ vectors for Agrobacterium-mediated plant transformation. *Trends in Plant Science* **7** (5), 193–195.

Kennelly, M. M., Gadoury, D. M., Wilcox, W. F., Magarey, P. A., Seem, R. C. (2007). Primary Infection, Lesion Productivity, and Survival of Sporangia in the Grapevine Downy Mildew Pathogen Plasmopara viticola. *Phytopathology* **97** (4), 512–522.

Kiefer, B., Riemann, M., Buche, C., Kassemeyer, H., Nick, P. (2002). The host guides morphogenesis and stomatal targeting in the grapevine pathogen Plasmopara viticola. *Planta* **215** (3), 387–393.

Kishimoto, K., Matsui, K., Ozawa, R., Takabayashi, J. (2005). Volatile C6-aldehydes and Allo-ocimene activate defense genes and induce resistance against Botrytis cinerea in Arabidopsis thaliana. *Plant & cell physiology* **46** (7), 1093–1102.

Knudsen, J. T., Eriksson, R., Gershenzon, J., Ståhl, B. (2006). Diversity and Distribution of Floral Scent. *The Botanical Review* **72** (1), 1–120.

Lam, E. (2004). Plant cell biology. Controlled cell death, plant survival and development. *Nat Rev Mol Cell Biol* **5** (4), 305–315.

Laudert, D., Weiler, E. W. (1998). Allene oxide synthase. A major control point in Arabidopsis thaliana octadecanoid signalling. *Plant J* **15** (5), 675–684.

Lee, D., Nioche, P., Hamberg, M., Raman, C. S. (2008). Structural insights into the evolutionary paths of oxylipin biosynthetic enzymes. *Nature* **455** (7211), 363–368.

Liu, X., Li, F., Tang, J., Wang, W., Zhang, F., Wang, G. (2012). Activation of the jasmonic acid pathway by depletion of the hydroperoxide lyase OsHPL3 reveals crosstalk between the HPL and AOS branches of the oxylipin pathway in rice. In: *PloS one* **7** (11), e50089.

Livak, K. J. & Schmittgen, T. D. (2001). Analysis of relative gene expression data using real-time quantitative PCR and the 2(-Delta Delta C(T)) Method. *Methods (San Diego, Calif.)* **25** (4), 402–408.

Maisch, J. & Nick, P. (2007). Actin Is Involved in Auxin-Dependent Patterning. *PLANT PHYSIOLOGY* **143** (4), S. 1695–1704.

Marino, D., Dunand, C., Puppo, A., Pauly, N. (2012). A burst of plant NADPH oxidases. *Trends in Plant Science* **17** (1), 9–15.

Matsui, K., Miyahara, C., Wilkinson, J., Hiatt, B., Knauf, V., Kajiwara, T. (2000). Fatty acid hydroperoxide lyase in tomato fruits: cloning and properties of a recombinant enzyme expressed in *Escherichia coli. Bioscience, biotechnology, and biochemistry* **64** (6), 1189–1196.

Matsui, K. (2006). Green leaf volatiles: hydroperoxide lyase pathway of oxylipin metabolism. *Current Opinion in Plant Biology* **9** (3), 274–280.

Matsui, K., Shibutani, M., Hase, T., Kajiwara, T. (1996). Bell pepper fruit fatty acid hydroperoxide lyase is a cytochrome P450 (CYP74B). *FEBS Letters* **394** (1), 21–24.

Melotto, M., Underwood, W., He, S. Y. (2008). Role of stomata in plant innate immunity and foliar bacterial diseases. *Annual review of phytopathology* **46**, 101–122.

Meyer, C., Lea, U. S.; Provan, F., Kaiser, W. M., Lillo, C. (2005). Is nitrate reductase a major player in the plant NO (nitric oxide) game? *Photosynthesis research* **83** (2), 181–189.

Miller, G. A.D., Suzuki, N., Ciftci-Yilmaz, S., Mittler, R. O.N. (2010). Reactive oxygen species homeostasis and signalling during drought and salinity stresses. *Plant, Cell & Environment* **33** (4), 453–467.

Mita, G., Quarta, A., Fasano, P., Paolis, A., Di Sansebastiano, G. P., Perrotta, C. (2005): Molecular cloning and characterization of an almond 9-hydroperoxide lyase, a new CYP74 targeted to lipid bodies. *Journal of Experimental Botany* **56** (419), S. 2321–2333.

Monetti, E., Kadono, T., Tran, D., Azzarello, E., Arbelet-Bonnin, D., Biligui, B. (2014). Deciphering early events involved in hyperosmotic stress-induced programmed cell death in tobacco BY-2 cells. *Journal of Experimental Botany* **65** (5), 1361–1375.

Mu, W., Xue, Q., Jiang, B., Hua, Y. (2012). Molecular cloning, expression, and enzymatic characterization of Solanum tuberosum hydroperoxide lyase. *Eur Food Res Technol* **234** (4), 723–731.

Mur, L. A. J., Kenton, P., Lloyd, A. J., Ougham, H., Prats, E. (2008). The hypersensitive response; the centenary is upon us but how much do we know? *Journal of Experimental Botany* **59** (3), 501–520.

Nagata, T., Nemoto, Y., Hasezawa, S. (1992). Tobacco BY-2 Cell Line as the “HeLa” Cell in the Cell Biology of Higher Plants. Kwang W. Jeon and Martin Friedlander (Hg.): International Review of Cytology, 132 // 132, 1–30.

Nick, P., Heuing, A., Ehmann, B. (2000). Plant chaperonins. A role in microtubule-dependent wall formation? *Protoplasma* **211** (3-4), 234–244.

Nick, P., Lambert, A. M., Vantard, M. (1995). A microtubule-associated protein in maize is expressed during phytochrome-induced cell elongation. *The Plant journal : for cell and molecular biology* **8** (6), 835–844.

Paschold, A., Bonaventure, G., Kant, M. R., Baldwin, I. T. (2008). Jasmonate perception regulates jasmonate biosynthesis and JA-Ile metabolism: the case of COI1 in Nicotiana attenuata. *Plant & cell physiology* **49** (8), 1165–1175.

Peressotti, E., Wiedemann-Merdinoglu, S., Delmotte, F., Bellin, D., Di Gaspero, G., Testolin, R. (2010). Breakdown of resistance to grapevine downy mildew upon limited deployment of a resistant variety. *BMC plant biology* **10**, 147.

Poland, J. A., Balint-Kurti, P. J., Wisser, R. J., Pratt, R. C., Nelson, R. J. (2009). Shades of gray. The world of quantitative disease resistance. *Trends in Plant Science* **14** (1), 21–29.

Popov, N., Schmitt, M., Schulzeck, S., Matthies, H. (1975). Reliable micromethod for determination of the protein content in tissue homogenates. *Acta biologica et medica Germanica* **34** (9), 1441–1446.

Qiu, Z. B., Guo, J., Zhu, A., Zhang, L., Zhang, M. (2014). Exogenous jasmonic acid can enhance tolerance of wheat seedlings to salt stress. *Ecotoxicology and environmental safety* **104**, 202–208.

Raguso, R. A. (2008). Wake Up and Smell the Roses. The Ecology and Evolution of Floral Scent. *Annu. Rev. Ecol. Evol. Syst.* **39** (1), 549–569.

Reid, K. E., Olsson, N., Schlosser, J., Peng, F., Lund, S. T. (2006). An optimized grapevine RNA isolation procedure and statistical determination of reference genes for real-time RT-PCR during berry development. *BMC plant biology* **6**, 27.

Riemann, M., Büche, C., Kassemeyer, H., Nick, P. (2002). Cytoskeletal responses during early development of the downy mildew of grapevine (*Plasmopara viticola*). *Protoplasma* **219** (1-2), 13–22.

Sano, T., Higaki, T., Oda, Y., Hayashi, T., Hasezawa, S. (2005). Appearance of actin microfilament 'twin peaks' in mitosis and their function in cell plate formation, as visualized in tobacco BY-2 cells expressing GFP-fimbrin. *The Plant journal : for cell and molecular biology* **44** (4), S. 595–605.

Sasaki, Y., Asamizu, E., Shibata, D., Nakamura, Y., Kaneko, T., Awai, K. (2001). Monitoring of Methyl Jasmonate-responsive Genes in Arabidopsis by cDNA Macroarray: Self-activation of Jasmonic Acid Biosynthesis and Crosstalk with Other Phytohormone Signaling Pathways. *DNA Research* **8** (4), 153–161.

Scala, A., Mirabella, R., Mugo, C., Matsui, K., Haring, M.A., Schuurink, R. C. (2013). E-2-hexenal promotes susceptibility to Pseudomonas syringae by activating jasmonic acid pathways in Arabidopsis. *Frontiers in plant science* **4**, 74.

Schattat, M. H., Griffiths, S., Mathur, N., Barton, K., Wozny, M. R., Dunn, N. (2012). Differential Coloring Reveals That Plastids Do Not Form Networks for Exchanging Macromolecules. *Plant Cell* **24** (4), 1465–1477.

Scholz, S. S., Reichelt, M., Boland, W., Mithofer, A. (2015). Additional evidence against jasmonate-induced jasmonate induction hypothesis. *Plant science : an international journal of experimental plant biology* **239**, 9–14.

Shabala, S. (2009). Salinity and programmed cell death: unravelling mechanisms for ion specific signalling. *Journal of Experimental Botany* **60** (3), 709–712.

Siedow, J. N. (1991). Plant Lipoxygenase. Structure and Function. *Annu. Rev. Plant. Physiol. Plant. Mol. Biol.* **42** (1), 145–188.

Smertenko, A. & Franklin-Tong, V. E. (2011). Organisation and regulation of the cytoskeleton in plant programmed cell death. *Cell death and differentiation* **18** (8), 1263–1270..

Stamp, N. (2003). Out Of The Quagmire Of Plant Defense Hypotheses. *The Quarterly review of biology* **78** (1), 23–55.

Stöhr, C., Strube, F., Marx, G., Ullrich, W. R., Rockel, P. (2001). A plasma membrane-bound enzyme of tobacco roots catalyses the formation of nitric oxide from nitrite. *Planta* **212** (5-6), 835–841.

Stuehr, D. J., Fasehun, O. A., Kwon, N. S., Gross, S. S., Gonzalez, J. A., Levi, R., Nathan, C. F. (1991). Inhibition of macrophage and endothelial cell nitric oxide synthase by diphenyleneiodonium and its analogs. *FASEB journal : official publication of the Federation of American Societies for Experimental Biology* **5** (1), 98–103.

Stumpe, M., Kandzia, R., Göbel, C., Rosahl, S., Feussner, I. (2001). A pathogen-inducible divinyl ether synthase (CYP74D) from elicitor-treated potato suspension cells 1. *FEBS Letters* **507** (3), 371–376.

Svyatyna, K., Jikumaru, Y., Brendel, R., Reichelt, M., Mithofer, A., Takano, M. (2014). Light induces jasmonate-isoleucine conjugation via OsJAR1-dependent and -independent pathways in rice. *Plant, Cell & Environment* **37** (4), 827–839.

Takayama, T., Mizutani, J., Tahara, S. (1998). Drop Method as a Quantitative Bioassay Method of Chemotaxis of Aphanomyces cochlioides Zoospore. *Jpn. J. Phytopathol.* **64** (3), 175–178.

Thaler, J. S., Stout, M. J., Karban, R., Duffey, S. S. (1996). Exogenous jasmonates simulate insect wounding in tomato plants (Lycopersicon esculentum) in the laboratory and field. *Journal of chemical ecology* **22** (10), 1767–1781

Thomas D. D. & April P. P. (1990). Chemotactic auto-aggregation in the water mould Achlya. *Journal of General Microbiology* (136), 847–853.

Thomma, B. P.H.J., Nürnberger, T., Joosten, M. H.A.J. (2011). Of PAMPs and Effectors. The Blurred PTI-ETI Dichotomy. *Plant Cell* **23** (1), 4–15.

Tijet, N., Schneider, C., Muller, B. L., Brash, A. R. (2001). Biogenesis of Volatile Aldehydes from Fatty Acid Hydroperoxides. Molecular Cloning of a Hydroperoxide Lyase (CYP74C) with Specificity for both the 9- and 13-Hydroperoxides of Linoleic and Linolenic Acids. *Archives of biochemistry and biophysics* **386** (2), 281–289.

Toporkova, Y. Y., Ermilova, V. S., Gorina, S. S., Mukhtarova, L. S., Osipova, E. V., Gogolev, Y. V., Grechkin, A. N. (2013). Structure-function relationship in the CYP74 family. Conversion of divinyl ether synthases into allene oxide synthases by site-directed mutagenesis. *FEBS Letters* **587** (16), 2552–2558.

Turlings, T. C., Loughrin, J. H., McCall, P. J., Rose, U. S., Lewis, W. J., Tumlinson, J. H. (1995). How caterpillar-damaged plants protect themselves by attracting parasitic wasps. *Proceedings of the National Academy of Sciences* **92** (10), 4169–4174.

Tyler, B. M., Wu, M., Wang, J., Cheung, W., Morris, P. F. (1996). Chemotactic Preferences and Strain Variation in the Response of Phytophthora sojae Zoospores to Host Isoflavones. *Applied and environmental microbiology* **62** (8), 2811–2817.

Vancanneyt, G., Sanz, C., Farmaki, T., Paneque, M., Ortego, F., Castanera, P., Sanchez-Serrano, J. J. (2001). Hydroperoxide lyase depletion in transgenic potato plants leads to an increase in aphid performance. *Proceedings of the National Academy of Sciences of the United States of America* **98** (14), 8139–8144.

Vance, R. E., Isberg, R. R., Portnoy, D. A. (2009). Patterns of pathogenesis: discrimination of pathogenic and nonpathogenic microbes by the innate immune system. *Cell host & microbe* **6** (1), 10–21.

Vickers, C. E., Gershenzon, J., Lerdau, M. T., Loreto, F. (2009). A unified mechanism of action for volatile isoprenoids in plant abiotic stress. *Nature chemical biology* **5** (5), 283–291.

Ward, H. M. (1902). On the Relations between Host and Parasite in the Bromes and their Brown Rust, Puccinia dispersa (Erikss.). *Annals of Botany* os-**16** (2), 233–316.

Wasternack, C. & Hause, B. (2013). Jasmonates: biosynthesis, perception, signal transduction and action in plant stress response, growth and development. An update to the 2007 review in Annals of Botany. *Annals of Botany* **111** (6), 1021–1058.

Wasternack, C. (2014). Action of jasmonates in plant stress responses and development - Applied aspects. *Biotechnology Advances* 32 (1), 31–39.

Wasternack, C. & Parthier, B. (1997). Jasmonate-signalled plant gene expression. *Trends in Plant Science* **2** (8), 302–307.

Williams, M. G., Magarey, P. A., Sivasithamparam, K. (2007). Effect of temperature and light intensity on early infection behaviour of a Western Australian isolate of Plasmopara viticola, the downy mildew pathogen of grapevine. *Austral. Plant Pathol.* **36** (4), 325.

Wong, F. P., Burr, H. N., Wilcox, W. F. (2001). Heterothallism in *Plasmopara viticola*. *Plant Pathology* **50** (4), 427–432.

Wu, J., Wu, Q., Wu, Q., Gai, J., Yu, D. (2008). Constitutive overexpression of AOS-like gene from soybean enhanced tolerance to insect attack in transgenic tobacco. *Biotechnol Lett* **30** (9), 693–1698.

Yan, C. & Xie, D. (2015). Jasmonate in plant defence: sentinel or double agent? *Plant biotechnology journal* **13** (9), 1233–1240.

Zeringue, H. J. & McCormick, S. P. (1989). Relationships between cotton leaf-derived volatiles and growth ofAspergillus flavus. *JAOCS* **66** (4), 581–585.

Zhu, B., Xu, X., Wu, Y., Duan, C., Pan, Q. (2012). Isolation and characterization of two hydroperoxide lyase genes from grape berries. *Mol Biol Rep* **39** (7), 7443–7455.

Ziegler, J., Keinänen, M., Baldwin, I. T. (2001). Herbivore-induced allene oxide synthase transcripts and jasmonic acid in Nicotiana attenuata. *Phytochemistry* **58** (5), 729–738.

Parts of this work have been submitted:

Akaberi S, Claudel P, Riemann M, Hause B, Hugueney P, and Nick P (2016) Grapevine hydroperoxide lyase acts in cell-death related immunity.